APPLICATION OF DECADE BEAM DEFLECTION TUBES TO FAST COUNTING CIRCUITS

Lloyd Irving Biscomb, Jr.

APPLICATION OF DECADE BEAM DEFLECTION TUBES TO FAST COUNTING CIRCUITS

* * *

Lloyd I. Biscomb, Jr.

Letter on cover:

APPLICATION OF DECADE BEAM DEFLECTION TUBES TO FAST COUNTING CIRCUITS

Lloyd Irving Biscomb, Jr.

APPLICATION OF DECADE BEAM DEFLECTION TUBES TO FAST COUNTING CIRCUITS

by

Lloyd Irving Biscomb, Jr.

Lieutenant, United States Navy

Submitted in partial fulfillment
of the requirements
for the degree of
MASTER OF SCIENCE
IN
ENGINEERING ELECTRONICS

United States Naval Postgraduate School
Monterey, California

1 9 5 6

This work is accepted as fulfilling

the thesis requirements for the degree of

MASTER OF SCIENCE

IN

ENGINEERING ELECTRONICS

from the

United States Naval Postgraduate School

PREFACE

This work on the Application of Decade Beam Deflection Tubes to Fast Counting Circuits was accomplished in major part at the U. S. Naval Postgraduate School, Monterey, California. The circuit development work described in Chapter III was performed at the Hewlett-Packard Company, Palo Alto, California.

Some of the applications and proposals for further investigation described in Chapter IV have not been previously described, to the author's knowledge.

Figures 8 and 10, and Appendix I are reproduced with permission of the Amperex Electronic Corporation, Hicksville, New York. The substance of Appendices II and III are reproduced from reference [3] of the Bibliography with permission of the Philips' Laboratories, Irvington-on-Hudson, New York.

Acknowledgement is gratefully made to Professors M. L. Cotton and J. B. Turner of the Engineering Electronics Department, U. S. Naval Postgraduate School, for their advice and assistance. Appreciation is also expressed to Mr. A. S. Bagley of the Hewlett-Packard Company for his cooperation and advice in the work described in Chapter III.

TABLE OF CONTENTS

LIST OF ILLUSTRATIONS

TABLE OF SYMBOLS AND ABBREVIATIONS

usec	Microsecond(s)
musec	Milli-Microsecond(s)
kc	Kilocycle(s)
Mc	Megacycle(s)
cps	Cycle(s) per Second
a.c.	Alternating Current
d.c.	Direct Current
Ω	Ohm(s)
K	1,000 Ohm(s)
M	1,000,000 Ohm(s)
H.P.	Hewlett-Packard
P.R.F.	Pulse Repition Frequency
R-C	Resistance - Capacity
A.V.C.	Automatic Volume Control
g_m	Transconductance
ma	Milliampere(s)
uf	Microfarad(s)
uuf	Micro-Microfarad(s)
uh	Micro-Henry(s)
I_b	Plate Current
E_c	Grid Voltage
i_b	Instantaneous Plate Current
e_c	Instantaneous Grid Voltage
R_k	Cathode Circuit Resistance

φ	Angle Defined in Figure III-2
-C	Cutoff Bias
C	Interelectrode, Stray and Wiring Capacity Existing at Electrodes D' and a_2 of ElT

ElT Electrodes:

f	Heater
k	Cathode
s	Screen
g_1	Control Grid
b	Beam Forming Electrodes
g_2	Accelerating Electrode
D	Left Deflecting Electrode
D'	Right Deflecting Electrode
A_h	Auxiliary Anode
g_3, g_5	Suppressor Grids
g_4	Slotted Electrode
a_1	Reset Anode
a_2	Anode
l	Conducting Layer Coated With Fluorescent Material

CHAPTER I

INTRODUCTION

The need for fast counting circuits, particularly as a means of measuring radioactive radiation and other phenomenon associated with nuclear physics, has increased considerably in recent years. Radiation intensities can be measured by means of a Geiger-Müller tube, in which an incident particle causes a discharge that produces an electric pulse, or with a scintillation counter, in which a fluorescent substance scintillates under radioactive radiation, the scintillations being converted into electric pulses by a photo-multiplier.

Circuits for counting regular and random pulses can also be adapted to the following functions: distributing, gating, multiplexing, modulating, cascading, frequency dividing, sampling, coding, memory, timing, matrixing, and oscillating. In addition to nuclear physics, such circuits have wide application in other fields, such as communications, computers, industrial counting and indicating, and automatic controls.

In recent years several beam-deflection counting devices have been developed in which an electron beam is deflected from one stable position to the next every time a pulse arrives at the input to the device. These devices have found application performing some or all of the functions indicated above for counting circuits.

Three general types of beam-deflection tubes will be described in Chapter II: gas-filled tubes, trochotrons, and cathode-ray tubes.

In Chapter III, an example of the cathode-ray tube type of beam-deflection counting tube (the Philips ElT) is selected for more

detailed investigation, with particular emphasis on extending its frequency response to higher counting rates.

Chapter IV describes some proposed improvements to the auxiliary circuitry for operating the ElT tube, and also describes a proposal for a new type of beam deflection device with possibly a much higher counting rate than those described in Chapter II.

Appendix I presents some technical data on the ElT tube and associated circuit parameters. Appendix III contains a summary of an article by van Barneveld [3] describing circuits enabling the ElT tube to count at frequencies up to 2.2 Mc. Appendix II defines some parameters and develops some expressions useful for measuring the counting of random pulses with the ElT tube. In appendix V the maximum transit time of an electron in the ElT tube is calculated.

Appendix IV presents some theoretical and practical material on the parallel-triggered blocking oscillator, which is used in circuit development work described in Chapter III to reset the ElT tube to zero.

CHAPTER II

GENERAL DESCRIPTION OF SEVERAL BEAM-DEFLECTION DECADE-COUNTING TUBES NOW COMMERCIALLY AVAILABLE

1. Introduction.

Three general categories of beam deflection tubes will be described in this chapter. The first type of tube contains a number of independent cathodes placed around a common anode in a gas-filled envelope. There are ten index cathodes separated by transfer cathodes. The number of transfer cathodes between any pair of index cathodes varies from one to three, depending on the type of tube. A glow discharge is made to rest on one of the index cathodes, and the tube is designed to count by moving the discharge from one index cathode to the next by the application of suitable pulses to the transfer cathodes. The resolving time between two consecutive counts varies from 30 to 250 usec., depending on the geometry of the electrodes and the gas-filling.

The second category of tubes, called trochotrons, uses an electron beam from a thermionic cathode. In this case, the beam is confined to an equipotential path by crossed electrostatic and magnetic fields. The beam is made to take up one of the ten stable positions by providing anodes and shields with load resistors which deflect the beam into one of ten pockets. The application of a negative pulse at the anodes results in the movement of the beam from one pocket to the next.

The third category of beam-deflection tubes to be considered here, known as the cathode-ray tube type, also uses a thermionic cathode in conjunction with an electrostatic focusing and deflection system. A

focused electron beam is arranged to have ten stable positions by placing load resistors in series with plates which collect the beam current and connecting these to deflector plates. The application of a pulse to a deflector plate causes the beam to move from one stable position to the next. The position of the beam is indicated on a fluorescent screen.

2. Gas-Filled Tubes.

The arrangements of electrodes and internal connections in a typical gas-filled beam-deflection counting tube are as shown in Figure 1. A circular central anode is surrounded by 30 cathode pins arranged symmetrically around the anode. The ten cathodes K_0 - K_9 are normally used as the index cathodes. The cathode K_0 is brought out to a separate connection in order to obtain an output pulse and reset the tube to zero. Between these index cathodes are the transfer cathodes connected in two groups, A_0 - A_9, and B_0 - B_9. The external connections are shown in Figure 2 and a simple method of driving the tube with negative input pulses is shown in Figure 3. All the transfer cathodes are normally held at about 40 volts, so that the glow rests on one of the index cathodes, such as K_9. Application of the negative pulses to cathodes A and B in turn transfers the glow to these cathodes, and then to K_0. The current through R_2 in Figure 2 develops the output waveform of the form shown in Figure 3. This output may be used to generate a pair of driving pulses for a succeeding tube. Due to the extinction time required by the gas in the tube, the minimum resolving time for two pulses arriving at the input to the counter is about

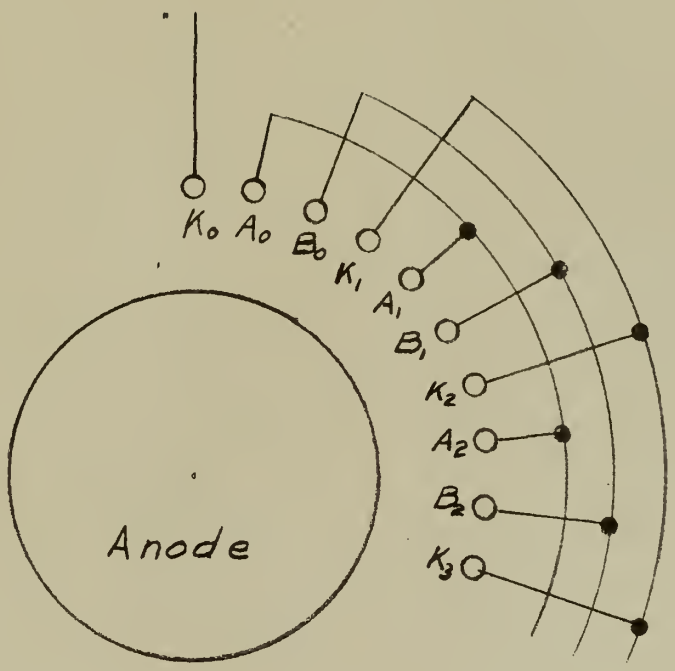

Fig. 1. Arrangement of Electrodes in a Typical Gas-Filled Decade Counting Tube

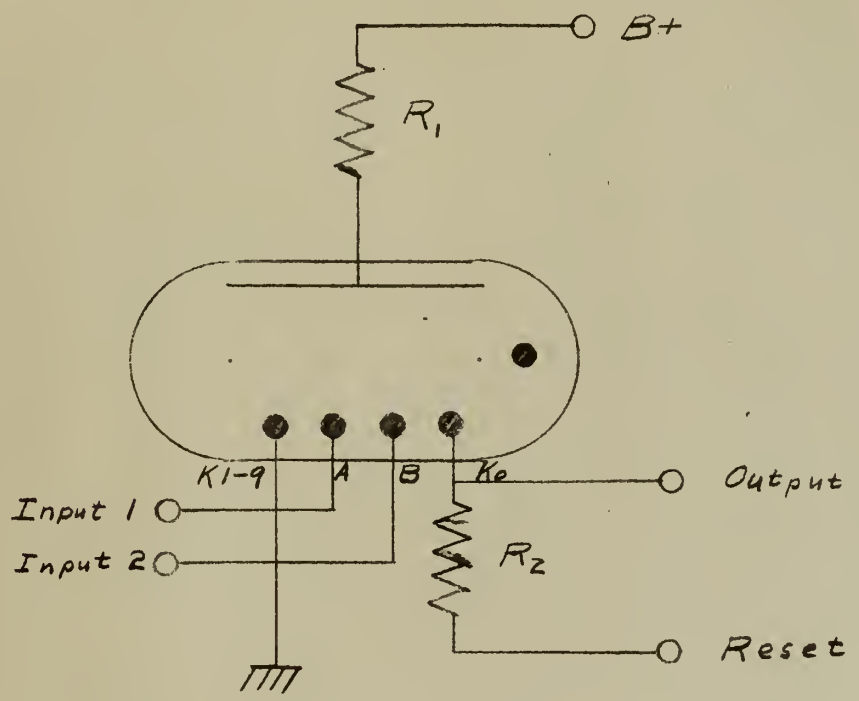

Fig. 2. Schematic Representation of Typical Gas-Filled Decade Counting Tube

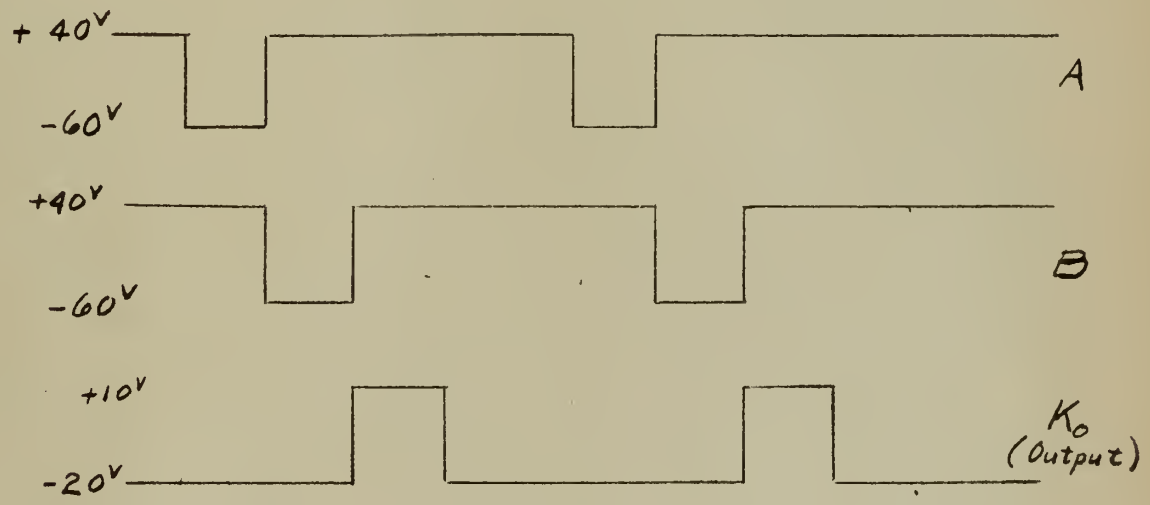

Fig. 3. Driving Pulses Required for Gas-Filled Counting Tube of Fig. 2.

250 usec (approximately 80 usec per transfer). Thus, the upper frequency limit for this type of counter tube is approximately four kc., a serious disadvantage for many applications. Another disadvantage arises from the necessity of providing two transfer pulses per decade stage, assuming multi-decade operation. This requires a rather elaborate interstage coupling circuit, consisting of pulse generating and shaping circuits. For satisfactory operation of tubes of this type, the range of driving pulse widths and amplitudes can be very wide. However, it is desirable to provide well-defined pulses in a complete equipment, in order to insure that the equipment will operate satisfactorily in spite of production tolerances, tube ageing, and drift of supply voltages and component values. The greatest advantage of this type of tube is that it is relatively easy to make it operate as a reversible counter. Also, it posesses the advantage of stability of characteristics over long periods even when the glow is left stationary on one index cathode.

Gas-filled tubes using only one transfer cathode between adjacent index cathodes have been designed, employing specially shaped cathodes in order to obtain directional properties when the discharge is moved from one index cathode to the next. The ten transfer cathodes are connected together internally and a negative driving pulse is applied to them. Resolving times between pulses of the order of 50 usec are obtainable using this technique.

Another type of tube in this category employs three transfer cathodes between each pair of index cathodes. Directivity is obtained by means of R-C circuits in the cathode circuits of alternate transfer

cathodes. Resolving times of the order of 50 usec are obtained with this type of tube.

In the cases of the last two tubes mentioned, it is not advisable to leave the discharge stationary on one cathode for long periods of time.

Still another type of gas-filled tube has been designed which differs from the other gas-filled tubes in two respects. There are two sets of ten cathodes in this tube, but both sets have directional properties. One set is used as the index cathodes K and the other as the transfer cathodes B. Each cathode is shaped in such a way that the discharge is taken over from a preceding cathode at the end nearest to this cathode, but soon moves over to the other end so that it "primes" the succeeding cathode. This tube can be driven with a single negative pulse and does not require any R-C circuits as do other tubes which are driven with single pulses. Another feature of this tube is that an auxiliary anode is built into the tube in close proximity to K_0 so that when the discharge moves to this index cathode the auxiliary gap breaks down and produces a large negative pulse at the auxiliary anode. This eliminates the need for a separate trigger tube for coupling from one counting tube to another. The resolving time of this tube is about 100 usec.

3. Trochotrons.

The trochotron is a high-vacuum tube in which a magnetic field is used in addition to electrostatic fields in order to control the position of the beam, utilizing the magnetron principle. Figure 4

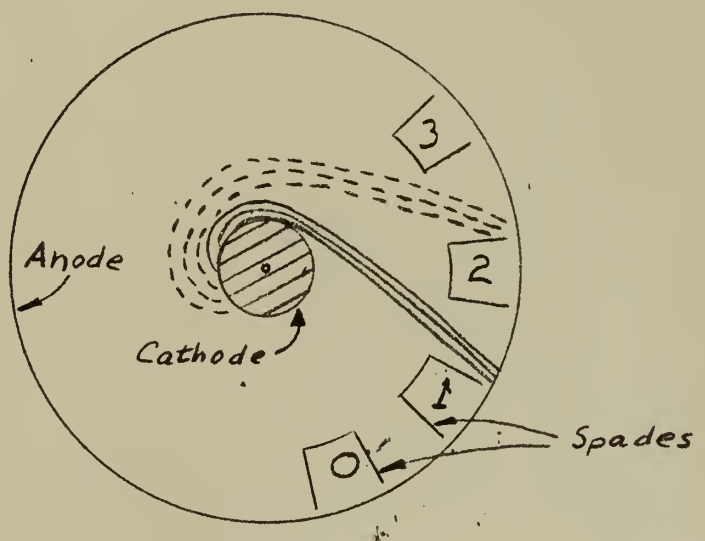

Fig. 4. Cross-Section of a Trochotron Showing Electron Trajectories

shows a cross-section of this type of tube in a plane perpendicular to the cathode. The tube electrodes consist of a central cylindrical cathode, a cylindrical anode, and ten spades spaced symmetrically around the cathode and in front of the anode. An external cylindrical permanent magnet provides a uniform magnetic field parallel to the cathode in the cathode-to-anode space. To explain the operation of the tube, assume that spade #1 is initially at cathode potential, while the anode and all other spades are kept at about +100 volts with respect to the cathode. The trajectory of the electrons will then be as shown in the heavy lines of Figure 4, this being an equipotential path for the electrons. This is a stable position for the beam as long as the above potentials are applied. Most of the electrons will proceed to the anode through the space between spades #1 and #2, but a small current will flow to spade #1. By momentarily reducing the potential of the anode to that of the cathode, reducing the potential of spade #2 to cathode potential, and raising the potential of spade #1 permanently, the position of the beam will be transferred to that of the dotted lines in Figure 4, corresponding to a transfer of one digit.

Figure 5 shows the circuit diagram of a typical counting stage using a trochotron. The 15K cathode resistor is required to stabilize the tube current. The magnetic field required is 320 gauss. The spades are connected to +250 volts, through an R-C circuit, and a negative pulse is applied to the anode through a pulse transformer. The tube current will be about 10 ma, causing a cathode potential of +150 volts. Assuming that the beam is in the position indicated by

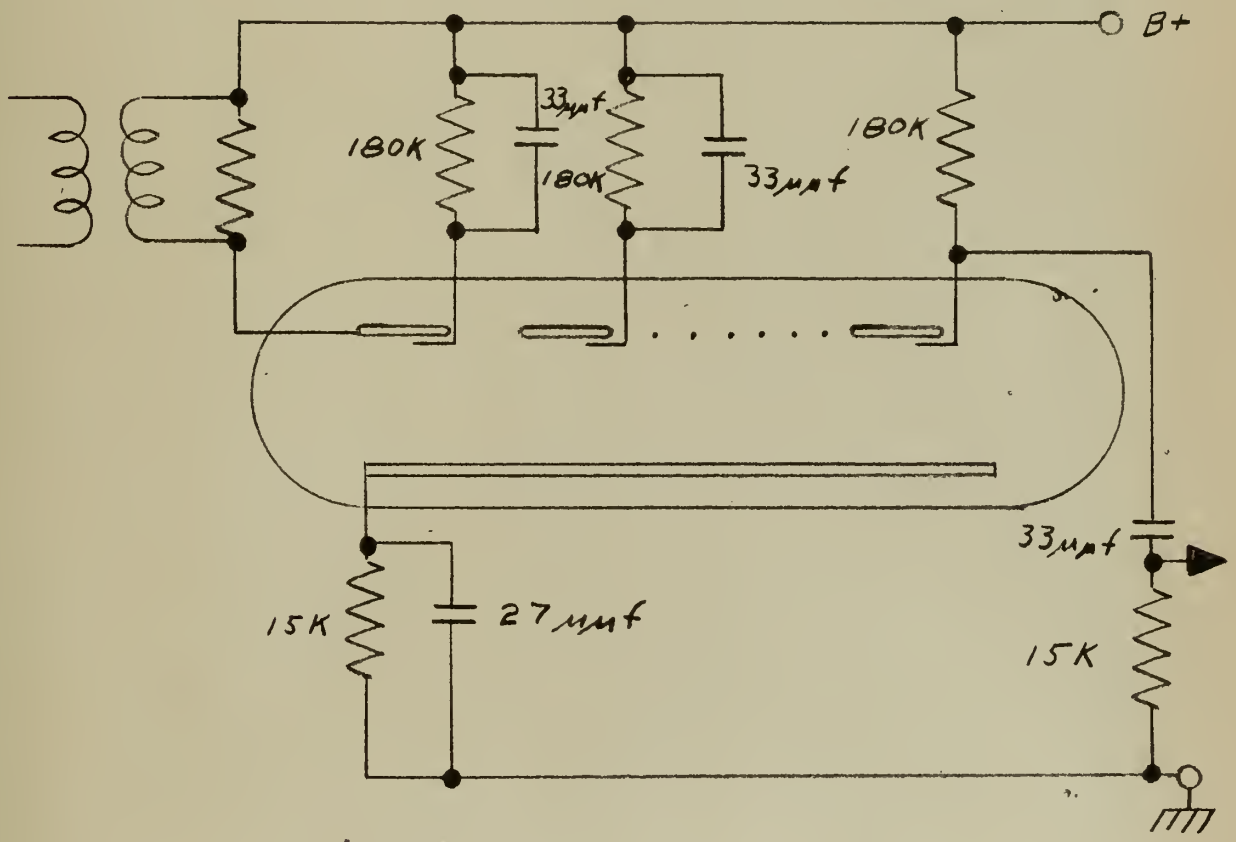

Fig. 5. Schematic Circuit of Trochotron Decade Counting Tube

the heavy lines in Figure 4, spade #1 will pass about 0.5 ma, causing the potential of this spade to be approximately equal to the cathode potential. The remainder of the tube current will be drawn by the anode, the other spades receiving a negligible amount of current.

When a negative pulse of more than 150 volts is applied to the anode of Figure 5, most of the current will flow to spade #2, and the potential of spade #2 will fall at a rate determined by the beam current of 10 ma and the 33 uuf capacitor in the spade circuit. At the same time the potential of spade #1 will rise exponentially with a time constant of 180K X 33 uuf, much slower than the rate of fall of potential of spade #2. By terminating the negative pulse at the anode when the potential of spade #2 has fallen to less than 150 volts, the beam will shift to the next stable position corresponding to the dotted lines of Figure 4. The amplitude of the negative anode pulse should be greater than 150 volts in order to effect this transfer by one digit. The duration of this pulse should be approximately equal to the time required for the potential of spade #2 to fall to cathode potential. If the pulse duration is much longer than this the beam will move too far and transfer by more than one digit. The duration of this pulse is therefore rather critically dependent on the beam current and spade circuit time constant. When the beam is moved from digit nine to digit zero a negative pulse output of about 50 volts is obtained from spade #0 for carry to the next decade stage.

A modification of the trochotron has the anode separated into ten target electrodes, with a switching grid located between each pair of spades, as shown in Figure 6. The operation is essentially the same as

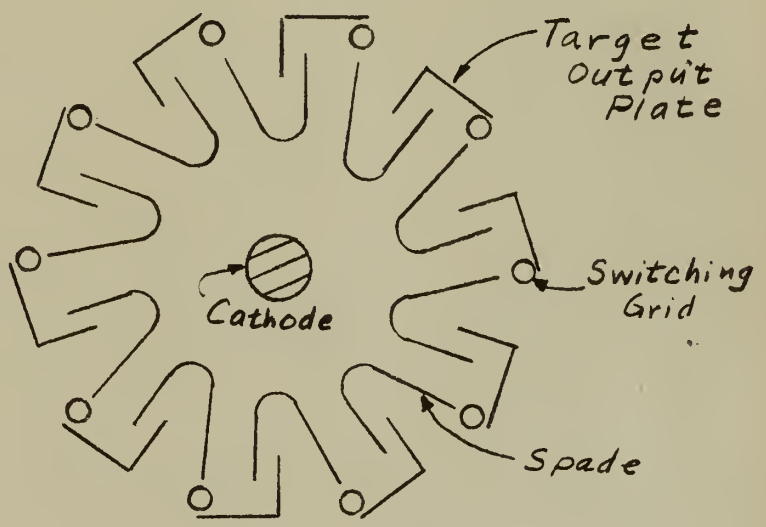

Fig. 6. Cross-Section View of Improved Trochotron

in the trochotron previously described, except that negative pulses are applied to the switching grids to effect the stepping of the beam from one spade to the next. Each spade has a negative characteristic due to the crossed electric and magnetic fields, show in Figure 7, and is capable of two stable states. The beam is formed "on" in a given spade by lowering its potential until the load line for R_g = 100K intersects the positive-slope portion of its static characteristic curve. At this point the negative characteristic will take over and lock in point A at near zero or cathode potential. This beam formation may be accomplished by a DC voltage or a fast pulse. The spade which has thus formed and locked the beam can remain at or near cathode potential indefinitely, while the other spades are at a high positive level.

An advantage of this type of tube is that the switching need not be sequential from one spade to the next. Since each spade has its own switching grid, from one to five spades may be eliminated or "jumped" by lowering the potential of the appropriate spade. Eliminating more than five spades per switching operation may be accomplished with slight modification of the external circuitry.

Another advantage of this tube is that distributions of more than ten positions may be accomplished by appropriately interconnecting two or more tubes. Operation at switching frequencies up to one Mc or higher is quite feasible.

4. Beam-Deflection Counting Tubes of the Cathode Ray Tube Type.

Figure 8a shows a cross-section view and Figure 8b a schematic representation of a typical tube of this type (Philips ElT). The tube

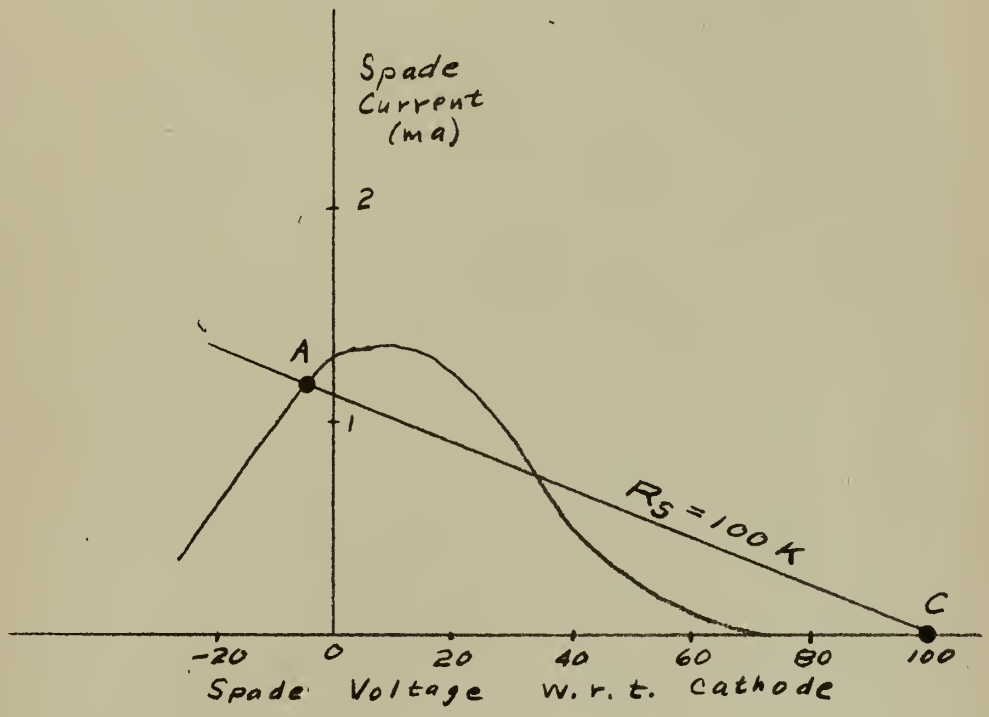

Fig. 7. Static Spade Characteristic for Improved Trochotron

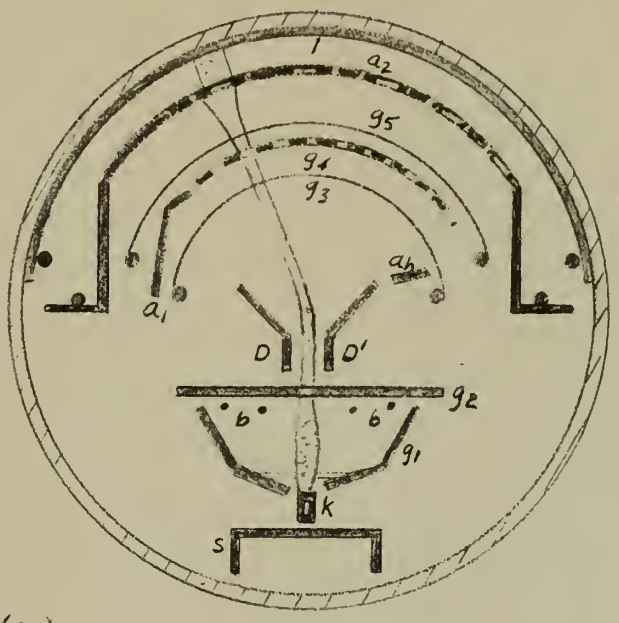

(a)

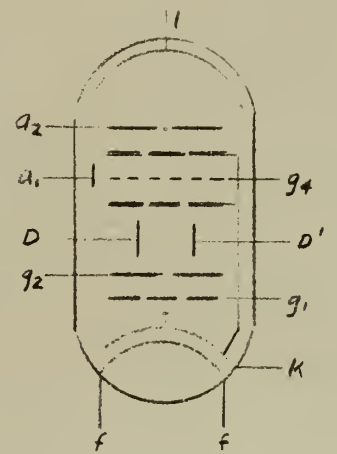

(b)

Fig.8. (a) Cross-Section of the E1T Counter Tube. (b) Diagram of the Electrode System. For Letter References See Text.

electrodes are designated as follows:

f	heater
k	cathode
s	screen
g_1	control grid
b	beam forming electrodes
g_2	accelerating electrode
D	left deflection electrode
D'	right deflection electrode
a_h	auxiliary anode
g_3, g_5	suppressor grids
g_4	slotted electrode
a_1	reset anode
a_2	anode
l	conducting layer coated with fluorescent material.

The heater f is mounted in a rectangular cathode k of relatively great height, the front of which is oxide-coated. This provides a narrow, ribbon-shaped beam, which is given the required shape by the action of control grid g_1, the internally connected beam-forming electrodes b, and the accelerating electrode g_2. The deflection of the beam takes place in the horizontal plane, requiring accurate alignment of the electrode system in only one dimension. Other advantages obtained by use of a ribbon-shaped beam are reduction of space-charge effects and current density, yet obtaining sufficient total beam current to provide rapid counting, and small values of interelectrode

capacitance due to the small physical dimensions of the electrodes. The maximum diameter of the ElT is 1.25 inches and maximum height is 2.15 inches.

The beam is shifted from its initial position at the extreme right (position zero) to the left by applying positive pulses to the left deflection electrode D or negative pulses to the right deflection electrode D'. The beam has ten stable positions, in each of which it passes through one of the ten apertures of the slotted electrode g_4. In each stable position some of the electrons also pass through one of the corresponding narrow slots in the anode a_2 and impinge on the fluorescent material lining the envelope of the tube, thus providing a luminous mark opposite the corresponding figure on the printed decal pasted on the outside of the glass envelope, even digits in the top row, and odd digits in the lower row.

When the beam is deflected beyond the last stable position (position nine) it strikes the reset anode a_1. The reset anode current pulse thus produced is made to trigger a reset circuit, by means of which the beam is reset to zero and a counting pulse is provided to the following decade stage.

The suppressor grids g_3 and g_5 and the screen s, which are internally connected to the cathode, serve to suppress any secondary emission from the slotted electrode g_4 and the anode a_2. The auxiliary anode a_h, which is internally connected to the accelerating electrode (and to B+), captures undesired stray electrons. The luminous screen is applied to a conducting layer 1, which is connected to B+ to remove the impinging electrons, thus preventing an accumulation of charge on the fluorescent screen.

Applying the electrode potentials shown in Figure 9, to the E1T, the static tube characteristic shown in Figure 10 is obtained. As $V_{D'}$, a_2 is decreased the beam is shifted toward the left. The undulating static characteristic curve is caused by the anode a_2 intercepting a large number of electrons as the beam strikes the portions of the anode between the ten slots, and a small number of electrons as the beam passes through the ten apertures. A horizontal slot in the bottom left portion of the slotted electrode g_4 causes an increase of anode current for positions of the beam to the left of the five position. With the assymetrical deflection used here ($V_{D'}$ = constant and $V_{D'}$ = variable) the beam is unavoidably defocused as it is deflected to the left. Therefore the apertures in g_4 are made wider for the positions corresponding to the higher digits.

Stability of the beam in each of the ten stable positions is accomplished by inserting a load resistor R_{a_2} of one megohm from the interconnected electrodes D' and a_2, to B+ (300 volts). The load line for this load resistor is indicated in Figure 10. The ten stable positions of the beam are the intersections of this load line with the positive-slope portions of the static characteristic curve. Point a is a stable position of the beam corresponding to digit zero, point c position one, point e position two, etc. Points b, d, f, r, s, and p are unstable positions of the beam due to the negative slope; if the beam is shifted to one of these positions it will return to the next stable position having a higher voltage level. If the beam tends to shift to the right of a stable point, such as point q, more of the

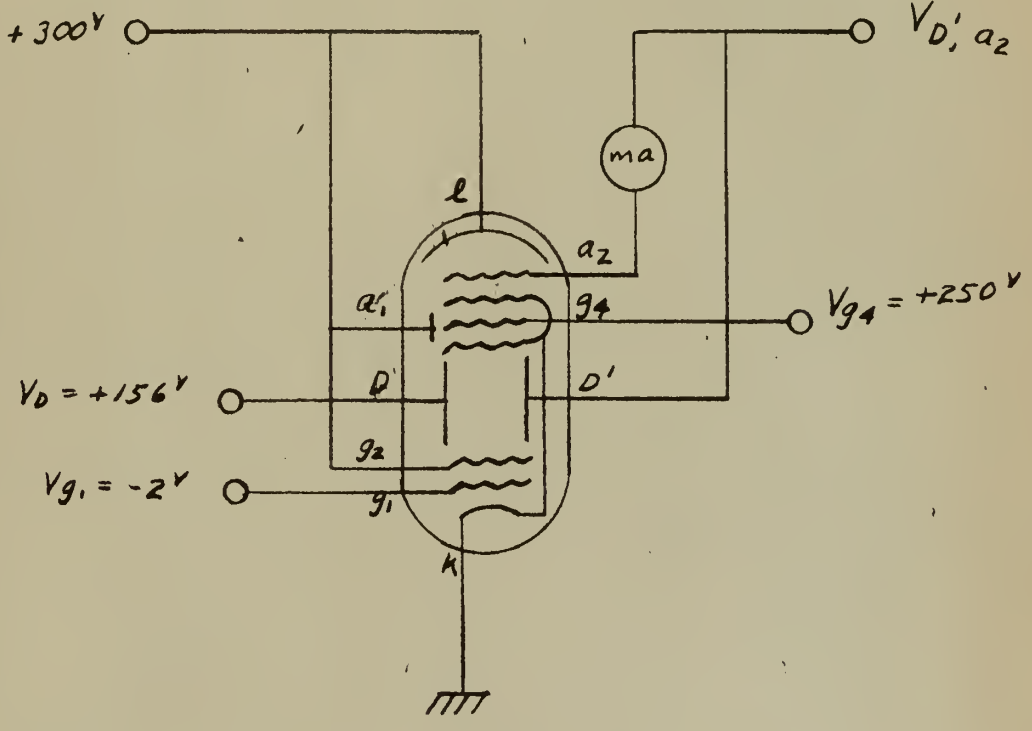

Fig. 9. Circuit for Measuring the $I_{a_2} = f(V_{D'a_2})$ Characteristic of the E1T

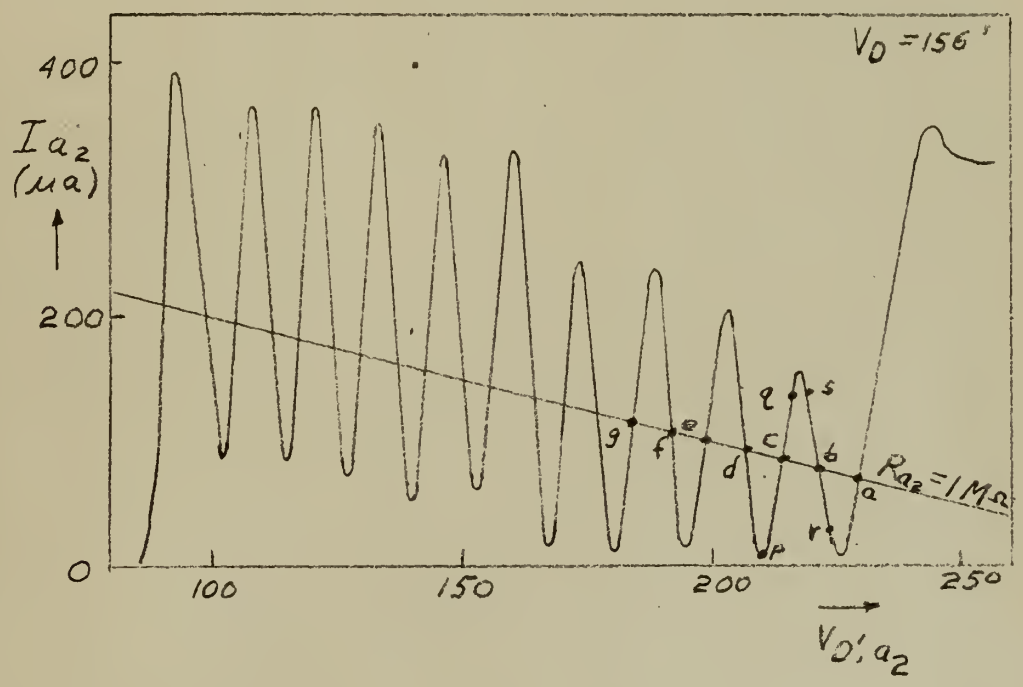

Fig. 10 E1T $I_{a_2} = f(V_{D'a_2})$ characteristic

beam will be intercepted by a_2, causing the potential of a_2 to decrease due to the increased current through R_{a_2}. Since the right deflection electrode D' is connected to a_2 its potential will also decrease by the same amount, deflecting the beam to the left, back to its stable position c.

In order to shift the beam from one stable point of operation to the next, positive pulses are applied to D or negative pulses to D', whose amplitude should be approximately equal to the voltage difference between two stable positions. When these pulses have a sufficiently short rise time, the voltage across R_{a_2} cannot follow them, due to the R-C time constant of R_{a_2} (one megohm) and the capacity that exists from D' and a_2 to all other electrodes, and stray and wiring capacitances (approximately 23 uuf.) Thus, for rise times of these stepping pulses of the order of one usec or less, the beam is displaced toward the left over a distance corresponding to the amplitude of the pulse. After the beam has been displaced to its new position, the stabilizing effect of the anode current flowing through R_{a_2} maintains the beam in its new stable position.

For resetting the beam to zero, a monostable multivibrator may be utilized, receiving its trigger from the negative pulse that occurs when the reset anode a_1 is struck by the electron beam. This multivibrator applies a negative pulse to g_1 of sufficient amplitude to cut the beam off completely, and of sufficient duration to allow V_{D', a_2} to rise from about 90 to 250 volts, at a rate governed by the R-C time constant at D' and a_2. Thus, the minimum reset time t for this method, which determines the maximum counting frequency, can be

calculated from:

$$E_{bb} - V_{a_2}(0) = E_{bb} - V_{a_2}(\text{reset})\ e^{\frac{-t}{R_{a_2} C_{max}}},$$

where E_{bb} = plate supply voltage (300 volts),

$V_{a_2}(0)$ = 240 volts,

$V_{a_2}(\text{reset})$ = 95 volts,

R_{a_2} = one megohm, and

C_{max} = 23 uuf.

This gives a value of t = 28.3 usec. Thus, a maximum counting frequency of 30 kc is readily obtainable by this method. Its advantage is that only one auxiliary tube (a twin triode) is required for the reset circuit.

The maximum counting frequency of the ElT may be increased to 100 kc by decreasing the reset time to 10 usec by connecting the cathode of the normally-conducting section of the monostable reset multivibrator to D' and a_2 as shown in Figure 11. When the beam of the ElT hits the reset anode, a negative pulse is applied to the grid of the normally-conducting triode V_2, cutting it off. The rise in plate voltage of this tube is transmitted to D' and a_2 of the ElT through V_1, which now acts as a cathode follower. Since $V_{D', a_2} \geq$ 90 volts, the plate voltage of V_2 between resets must be $\leq$ about 80 volts to render V_1 non-conducting. When V_1 conduts, the capacity C at D' and a_2 (interelectrode, wiring, stray, and cathode-to-ground capacity of V_1) is charged more rapidly than if the ElT were merely cut off allowing C to recharge through R_{a_2}. The negative-going pulse

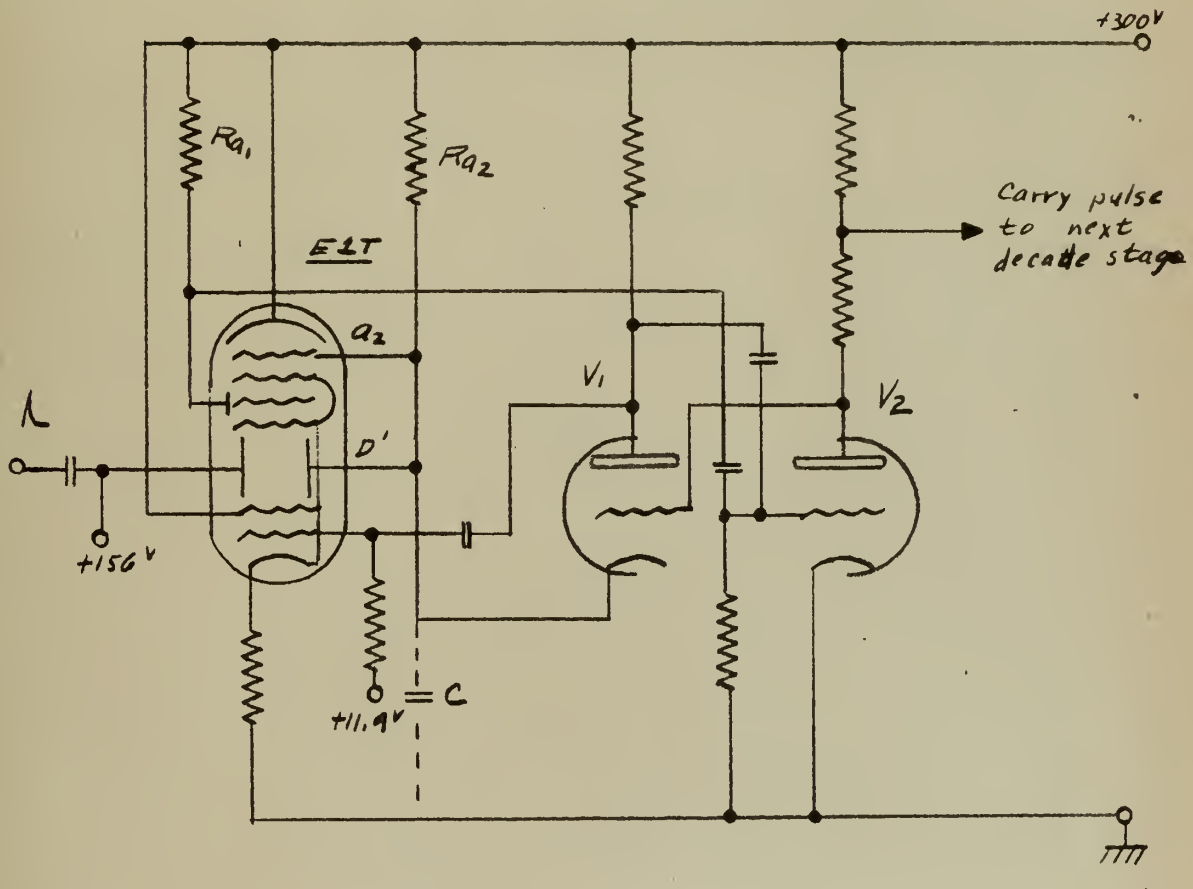

Fig. 11. E1T Decade Counter Tube and Monostable Multivibrator Reset Circuit

at the plate of V_1 is used both for blanking the ElT during reset and keeping V_2 cut off for the length of time required for $V_{D'}$, a_2 to rise from about 90 to 250 volts.

The disadvantages of such a circuit are high heater-to-cathode and grid-to-cathode voltages of V_1, and leakage current in V_1 causing an effective shunt in parallel with R_{a_2}. These disadvantages may be eliminated by installing a diode biased normally non-conducting between the multivibrator and the ElT.

A circuit for operating the ElT at frequencies up to 2.2 Mc is described in Appendix III.

CHAPTER III

DEVELOPMENT OF CIRCUITS USED IN INVESTIGATING THE HIGH-FREQUENCY RESPONSE OF THE ElT, AND EXPERIMENTAL RESULTS

1. Introduction.

This chapter will describe the work performed by the writer with the objective in mind of increasing the upper frequency limit of reliable counting operation of the ElT beyond the 2.2 Mc limit achieved by van Barneveld [3] in the circuit described in Appendix III.

Preliminary estimations were made of the minimum times required for the stepping and resetting operations of the ElT, using pulse generators. Reset circuits using a monostable multivibrator and/or R-C coupled pentodes were then tried, without success. Reset circuits utilizing a blocking oscillator are then described, which were used successfully throughout the remainder of the investigation. A one cps to one Mc square-wave generator and differentiating circuit were used as the input circuit until broad-band one cps to one Mc operation was accomplished, after which a 10 cps to 10 Mc sinusoidal oscillator, followed by a Schmitt trigger circuit was used as the input to the ElT circuit.

Several configurations of cascode amplifiers, as well as R-C coupled and pulse transformer coupled pentode amplifiers were tried in order to decrease the stepping time. Transformer coupling operated the best of the methods tried, giving a stepping time of 0.05 usec. A proposed modification to the R-C coupled stepping circuit used may equal or further reduce this stepping time.

The reset time was decreased to 0.3 usec by using a low value of reset anode resistance, R-C coupled pentode reset pulse amplifiers, and a pentode-triode parallel-triggered blocking oscillator with a three-winding pulse transformer.

2. Preliminary Estimation of the Minimum Time Required for the Stepping Operation.

The ElT tube and associated components were assembled as in Figure 12. A 6BC4 triode was used as the stepping or charging tube, using the technique described in Appendix III, Section 2. A Hewlett-Packard 212A Pulse Generator, providing pulses of 0.1 to 10 usec duration, and at pulse repetition frequencies up to five kc, furnished the input signal to the grid of the stepping tube. This pulse generator could be synchronized by a Hewlett-Packard 202A Low Frequency Function Generator, providing a square wave output at frequencies from 0.01 to 1200 cps. This is shown schematically in Figure 12. The amplitude and duration of the pulses applied to the grid of the stepping tube were examined on the oscilloscope at a p.r.f. of about five kc, then applied to the grid of the stepping tube at a slow enough p.r.f. to enable observation of the stepping of the ElT (three to eight pulses per second). By this technique, it was determined that all four of the available ElT's would step reliably with a stepping pulse applied to the grid of the stepping tube of 0.08 usec duration and 35 volts amplitude. The setting of the variable cathode resistor of the stepping tube was 15K.

The minimum pulse duration here was limited by the H. P. 212A to 0.08 usec. It is likely that the ElT would step with a shorter stepping

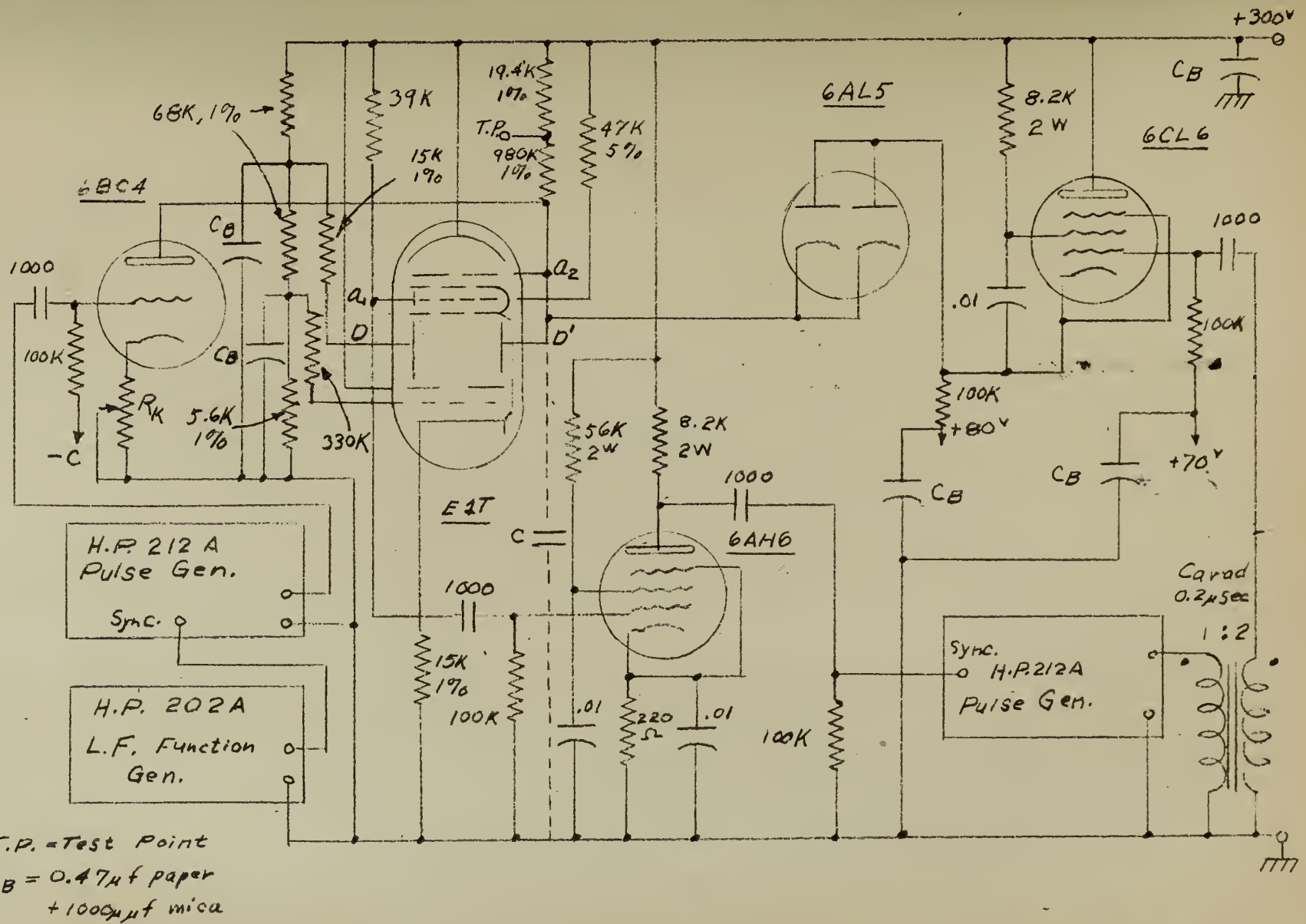

Fig. 12. Circuit for Estimating Minimum Stepping and Reset Times of the E1T.

pulse duration than this, since it is a vacuum tube, and, from Appendix V, the maximum transit time of electrons in the electrostatic fields from cathode to fluorescent screen is approximately 4.7 musec.

3. Preliminary Estimation of the Minimum Time Required for the Resetting Operation.

As explained in Chapter II, the maximum frequency for counting regularly recurring pulses will be determined by the length of time required to reset the ElT from nine to zero. The circuit described in Appendix III, Section 3 accomplishes this reset operation in 0.45 usec.

In order to determine the minimum time in which this reset operation can be accomplished, the circuit of Figure 12 was utilized. After the electron beam in the tube is advanced past the nine position, the reset anode is struck, providing a negative pulse at this anode. This negative reset pulse, approximately two volts in amplitude, was amplified by a 6AH6 pentode, the amplified reset pulse synchronizing a second H.P. 212A Pulse Generator. The output pulse from the second H.P. 212A, of approximately +175 volts amplitude and 0.2 usec duration, was then applied to the grid of a 6CL6 pentode through a 2:1 stepup pulse transformer, raising the pulse amplitude to about 300 volts. The cathode of the 6CL6 was connected, through a 6AL5 double diode, to D' and a_2 of the ElT, in a similar manner to that of the monostable flip-flop circuit described in Chapter II, Section 4. Both the 6CL6 and the 6AL5 were biased non-conducting between reset pulses.

For pulse durations of less than 0.2 usec, the amplitude of the pulse furnished by the H.P. 212A reset pulse generator decreased rapidly,

providing insufficient amplitude to reset the E1T to zero. Again, it is likely that the E1T can reset in less time than the duration of the pulse used here, for the same reason, i.e., it is a vacuum tube.

4. Reset Circuits Utilizing a Monostable Multivibrator, and/or Resistance-Capacity-Coupled Pentodes.

Initially, a circuit similar to that of Figure 11 was utilized to accomplish the resetting operation of the E1T, using a 6CL6 pentode in place of triode V_1 of Figure 11*, since the cathode of the 6CL6 is connected directly to deflecting plate D' of the E1T, whose potential varies from about +90 to +250 volts during normal operation, it was necessary to provide an isolating filament transformer for this tube, with its center tap connected to a +170 volt tap on a voltage divider. This reduced the maximum heater-to-cathode voltage to about ± 80 volts, which is near the maximum rated value for the 6CL6 of ± 90 volts. This reset circuit reset the E1T to two, the positive pulse at the plate of the 6CB6 being insufficient in amplitude to reset the E1T to zero.

The two salient disadvantages of the above circuit, i.e., severe strain on the heater-to-cathode insulation and in additional isolation transformer for the 6CL6 heater, were both eliminated by installing a biased 6AL5 double diode between the 6CL6 cathode and the E1T right deflecting plate, as shown in Figure 12.

Replacing the 6CB6 with a 6AQ5 did not increase the amplitude of the positive pulse applied to the grid of the 6CL6 sufficiently to reset the E1T to zero.

*and a 6CB6 pentode in place of the normally conducting triode V_2 of Figure 11.

Amplifying the reset pulse from the reset anode by means of two stages of resistance-capacity coupled 6AH6 pentodes, with interstage differentiation of the pulse, and followed by a 6CB6 pentode amplifier, also failed to provide a sufficiently large positive pulse to the grid of the 6CL6 to reset the ElT to zero. It is relatively easy to obtain a negative pulse of large amplitude at the plate of a miniature receiving-type pentode, but rather difficult to obtain a positive pulse of 175 volts or so, particularly when pulses of less than half a usec duration are sought. A 2:1 step-up pulse transformer for amplifying and inverting the negative pulse would have been of assistance here, had the writer been aware of the existance of such transformers capable of handling pulses of the order of half a usec or less. (The circuits described in this section were attempted prior to the estimation of the minimum reset time described in Section 3.)

5. Reset Circuits Using a Blocking Oscillator.

Some theoretical considerations on the parallel-triggered blocking oscillator are included in Appendix IV. The parallel-triggered blocking oscillator shown in Figure 13, using a 6BQ7A twin triode, provided a plate pulse of -150 volts, 0.2 usec duration. The pulse transformer T_1 was a Carad type 60S, having a ferrite core, a 1:1 winding, and was encased in plastic. The germanium diode clipped positive transient oscillations which occurred after the -150 volt pulse.

Considering the possibility that the ElT may ultimately operate at a frequency of ten megacycles, it would be necessary that the reset blocking oscillator fire every usec. Reducing the recovery time of a blocking oscillator can be accomplished by reducing the coupling

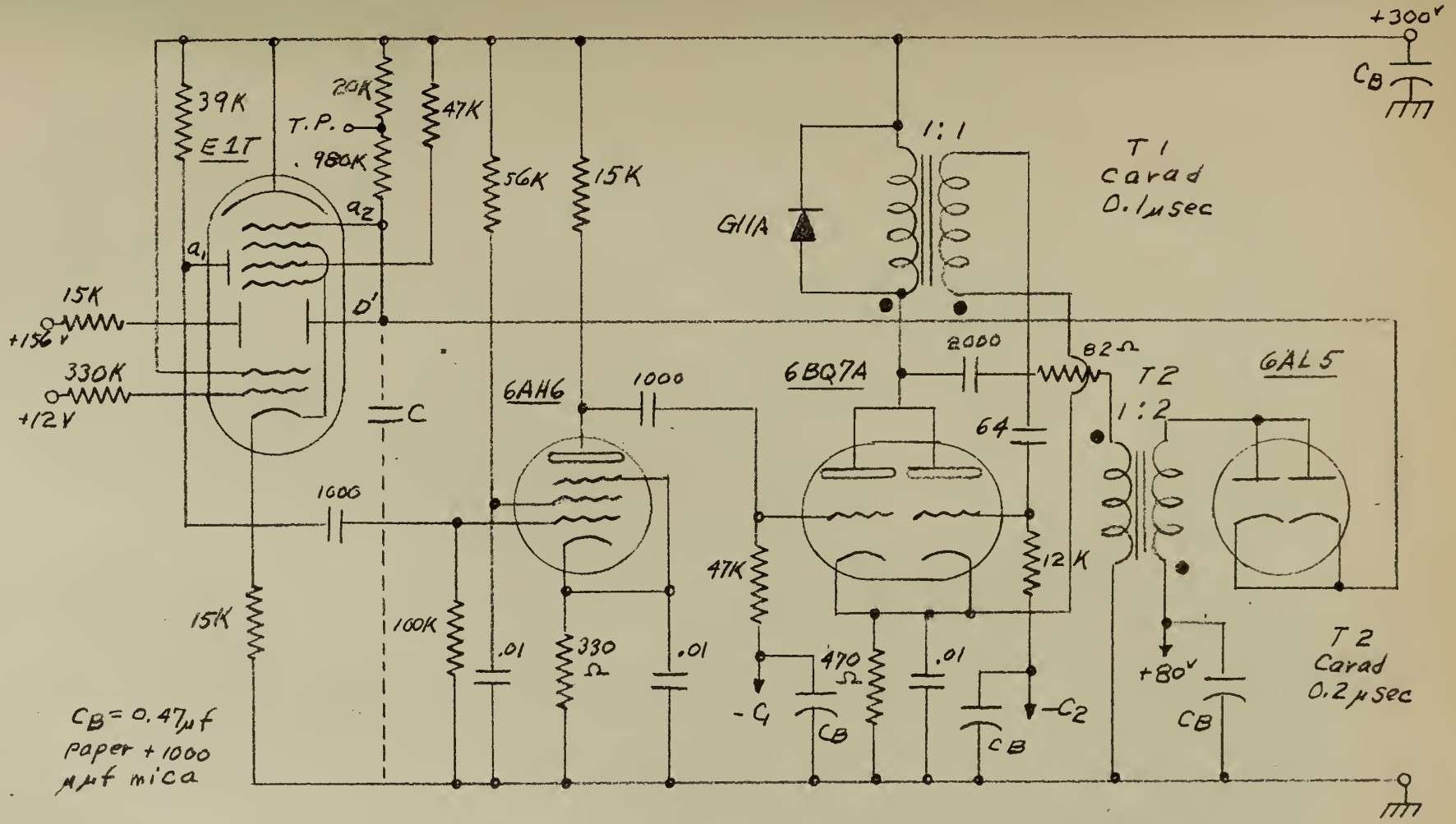

Fig. 13. E1T Reset Circuit Using a Parallel-Triggered Blocking Oscillator and Biased Diode

capacitor and/or grid resistor in Figure 13, providing they are not reduced to such low values that the circuit is unstable.

For Cg = 37 uuf and Rg = 2K, the recovery time of the blocking oscillator circuit of Figure 13 was about three usec. At two usec after the pulse, the grid voltage had recovered to 20 volts below its quiescent bias level and could have been triggered again at that time, since the positive grid pulse was about 50 volts. This corresponds to a maximum ElT counting frequency of five Mc.

For Cg = 27 uuf and slightly less bias, the blocking oscillator grid recovered to about 20 volts below its quiescent level in one usec, permitting a maximum ElT counting frequency of ten Mc. However, the amplitude of the negative plate pulse had decreased to 120 volts.

Decreasing Rg and Cg also caused a slight decrease in the pulse duration of the plate pulse from 0.2 to 0.15 usec, confirming qualitatively the theoretical prediction of equation (7) of Appendix IV.

An attempt was made to increase the amplitude of the negative plate pulse by increasing the plate current, using both halves of the 6BQ7A twin triode in parallel as the blocking oscillator, and parallel-triggering this tube with a 6J6 twin triode, also parallel-connected. Since the plate capacity to be driven was approximately doubled, this attempt provided no significant increase in the plate pulse amplitude.

For resetting the ElT to zero, a positive pulse of at least 160 volts is required at the right deflecting plate. For inverting the phase and increasing the amplitude of the plate pulse of the blocking oscillator, a second Carad type 60S pulse transformer T_2 (0.2 usec) was used, with three equal windings on a ferrite core. Two of the windings were

connected together to form a two-to-one step-up transformer. The primary of this transformer was capacitively coupled to the plate of the blocking oscillator, and the secondary was connected from the plates of the 6AL5 double diode to a positive bias of about 80 volts. All three windings of this transformer were wound with the same polarity (dots at the same end of each winding). Since a phase inversion was required, it was necessary to connect one of the secondary leads adjacent to the primary input lead to a.c. ground. The capacity existing between these two leads, due to their close proximity, resulted in the output pulse from the secondary of the step-up pulse transformer being somewhat attenuated to less than twice the amplitude of the plate pulse.

The 6BQ7A twin triode was replaced with a 5687 twin triode, providing greater plate current as the grid is driven positive during the pulse. This tube and transformer combination produced an output pulse at the secondary of the step-up pulse transformer of 300 volts, 0.25 usec when the transformer was disconnected from the 6AL5 diode, and 175 volts, 0.25 usec with the transformer connected to the diode through an 82 ohm parasitic suppressing resistor. This reset the E1T to zero reliably.

6. Development of Circuits for High-Frequency Operation of the E1T.

This section will describe, in approximately the chronological order of use, the circuits utilized to attempt to determine the upper frequency limit of reliable counting of the E1T. Reliable counting of the E1T is defined as ten steps per reset, and is observed on an oscilloscope as a steady "staircase" waveform of approximately 160 volts amplitude at the right deflecting plate of the E1T. The steps

corresponding to lower digits are greater in amplitude than those corresponding to the higher digits, as described in Appendix III.

A. Input circuit.

Referring to Figure 12, the H.P. 202A -- H.P. 212A pulse generating equipment used for low frequency checking of the stepping and reset times was replaced with a H.P. 211A Square Wave Generator, providing a square wave output of approximately 60 volts amplitude at frequencies from one cps to one Mc. This square wave was differentiated by a 15 uuf and 2K R-C network, amplified by a 6AH6 pentode, and R-C coupled to the grid of the 6BC4 stepping triode. The remainder of the stepping circuit was the same as in Figure 12, and the reset circuit was the same as in Figure 13, using a 5687 twin triode as the blocking oscillator tube.

B. Cascode amplifier stepping circuits.

By observing the negative pulse occuring at the reset anode of the E1T, with the reset circuit disabled, it was found that a small positive pulse occured at the initial time of the reset pulse, followed by the negative swing of the reset pulse. The duration of this small positive pulse increased with frequency over the 100-500 kc. frequency range, being about 0.18 usec long at f = 460 kc. This initial time delay before the reset anode waveform swings negative would limit the upper counting frequency of the E1T if it were not eliminated.

Believing this small positive pulse at the beginning of the reset pulse to be caused by capacitive coupling from grid to plate through the amplified grid-to-plate capacity of the stepping tube (Miller effect), various configurations of a cascode amplifier (shown in Figure 14) were tried in order to eliminate it. A cascode amplifier was chosen in order to reduce the grid-to-plate capacity by inserting two more

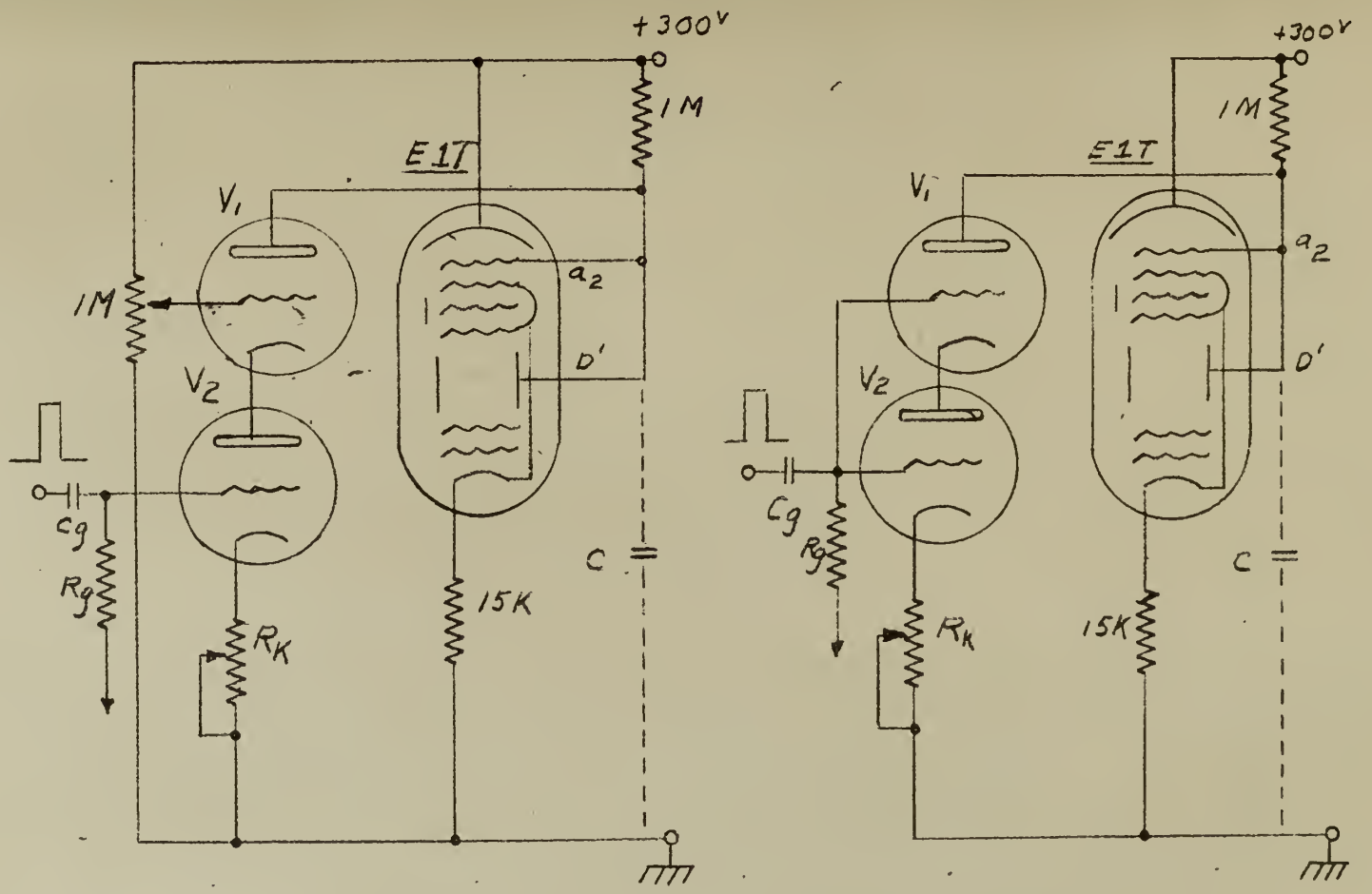

Fig. 14. Cascode Amplifiers Used to Step the E1T

electrodes between the input grid and output plate, yet retaining the transfer characteristics of a triode to provide a stepping pulse that decreased in amplitude as the plate voltage ($V_{D'}$, a_2) decreased, as explained in Appendix III.

From the Radiotron Designer's Handbook [6], Section 12.9, the amplification of V_2 of Figure 14 is given by:

$$A' = \frac{\mu R_L}{r_p + \frac{r_p + R_L}{\mu + 1}} \tag{1}$$

where $\frac{r_p + R_L}{\mu + 1}$ is the load into which V_2 works. Dividing by uR_L,

$$A' = \frac{1}{\frac{1}{g_m R_L} + \frac{r_p + R_L}{R_L} \cdot \frac{1}{\mu(\mu+1)}} \tag{2}$$

Equation (2) may be compared with the ordinary form for expressing amplification:

$$A = \frac{1}{\frac{1}{g_m R_L} + \frac{1}{\mu}} \tag{3}$$

Therefore, from equation (2), the composite characteristics of a cascode amplifiers, u', g_m', and r_p' are:

$$\mu' = \frac{\mu(\mu+1) R_L}{r_p + R_L} \tag{4}$$

$$g_m' = g_m$$

$$r_p' = \frac{\mu'}{g_m'} = (\mu+1) \frac{r_p R_L}{r_p + R_L} \tag{5}$$

This predicts that A' of a cascode amplifier should be considerably greater than A of a single triode, for $R_L \gg r_p$. This predicted increase in amplification of the cascode amplifier over that of a single triode was not observed in the application considered here, for the following reasons:

(a) The load driven by the cascode amplifier was not the one megohm resistor from D' and a_2 of the ElT to B+, but rather the inter-electrode, stray and wiring capacitances existing at D' and a_2, the output capacity of the cascode amplifier, and the cathode-to-ground capacity of the 6AL5 reset diode of Figure 13.

(b) Degeneration caused by the unbypassed cathode resistor of the cascode amplifier.

In fact the amplitude of the stepping pulses observed at the plate of the cascode amplifiers was less than that for a single triode, given the same values of bias and stepping pulse amplitude applied to the grid. This was true for all triodes used in the cascode stepping amplifier: 6BC4, 6BQ7A, 12AT7, and 5687. However, by increasing the pulse amplitude at the cascode grids, and/or decreasing the bias, these tubes operated satisfactorily as stepping cascode amplifiers at counting frequencies up to one megacycle. However, using the cascode amplifier stepping circuit, no one combination of the variable parameters (cascode bias, cascode grid pulse amplitude, cascode cathode resistance, blocking oscillator bias, and reset diode bias) was found that would given reliable counting of the ElT over a broad frequency band such as one cps to one Mc.

C.

Broad-band (one cps to one Mc) reliable counting was accomplished using R-C coupling from the 6AH6 stepping pulse amplifier to a 5687 triode (both halves in parallel), and using a parallel-triggered 5687 blocking oscillator with both grids tied together for resetting, for the following values of the variable parameters:

Step tube bias - 50 volts

Step pulse amplitude at grid of step tube - +56 volts

Step tube cathode resistance - 7.8K

Blocking oscillator bias - 48 volts

Blocking oscillator feedback capacitor - 64 uuf

Reset diode bias - +56 volts

The total reset time was 0.8 usec; 0.2 usec for the positive-going pulse, 0.4 usec for the step time, and 0.2 usec for the reset time. The above values of the variable parameters were change only slightly by changing the cathode resistance of the step tube from 7.8K on a 20K potentiometer to an 8.2K, 2 watt, 10% resistor. The circuit operated the same with the 15K, 1% resistor from the left deflection plate of the E1T to the +156 volt tap on the voltage divider either in the circuit or shorted out.

D. Transformer-coupled stepping circuit.

In order to improve the frequency response of the E1T to frequencies much in excess one Mc, it was now necessary to reduce the stepping time to considerably less than 0.4 usec, and to eliminate the 0.2 usec time delay caused by the positive-going pulse that occurred at the plate of the stepping tube prior to the negative-going step. Transformer coupling of the stepping pulse to the grid of the step tube was therefore attempted in order to eliminate this positive pulse by neutralization, as shown in Figure 15. This type of neutralizing circuit is used in radio receivers employing automatic volume control, and requiring an A.V.C. bypass capacitor from the bottom of the transformer secondary to ground. In such a circuit, from Radiotron Designer's Handbook [6], Section 26.8,

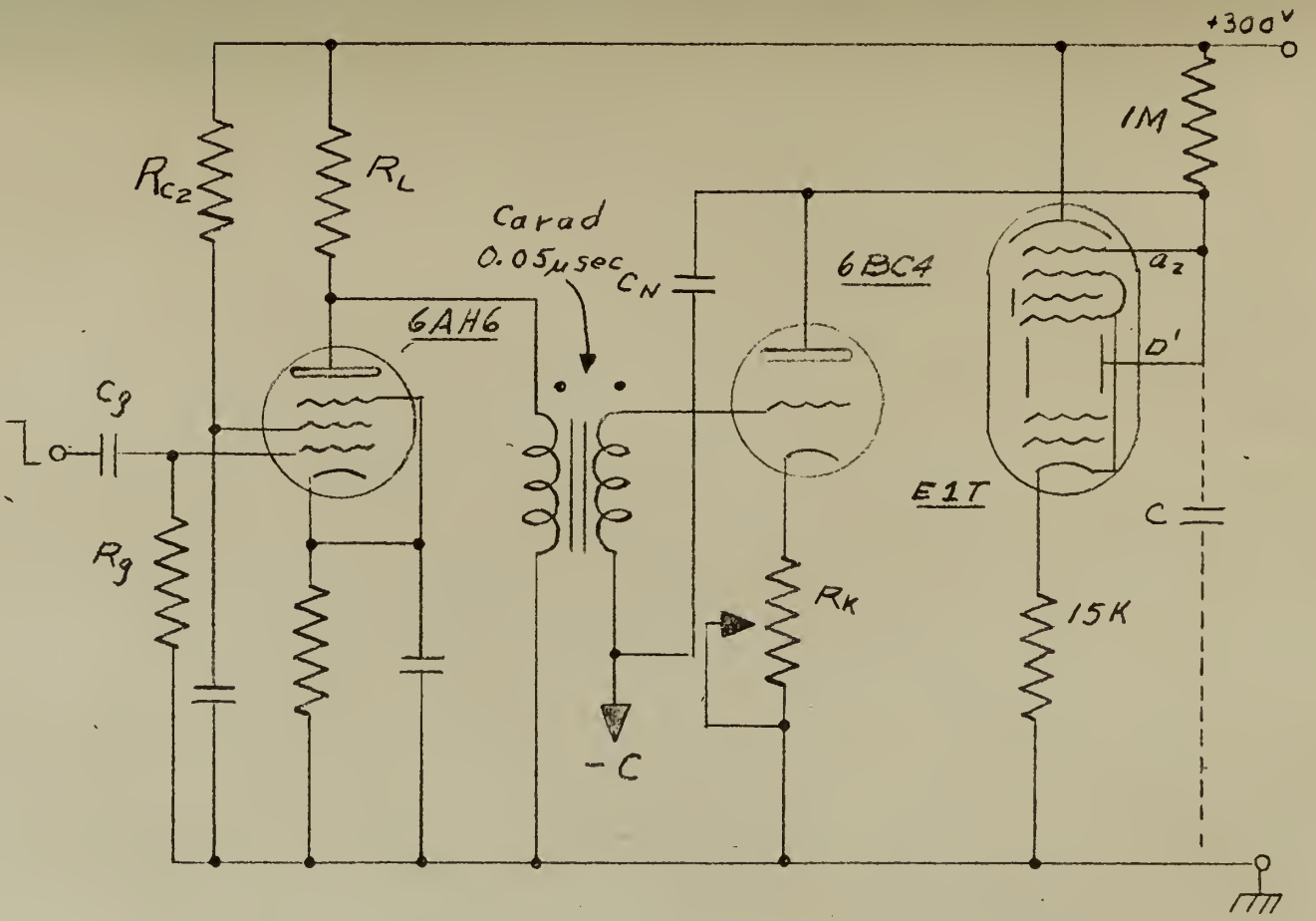

Fig. 15. Transformer-Coupled Stepping Pulse Amplifier and Stepping Triode

$$C_N = \frac{C_{gp}}{C_{gk}} C ,$$

where C_N is the neutralizing capacitance required, C the A.V.C. bypass capacitance, C_{gp} the total grid-to-plate capacitance including strays, and C_{gk} the total grid-to-cathode capacitance including strays. Since C is zero in the case of the stepping tube application (no A.V.C. bypass capacitor required), C_N also is equal to zero, and the circuit is automatically neutralized. The transformer used for this coupling was a Carad 0.05 usec pulse transformer. This technique completely eliminated the positive pulse that formerly occurred at the beginning of the stepping pulse observed at the plate of the stepping tube, and at the beginning of the reset pulse.

Eliminating the coupling capacitor from the stepping pulse amplifier (6AH6) to the stepping triode (6BC4) by means of transformer coupling eliminated the positive-going pulse at the beginning of the negative stepping waveform at the stepping triode plate. This indicates that this initial positive pulse must have been caused by grid current in the stepping triode charging the coupling capacity during the stepping pulse, which then discharged exponentially through the grid resistor between pulses.

Reducing this coupling capacitor from 1800 uuf to 100 uuf in the R-C coupled circuit practically eliminated the positive pulse at the beginning of the stepping time, which also bears out the above conclusion that it must have been due to grid current.

E. Input and stepping circuits at frequencies above one Mc.

In order to test the circuit at frequencies above one Mc, an H.P.

650A Test Oscillator was used, providing a sin wave output of up to three volts amplitude, and at frequencies from ten cps to ten Mc. It was thus necessary to abandon the input differentiating circuit used with the H.P. 211A Square Wave Generator. A Schmitt trigger circuit was employed here to provide a square wave output for a sin wave input.

Figure 16 shows schematically the Schmitt trigger circuit and amplitude discriminator used, which is a standard H.P. plug-in unit used in several H.P. frequency counters. V1A (1/2 5693) is an amplifier with a gain of one. V1B (1/2 5693) is an amplitude discriminator, the triggering level of the Schmitt trigger circuit (V2 and V3) being determined by the setting of the bias potentiometer connected to pin three of the octal socket. V2 is normally conducting, with a plate current of ten milliamperes, and V3 is biased non-conducting. A negative input to V1A of sufficient amplitude to overcome the triggering level at the grid of V1B appears at the grid of V2 as a negative excursion, cutting V2 off. The plate of V2 rises and V3 conducts. The cathode of V3 follows its grid, raising the cathode potential of V2, thus accelerating the switching action. V3 remains conducting until a positive input to V1A (and V2) causes V2 to conduct again and the original stable state is obtained. The plate load impedance of V3 is arbitrary. In this case a Doba network (Moskowitz and Racker [7], Article 4.3, p. 130) was selected as the plate load impedance, with a resistance of about 500 ohms in series with a 2.2 uh inductance, the inductance being paralleled by a 50 uuf capacitor. This provided a negative step-function of five volts amplitude with a rise time of 0.05 usec at the plate of V_3 for frequencies up to about four Mc. For frequencies above about four Mc, the square wave becomes increasingly sinusoidal.

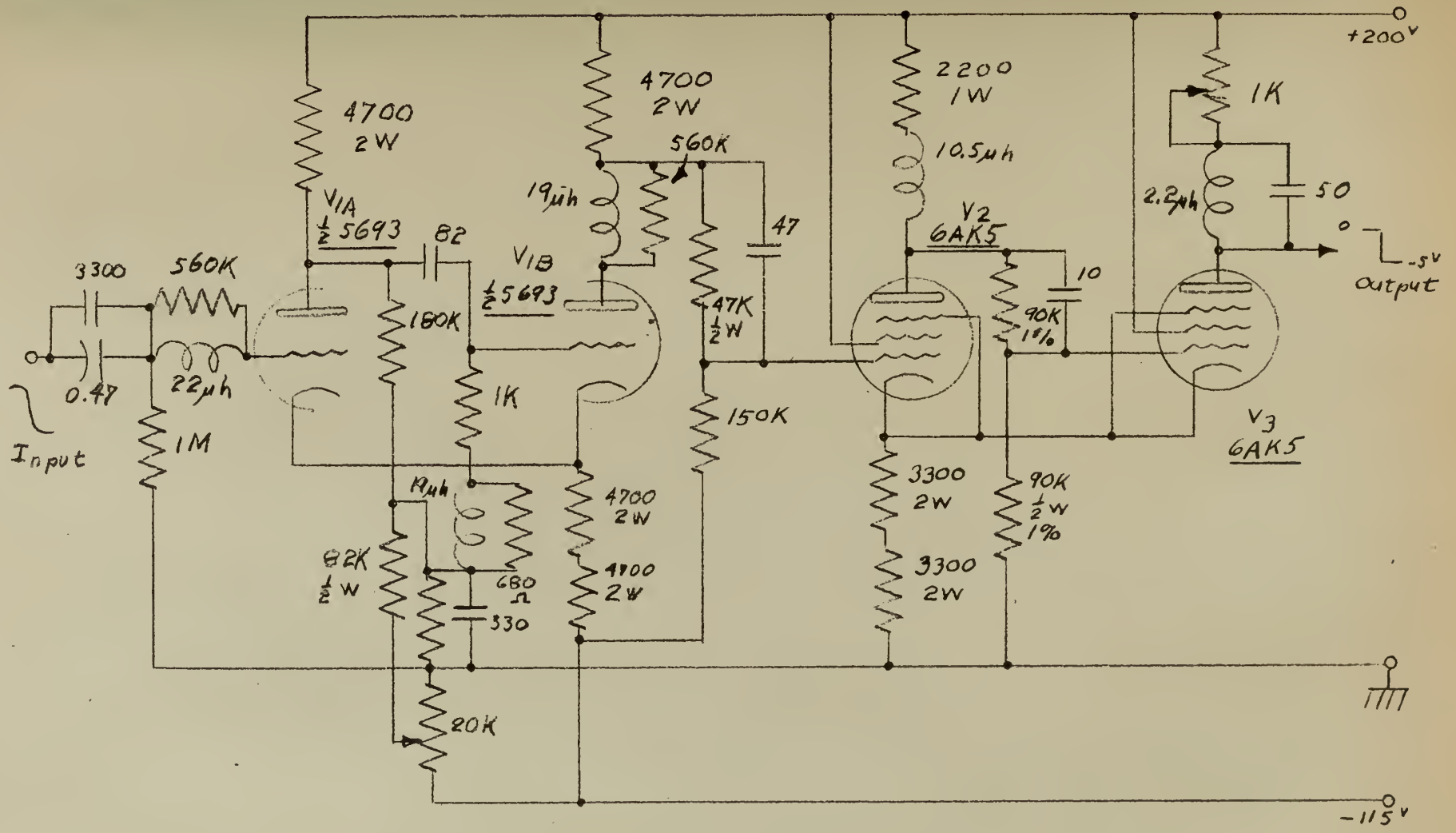

Fig. 16. Schematic Diagram of Schmitt Trigger Plug-in Unit

This negative step-function output from the Schmitt trigger circuit was then amplified and inverted by a 6AH6 pentode, as shown in Figure 17. The plate load of the 6AH6 consisted of the primary of a Carad 0.05 usec pulse transformer, in series with a 33K current-limiting resistor, decoupled to ground. At the secondary of the pulse transformer a positive pulse of 12 volts amplitude and 0.1 usec duration occurred, which was applied to the grid of the stepping triode (1/2 of a 12AT7). Using this circuit for stepping the E1T, a stepping time of 0.05 usec was achieved.

R-C coupling from the 6AH6 stepping amplifier to the 12AT7 step tube was also tried, as shown in Figure 18, providing a positive step-function of approximately 60 volts amplitude and 0.05 usec rise time at the grid of the 12AT7 step tube. (A stepping time of considerably less than 0.05 usec could probably have been achieved here, by clamping the plate swing of the 6AH6 to about 15 volts in the high-g_m portion of its plate characteristics.) The E1T stepped properly using this technique (square waves instead of short pulses) due to the stability of the beam in its ten stable positions. However, the plate waveform of the 12AT7 initially went positive for about 0.05 usec prior to the negative step, as was observed before when using R-C coupling to the step tube. A grid-current limiting resistor at the grid of the 12AT7 step tube probably would have eliminated or greatly reduced this time delay.

F. Decreasing the reset time.

Having decreased the stepping time to 0.05 usec, it was next necessary to decrease the reset time in order to extend the upper counting frequency limit. By observing the waveform at the reset anode, with the reset circuit disabled, it was determined that the R-C transient decay after the

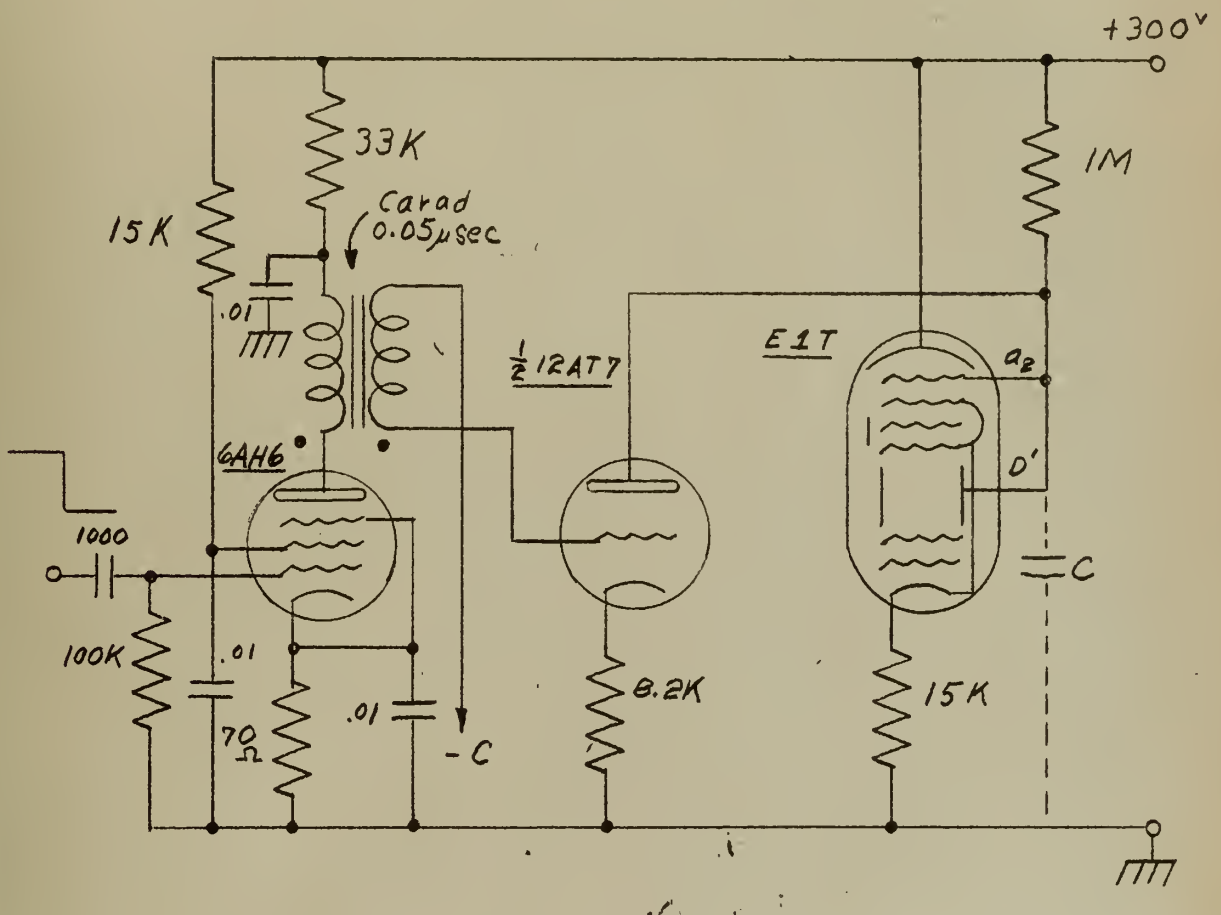

Fig. 17. Transformer-Coupled Stepping Circuit

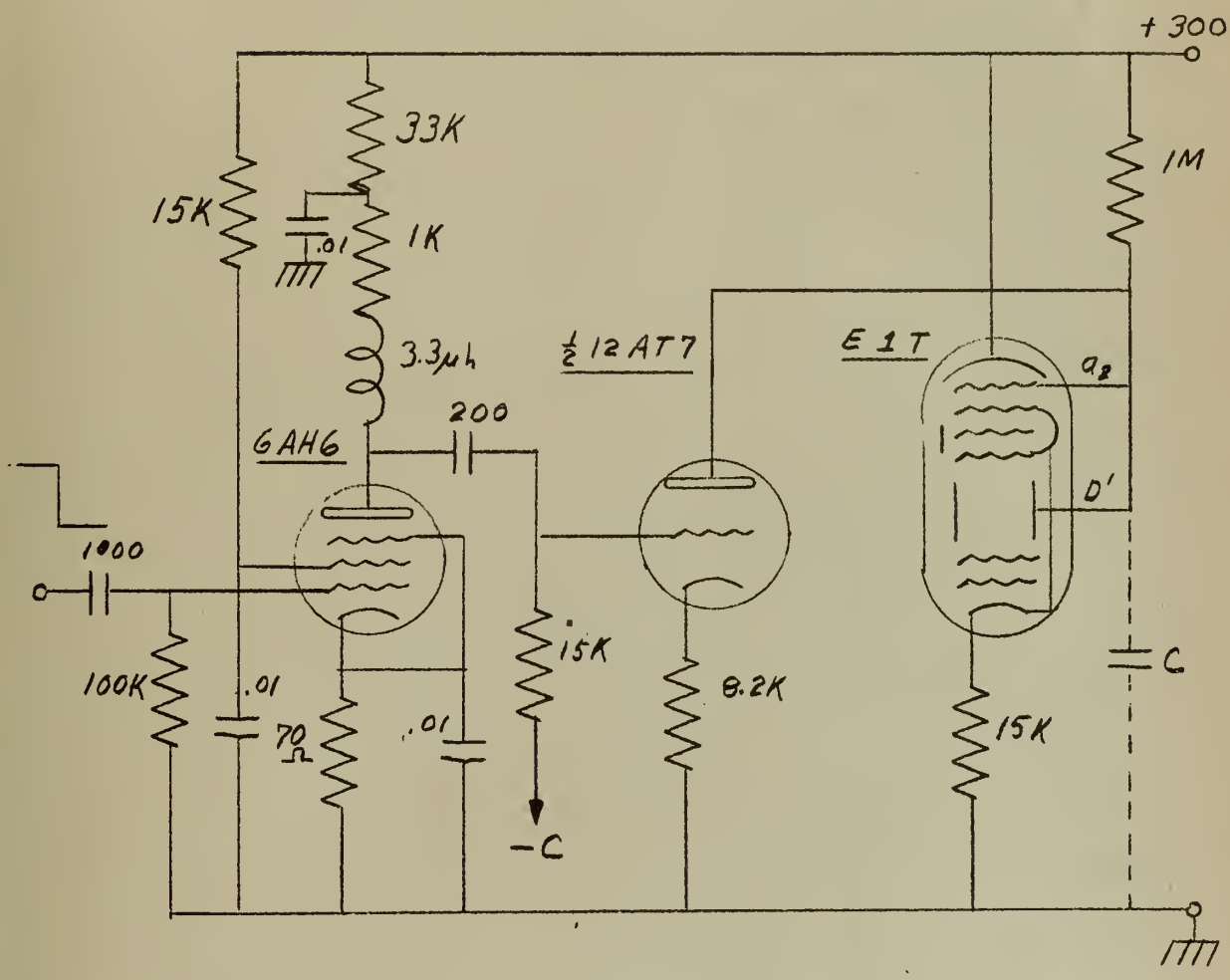

Fig. 18. R-C Coupled Stepping Circuit

reset anode was struck by the electron beam lasted approximately two usec when the resistance from the reset anode to B+ was 39K. The amplitude of this negative pulse was about six volts. Decreasing this reset anode load resistor to 500 ohms decreased the R-C transient decay time to about 0.1 usec, while decreasing the amplitude of the negative reset pulse to about 0.2 volts. This negative reset pulse was capacitively coupled through an RG-55/U coaxial cable to the grid of the first of three 6BH6 pentode reset pulse amplifiers, as shown in Figure 19. Three reset pulse amplifiers were necessary because of the small input signal to the first amplifier, the low values of AC plate load resistances (in order to maintain the fast rise time of the reset pulse), and to obtain the proper polarity (positive) of the reset trigger pulse applied to the grid of the trigger tube of the parallel-triggered blocking oscillator. Plate decoupling capacitors were utilized in all three reset pulse amplifiers in order to establish the DC operating point of the amplifier at an optimum point on its plate characteristics.

Using a 5687 twin triode as the blocking oscillator and parallel trigger tube, it was observed that a 0.3 usec delay occurred between the time that the trigger tube was triggered and the blocking oscillator fired. Reasoning that this delay must have been caused by Miller effect in the 5687 triode, a 6AW8 sharp cutoff pentode - high mu triode was substituted for the 5687, using the pentode section as the trigger tube and the triode section as the blocking oscillator, as shown in Figure 20. Using this technique the time delay between the application of a positive pulse to the trigger tube and the blocking oscillator firing was about 0.05 usec. The total reset time was 0.3 usec (0.05 usec for the nine-to-reset anode step, 0.05 used delay, and 0.2 usec blocking

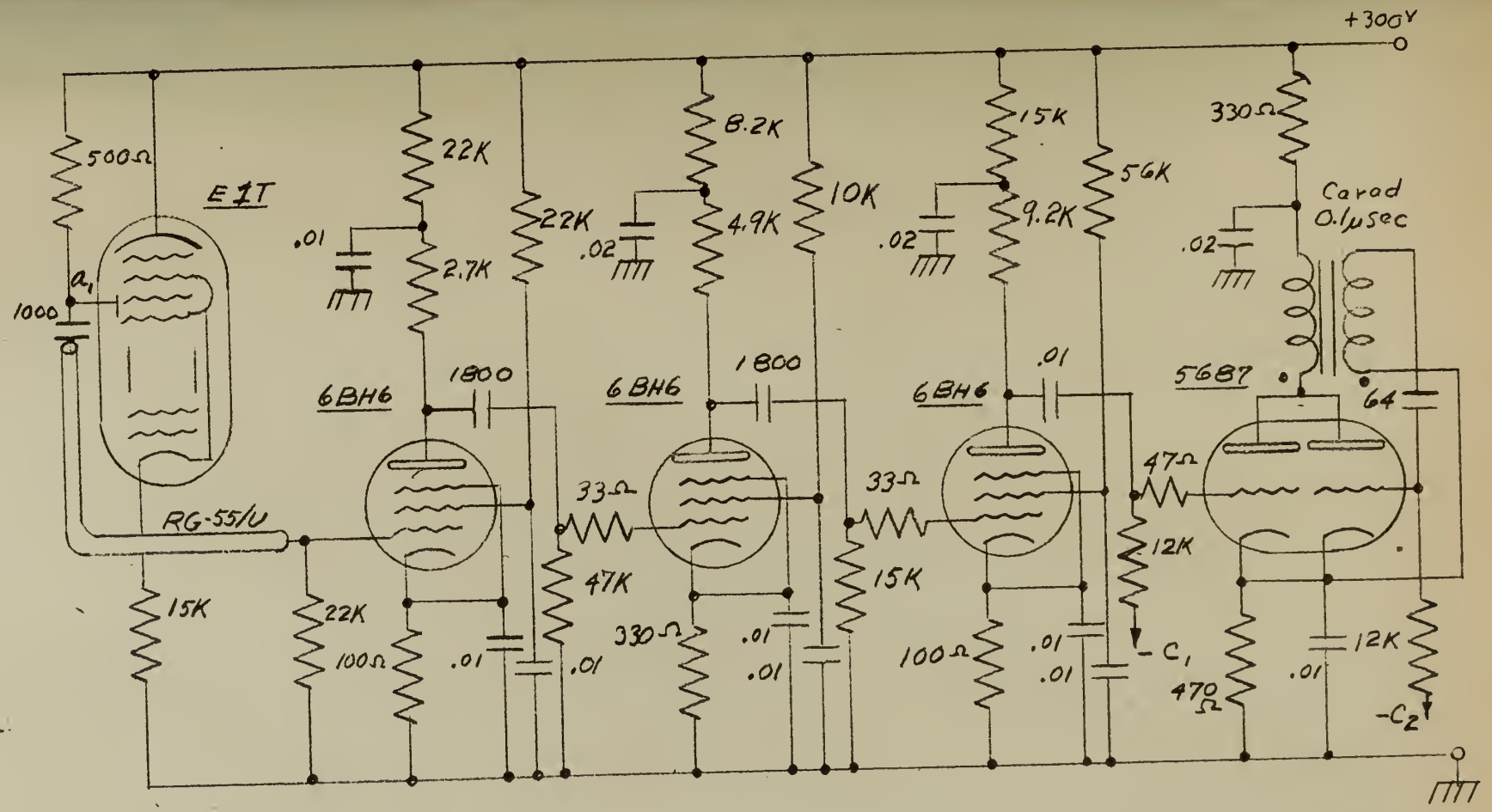

Fig. 19. Three-Stage R-C Coupled Reset Pulse Amplifier and Blocking Oscillator

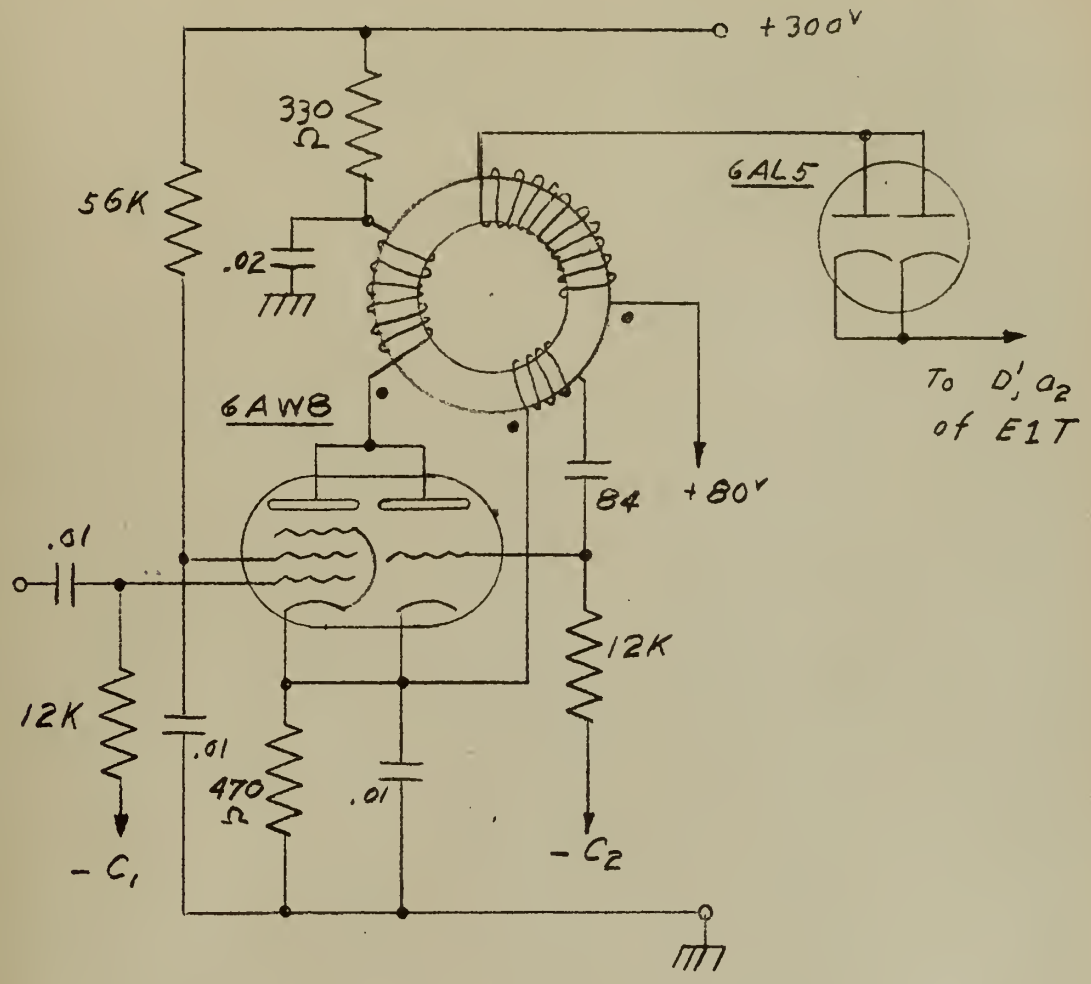

Fig. 20. Reset Blocking Oscillator Using a 6AW8 Triode-Pentode and Three-Winding Pulse Transformer

oscillator pulse). This corresponds to an upper counting frequency of about 3.3 Mc (with zero counting loss) for regularly recurring pulses. Above this frequency counting will be less accurate as the frequency increases, due to more than one pulse arriving during the reset period, and not being counted.

For counting of random pulses, from Appendix II:

τ_s = 0.05 usec,

τ_r = 0.3 usec,

$\tau_m = 0.9\tau_s + 0.1\tau_r = 0.045 + 0.03 = 0.075$ usec

Accepting a counting loss of 1%, $n = \frac{1}{11\tau_m}$ = 133 kc, which is an improvement by a factor of more than three over that obtainable using the circuit of Appendix III.

The method of coupling the blocking oscillator plate pulse to the E1T shown in Figure 13 requires two pulse transformers, at a cost of about $5.00 each. Therefore, this circuit was modified as shown in Figure 20. Three windings were wound on a Ferramic H 3/8" ferrite torroidal core, using #34 wire: 20 turns on the primary winding, 10 turns on the grid feedback winding, and 40 turns on the third winding to invert and increase the amplitude of the reset pulse for application to D' and a_2 of the E1T through the 6AL5 reset diode. This provided a pulse at the plate of the 6AL5 reset diode of +160 volts, 0.1 usec duration. The 330 ohm resistor in series with the plate winding of the transformer (decoupled to ground) was inserted to keep the blocking oscillator plate pulse out of the power supply.

Figures 16, 17, 19, and 20 combined show the final circuit of this investigation.

In an attempt to reduce the reset time below 0.3 usec, the circuit of Figure 21 was utilized. The 6AW8 triode-pentode operates as a parallel-triggered blocking oscillator, as before. The positive blocking oscillator pulse is taken from the triode cathode, amplified by the 6AH6, inverted and applied to the 6AL5 reset diode plates. T_1 was a Ferramic S-2 ferrite core. In order to provide sufficient positive feedback to the blocking oscillator grid, 16 turns on the primary winding and eight turns on the secondary winding T_1 were required. This resulted in a pulse at the cathode of the blocking oscillator of about 0.15 usec duration and 10 volts amplitude. This was comparable to the duration and rise time of the blocking oscillator pulse previously obtained with the circuit of Figure 20, so the circuit was not investigated further.

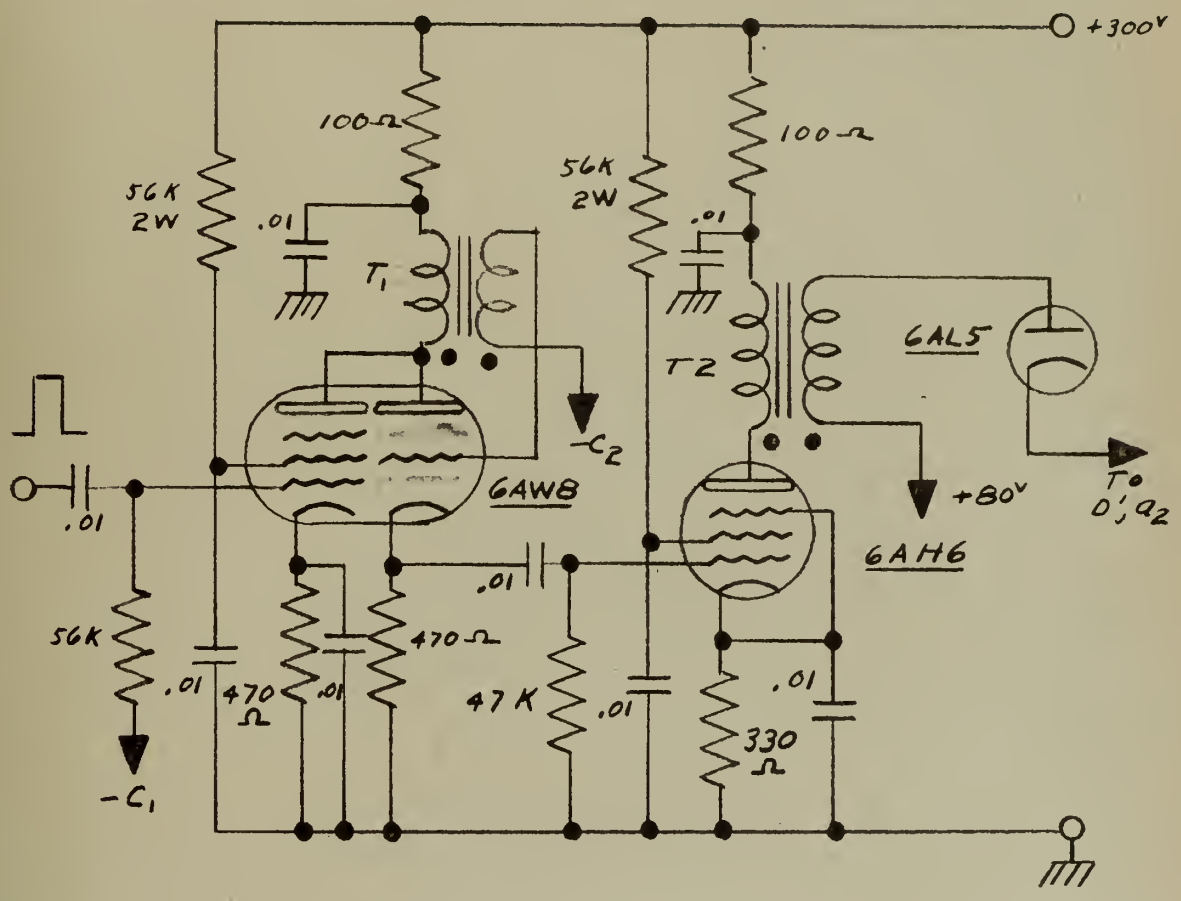

Fig. 21. Blocking Oscillator Circuit for Obtaining a Fast Pulse at the Blocking Oscillator Cathode

CHAPTER IV

APPLICATIONS AND PROPOSALS FOR FURTHER INVESTIGATION

1. Comparison of the Final ElT Counting Circuit of Chapter III With Conventional High-Speed Counting Techniques.

As an example of a fast counting circuit using conventional techniques, the 10-Mc circuit of the H. P. 524A Frequency Counter may be considered. This circuit employs nine pentodes (two each for four flip-flops) and a gate tube. The flip-flops operate sequentially, dividing by two at each stage, with feedback from the output of the fourth to the inputs of the second and third flip-flops to provide a scale-of-ten output. Plate clamping is used for each pentode to limit the plate swing to 20 volts, insuring a fast enough rise time for 10 Mc operation of the circuit. In addition, a Schmitt trigger input circuit is required. Residual count is indicated on a meter.

The final ElT circuit described in Chapter III requires seven auxiliary tubes in addition to the ElT and Schmitt trigger input circuit. Residual count is indicated directly on the ElT tube face. Estimating the retail cost of a circuit at $10.00 per tube, the ElT circuit would cost almost as much as the scale-of-ten flip-flop circuit, with approximately one-third the frequency response. Therefore, the ElT circuit described is not economically competitive at present with the 10 Mc flip-flip circuit. However, by increasing the reset anode resistance in Figure 19, and employing clamping and/or decoupling, the number of reset amplifiers required may be reduced from three to one, leaving four or five auxiliary tubes and the ElT. This circuit probably could have a frequency response

of greater than one Mc, and may be economically competitive with the one Mc circuit used in the H. P. 524A, which uses four twin-triode flip-flops, a gate tube, and a meter for residual count readout.

For lower frequencies, the circuit of Figure III-3, requiring only two or three auxiliary tubes per ElT stage (an input stepping tube and a monostable multivibrator reset tube, and perhaps a reset diode), might be economically competitive with the H. P. AC-4A decade counter plug-in unit, which requires four twin-triode flip-flops, provides neon bulb readout for each digit, and has an upper frequency of 120 kc. If necessary, a stepup pulse transformer may be used to couple the multivibrator output to the ElT.

The higher the g_m of the monostable multivibrator tube, the lower the value of the reset anode a.c. resistance necessary to provide a reset pulse of sufficient amplitude to trigger the multi-vibrator, with a resultant increase in frequency response of the circuit.

Figure 22 compares the estimated costs of various counting circuits graphically.

Reference [2] of the Bibliography describes a circuit for operating the ElT at frequencies up to 2 kc with no auxiliary tubes.

2. Proposed Reversible Counter Using the ElT.

In order to determine whether or not the ElT can operate as a reversible counter, it will be necessary to modify the circuit of Figure 17 to provide a positive pulse at D' and a_2 of the ElT for reverse stepping of the ElT from nine to zero. To accomplish this the circuit of Figure 23 might be utilized. The cathode of the reverse stepping triode V_2 is connected to D' and a_2 of the ElT. When a positive trigger

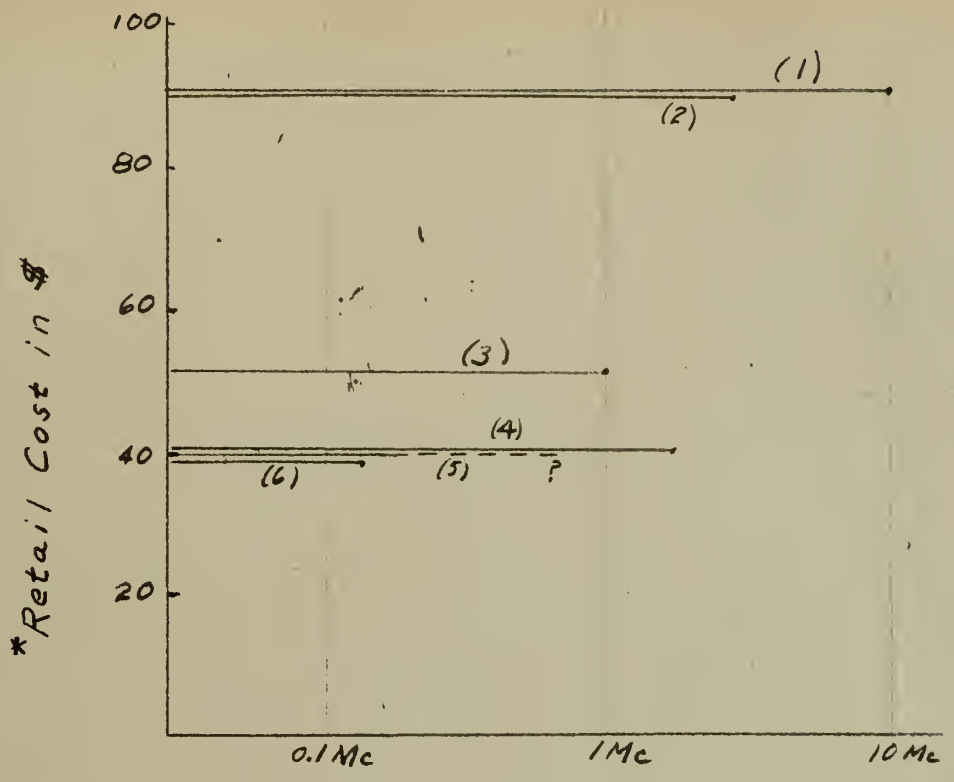

*Estimated at $10 per tube + $20 per E1T

(1). H.P. 524A 10 Mc. Circuit (9 tubes, 1 Meter)

(2) E1T 3 Mc Circuit of Figs. 17, 19 & 20 (8 tubes)

(3) H.P. 524A 1 Mc Circuit (5 tubes, 1 Meter)

(4) E1T 2.2 Mc Circuit of Fig. III-5 (3 tubes)

(5) E1T Circuit of Fig. III-3 (3 tubes)

(6) H.P. AC-4A 120 kc Circuit (4 tubes, 10 neon bulbs)

Fig. 22. Cost vs. Frequency Comparision of Several Fast Counting Circuits

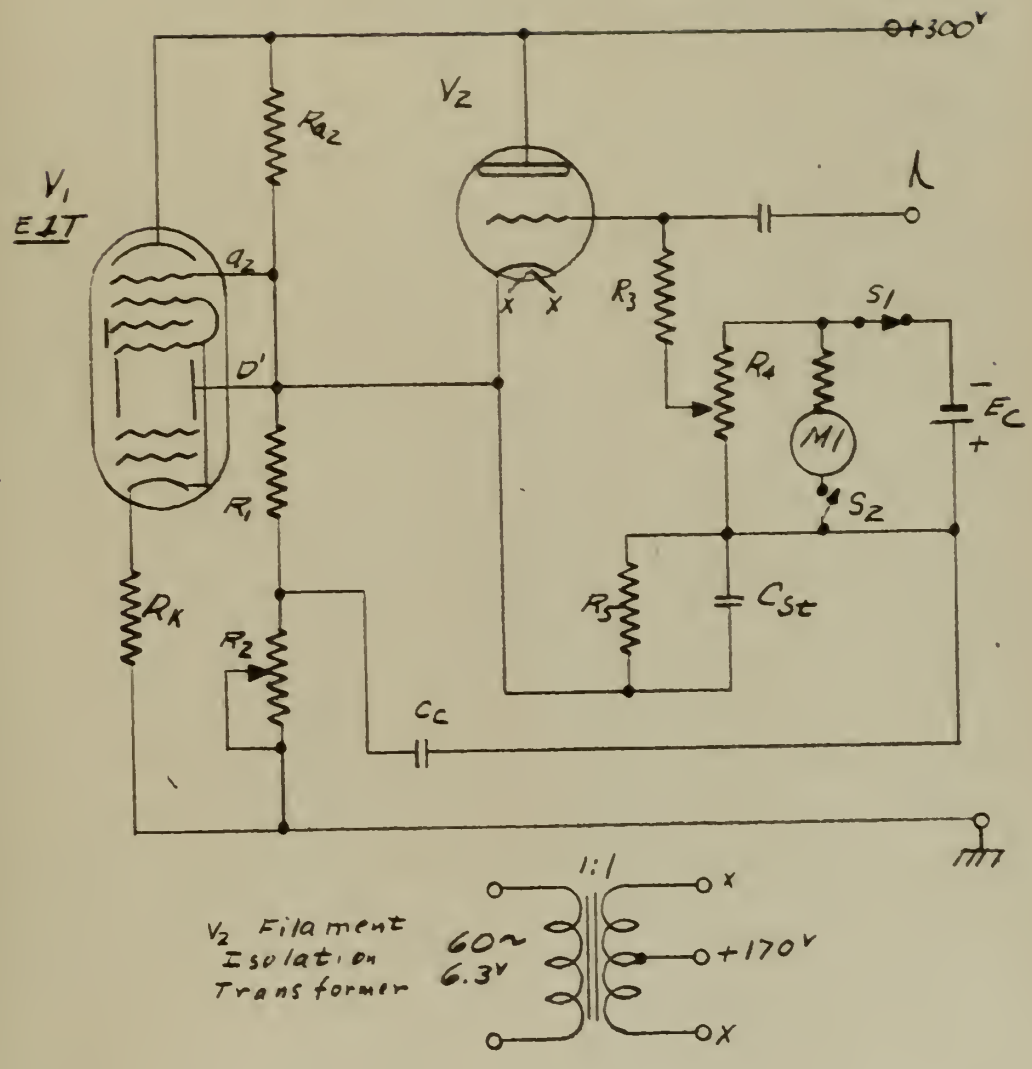

Fig. 23. Reverse Stepping Circuit

is applied to the grid of V_2 electrons are drawn from the stray, wiring and interelectrode capacity at D' and a_2, raising the potential of D' and a_2. In order to raise this potential sufficiently to make the ElT step to the next stable position (corresponding to the next lower digit) the plate current of V_2 must vary from some minimum value (corresponding to the step from nine to eight) to some maximum value (corresponding to the step from one to zero). This variable plate current may be obtained by a series combination of fixed and variable bias at the grid of V_2.

The fixed bias is obtained by a potentiometer across a battery, adjusted so that V_2 is held cut off between reverse stepping pulses. The amount of this bias will vary with the type of triode used as V_2. The variable bias is obtained by connecting D' and a_2 to a voltage divider (R_1 and R_2), tapping a small fraction of this waveform (V_{D', a_2}) across R_2 (the exact value will again depend on the triode used as V_2), and coupling this small waveform to a storage capacitor, C_{st}. $R_1 + R_2 >> R_{a_2}$. It will be seen that for low digits (V_{D', a_2} high) the bias on V_2 is reduced, providing a larger plate current when triggered by a trigger pulse of constant amplitude. The time constant of R_5 and C_{st} must be large enough to allow negligible decay of the stored charge on C_{st} between steps at very low stepping frequencies, yet R_5 is limited by the maximum grid circuit resistance permitted for the triode used as V_2. For R_5 = 100K and C_{st} = 1 uf, R_5C_{st} = 0.1 second. If this were not long enough for the lowest stepping frequencies required, C_{st} could be increased to about 10 uf, since only a few volts would appear across it during operation.

To prevent discharging the fixed bias battery ($-E_c$) when the counter is not in use, switch S_1, ganged to the main power switch, opens. For checking the battery voltage during operation, switch S_2 (a front-panel function-selector switch) is closed, providing an indication of battery voltage on M_1, a front panel meter.

Since the cathode voltage of V_2 will vary from about 90 to 250 volts above ground, it will be necessary to provide an isolation transformer for its filament voltage, with the center tap of the secondary connected to about +170 volts on a voltage divider from 300 volts to ground. Thus, the maximum heater-to-cathode voltage stress on the insulation will be about 80 volts, which is within the tolerance of most triodes.

The reverse reset pulse for resetting the ElT from zero to nine could be taken from D' and a_2 by means of an amplitude discriminating diode, as shown in Figure 24. The value of the resistor R will depend on the desired maximum operating frequency of the reversible counter. The higher the maximum operating frequency desired, the smaller the value of R that can be used, and consequently a reverse reset pulse of smaller amplitude will be developed across R. This in turn will mean more amplification of the reverse reset pulse will be required to provide a pulse of sufficient amplitude to trigger the reverse reset blocking oscillator. No reversal of polarity of the reverse reset blocking oscillator plate pulse will be necessary, but a three-winding pulse transformer may still be necessary to apply the negative blocking oscillator pulse to D' and a_2 through the biased diode, as shown in Figure 25 (a), or the negative pulse may be capacitively coupled from the blocking oscillator plate to the biased diode cathode, as shown in Figure 25 (b).

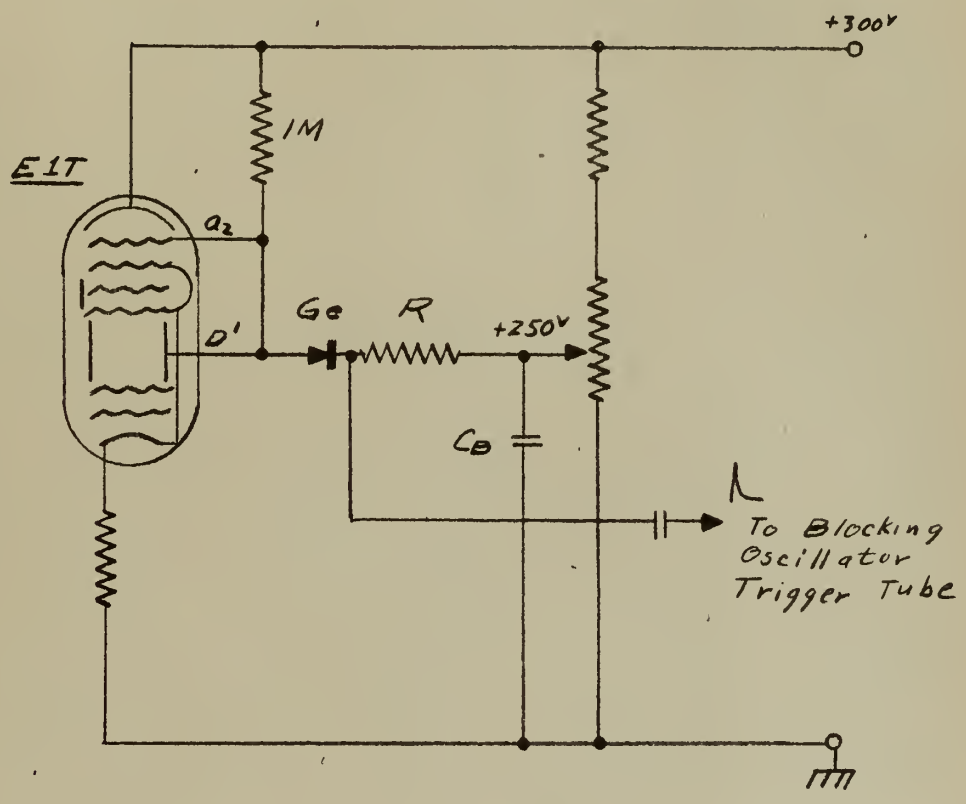

Fig. 24. Circuit for Obtaining a Reverse Reset Pulse

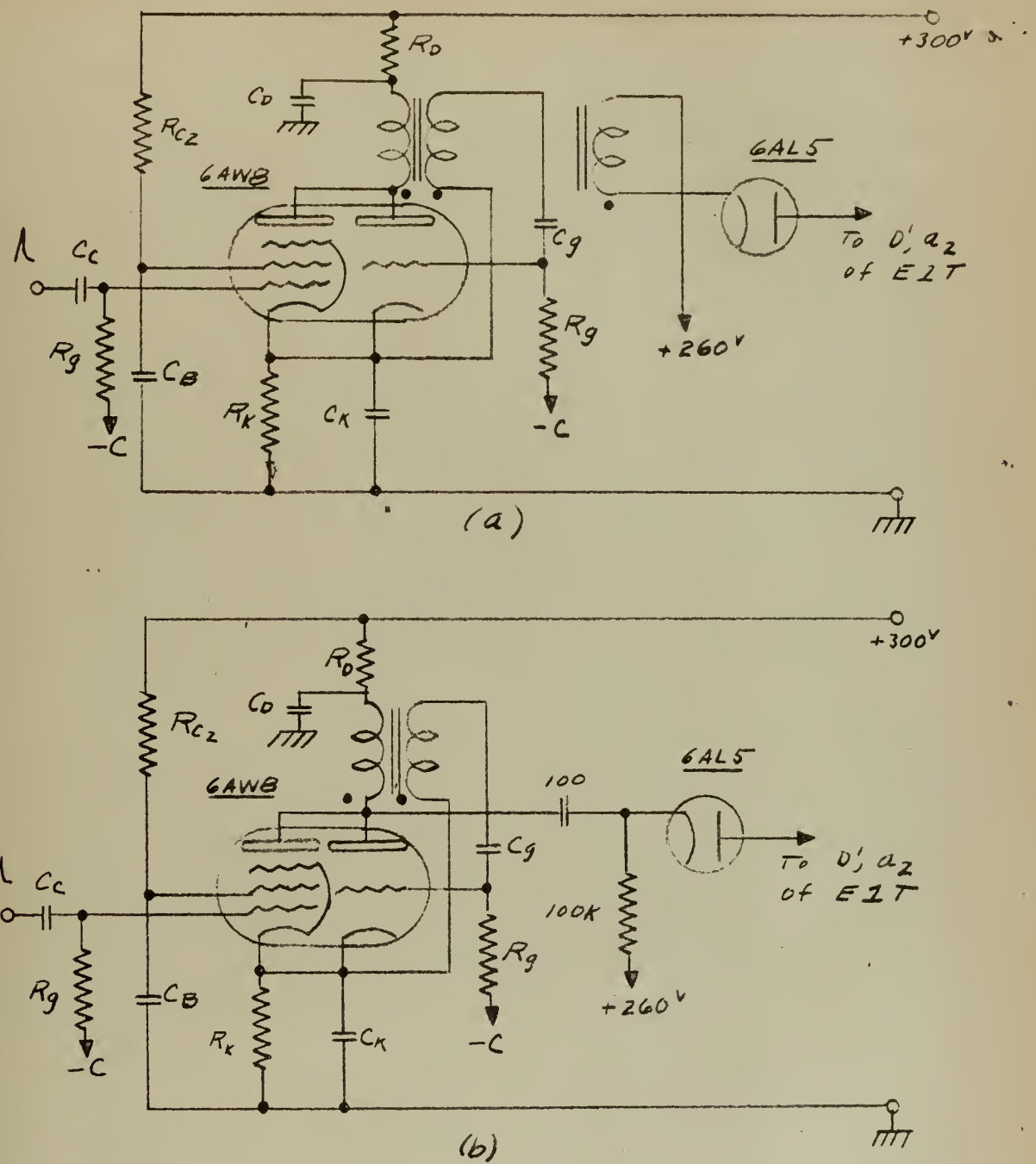

Fig. 25. Reverse Reset Blocking Oscillators

An overall block diagram for a proposed ElT reversible counter is shown in Figure 26. The derivation of inputs A and B' will be explained in the following section. For forward counting, input A enables Gate #1, permitting the positive B' pulse to step the ElT to the next higher digit. For reverse counting, input A enables Gate #2, permitting the negative B' pulse (after inversion) to step the ElT to the next lower digit. For forward resetting a coincidence of a reset pulse at the reset anoide (a_1) and a forward stepping pulse is required at Gate #3. Otherwise the forward reset action might occur immediately following a reverse reset. For reverse reset, a coincidence of a reverse reset pulse (obtained as in Figure 24) and a reverse step pulse is required at Gate #4, for the same reason.

3. Optical Grating Transducer to Provide Input Pulses to Operate a Reversible Counter.

Figure 27 illustrates a method for converting forward and reverse motion of an optical grating into pulses suitable for forward and reverse counting of the ElT. The optical grating is scribed with opaque lines and transparent spaces of equal width. Microscopes A and B are focused one-quarter of a cycle of the optical grating apart. Phototubes A and B receive the light transmitted by microscopes A and B, and provide output current waveforms indicated. These waveforms are amplified, and the B waveform is differentiated, providing the inputs to the reversible counter of Figure 26. The optical grating is mounted on a moving object, such as a machine tool, whose motion is to be accurately controlled by the output of the counter, as shown in Figure 28.

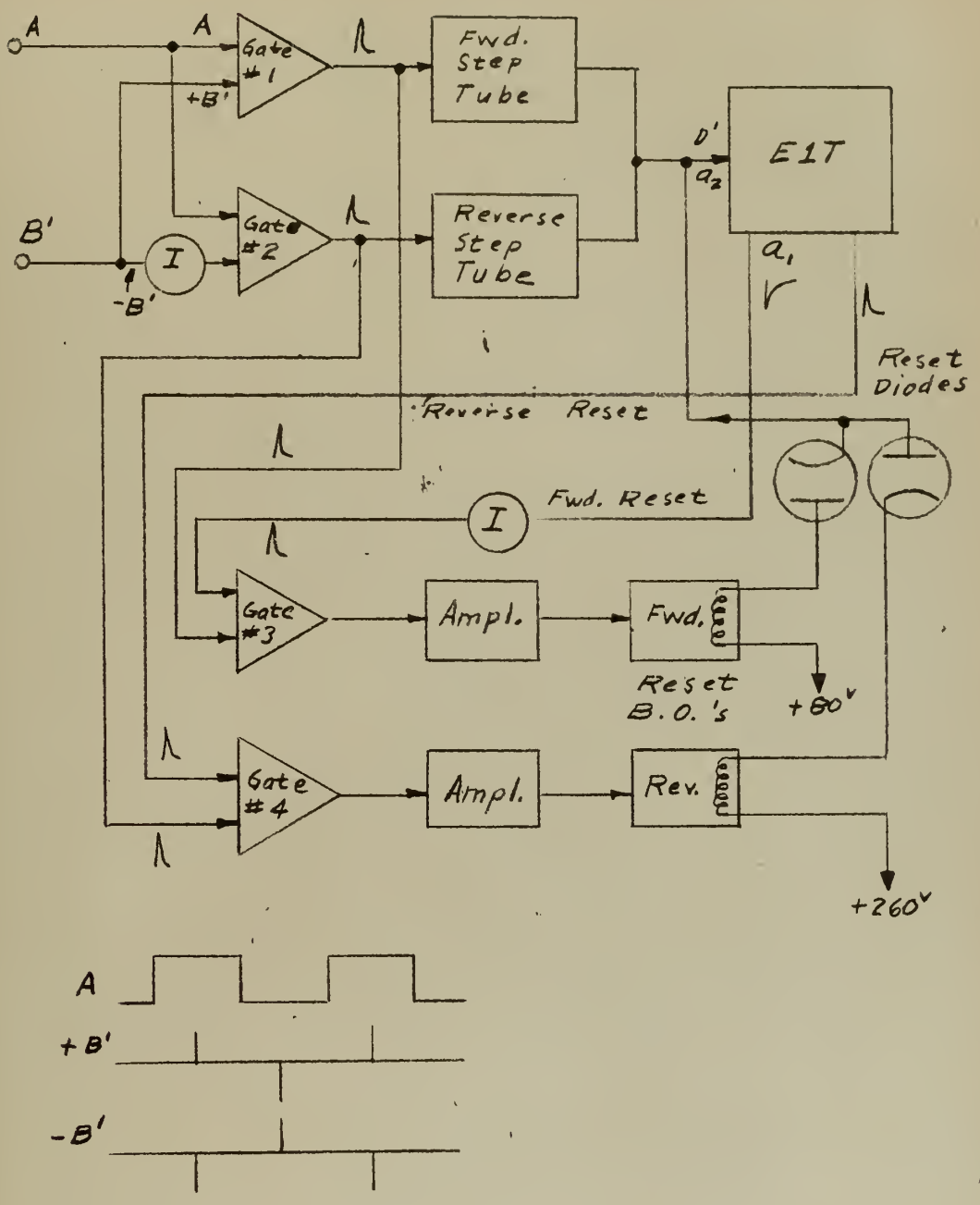

Fig. 26. Block Diagram of Reversible E1T Counter

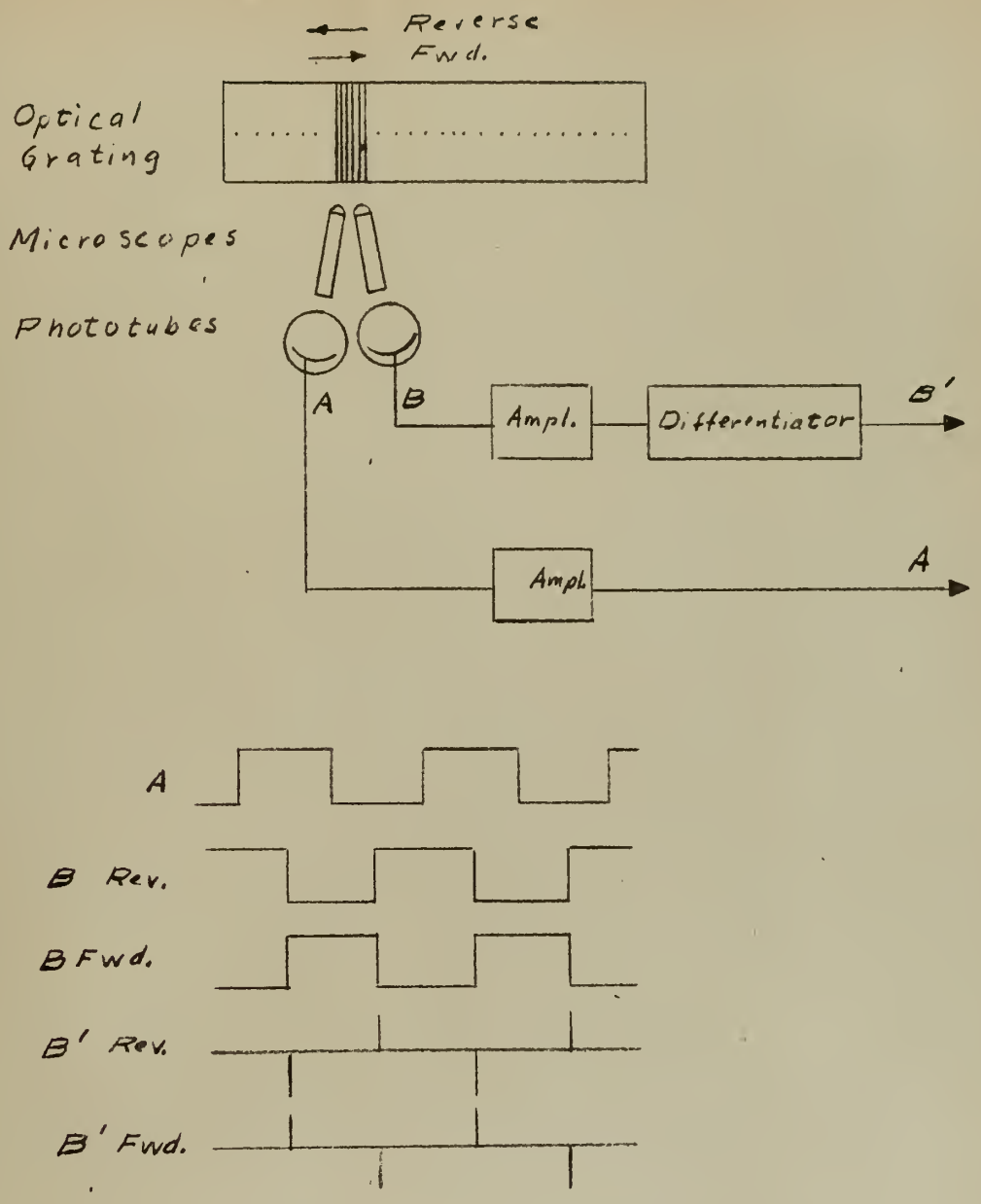

Fig. 27. Optical Grating Transducer

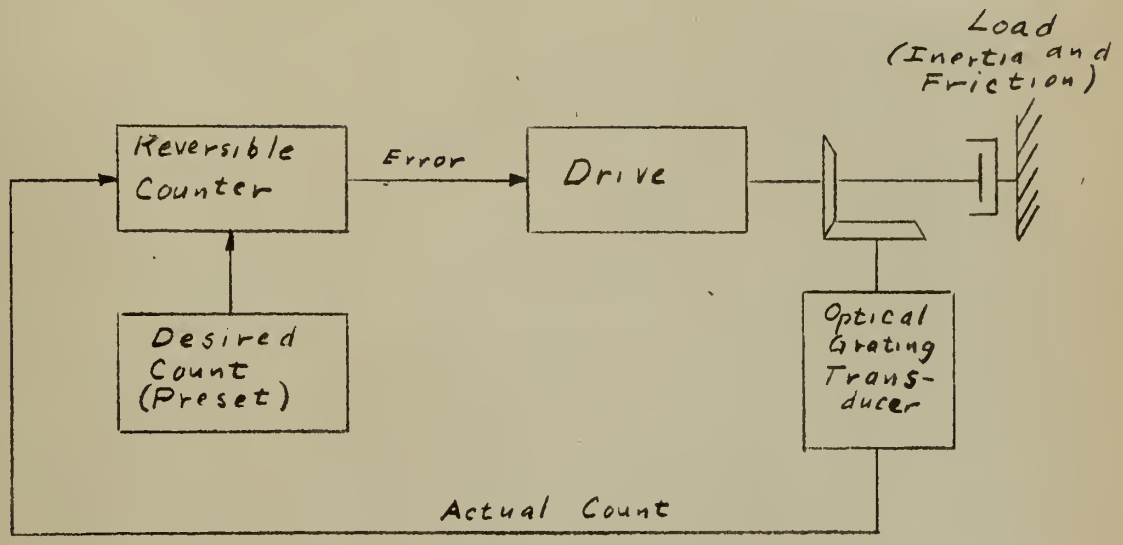

Fig. 28. Block Diagram of Reversible Counter Incorporated Into a Feedback Loop to Control the Position of a Driven Load

In lieu of the optical grating transducer, a rotary analog-to-binary converter, providing accuracies up to one part in 2^{13} may be substituted, using a suitable gear reduction ratio.

4. Reducing and/or Compensating for the Non-Linearity of ElT Stepping Pulse Amplitudes.

It has been pointed out previously that the "staircase" counting waveform at D' and a_2 of the ElT is non-linear, i.e., the amplitude of the steps for the lower digits is greater than the step amplitudes for the higher digits. It may be possible to minimize this non-linearity by varying any or all of the following parameters which were held fixed at the values given throughout the work described in Chapter III: V_{g1} (12.9 volts), V_D (156 volts), V_{g2} (300 volts), R_K (15K), R_{a2} (1M), and R_{g4} (47K). If this non-linearity of the step amplitudes were sufficiently minimized, it might be possible to eliminate the stepping triode altogether, and couple the negative stepping pulse to D' and a_2 directly from the Schmitt trigger circuit output, as shown in Figure 29. The amplitude of this step would have to be that of the largest step (zero to one). A large Schmitt circuit plate load resistor and clamping diode may be used here to decrease the stepping time.

This non-linearity may also be a disadvantage in other applications, such as operating a succeeding decade counter stage of a different type, which requires stepping pulses of constant amplitude, using the output of the ElT. It might be possible to correct this non-linearity by introducing a compensating non-linearity, thus making all the steps of nearly constant amplitude. Figure 30 shows a possible circuit for

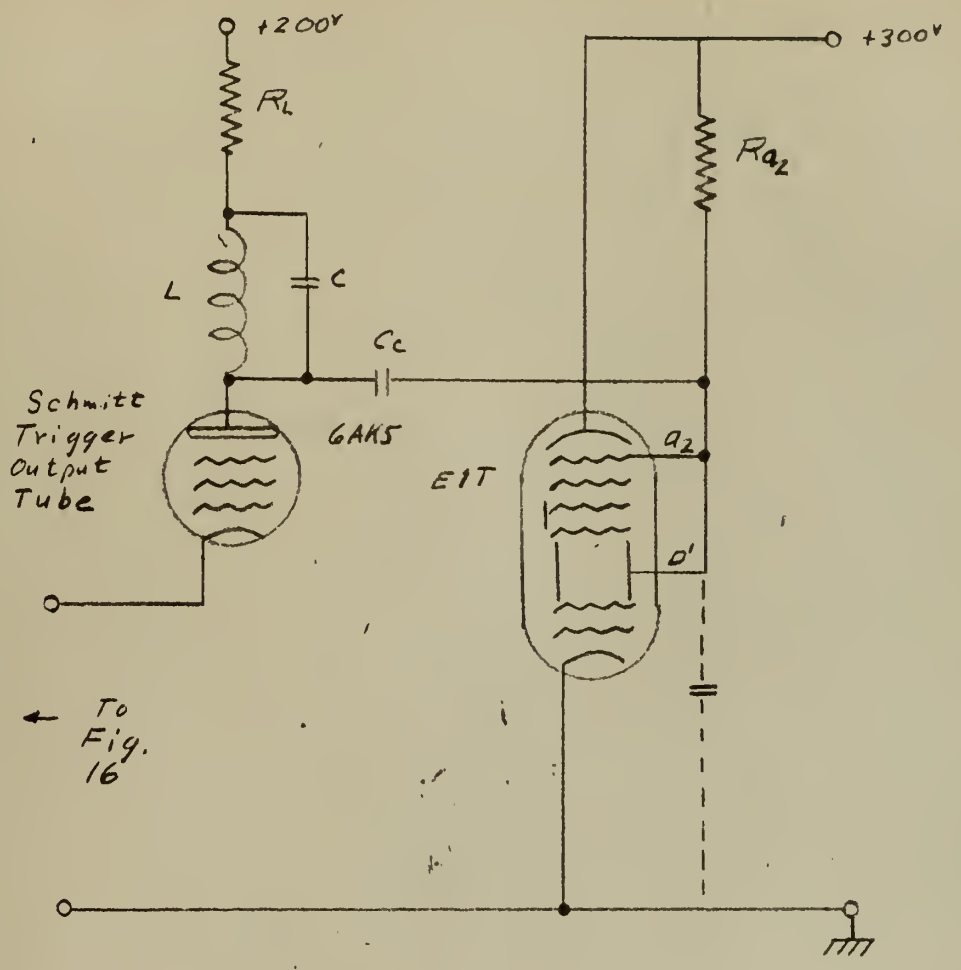

Fig. 29. Schmitt Trigger Circuit Output Coupled Directly to the E1T for Stepping

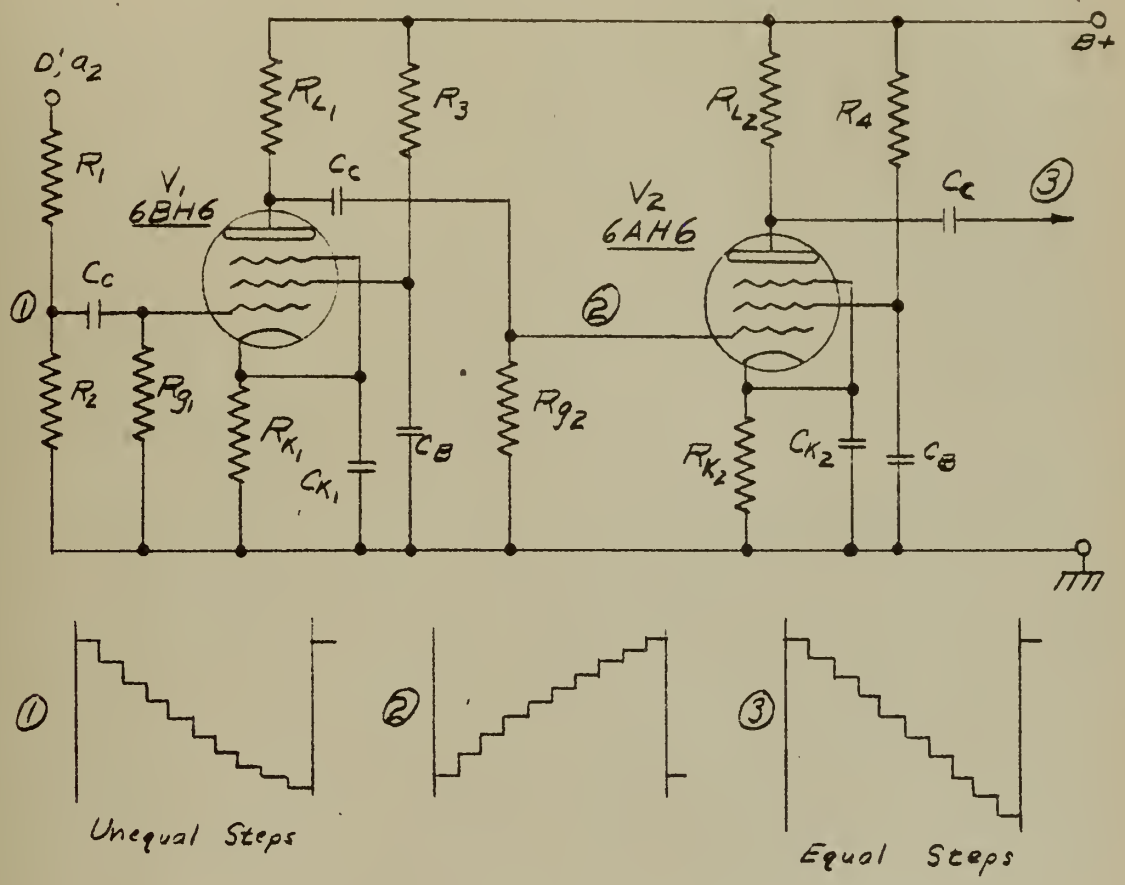

Fig. 30. Circuit for Introduction of a Compensating Non-linearity to Equalize the E1T Step Amplitudes

accomplishing this. The staircase waveform at D' and a_2 is applied to a high-resistance voltage divider, the output of which is only a small fraction of its input. V_1 has a gain of approximately one, by proper adjustment of R_{L1} and R_{K1}. Its purpose is to invert the voltage divider output for application to the grid of V_2. V_2 is biased, by its cathode and plate load resistors, to take advantage of the non-linear amplification of a 6AH6 (greater amplification in the regions of less bias), thus serving to equalize the amplitudes of the steps. V_1 and V_2 may be a twin-triode for frequencies below about one Mc, but should be pentodes for higher frequencies.

5. Proposed Circuit for Push-Pull Deflection of the E1T, With a Possible Increase in Counting Speed.

Figure 31 shows a possible circuit for push-pull deflection of the E1T using two 6AK5's as a paraphase amplifier. A negative step input to V_1 provides a positive step at D and a negative step at D', which should increase the speed of the stepping operation. For resetting the E1T to zero, the reset pulse at the reset anode a_1 is inverted by V_4, amplified, and coupled to the grid of V_1. Since higher speeds seem possible using this technique, R_{a1} (a.c.) will have to be small, and considerable amplification may be required of V_4, or a large R_{a1} and clamping might be used.

Since the E1T is designed for single-ended deflection, as explained in Chapter II, push-pull deflection may not prove to be feasible. In any case, considerable experimentation will be required to determine proper electrode potentials and resistance values.

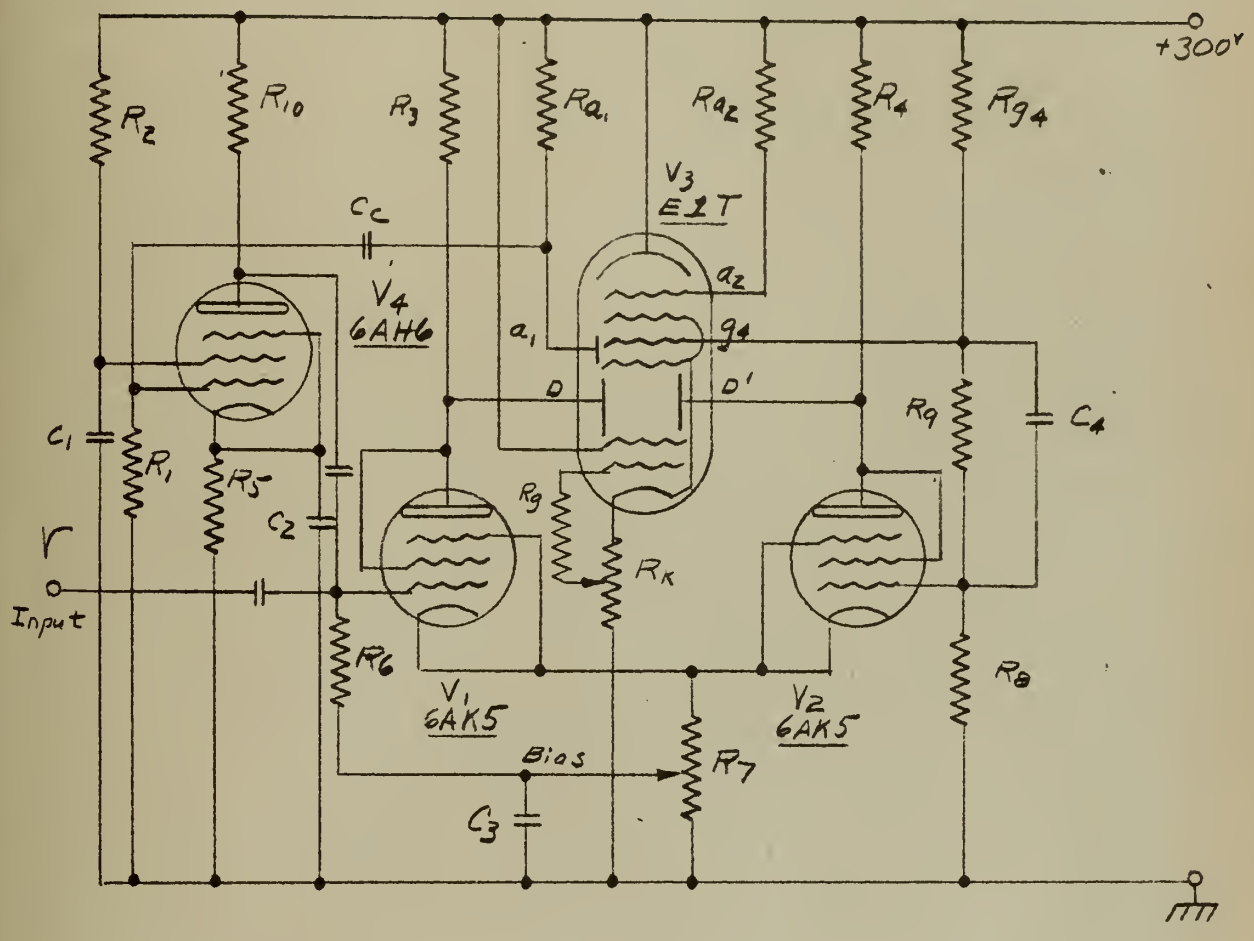

Fig. 31. E1T Push-Pull Deflection Circuit

Note that the feedback to provide stability of the beam between steps is obtained from g_4, the slotted electrode, rather than from the anode a_2. The potential of g_4 increases during a step to a higher digit. Separating electrodes a_2 and D' reduces the capacity to be driven at D', which may increase the maximum counting speed.

Obtaining the control grid bias for the E1T from a tap on its own cathode resistor (as indicated in Figure 31) may or may not be feasible.

6. Recommended Modifications of the Circuits of Figure III-5 and Figure 16 to Increase the Upper Counting Frequency Limit of the E1T.

Figure 32 includes some modifications to the circuit of Figure III-5 which may increase its frequency above the 2.2 Mc limit quoted by van Barneveld [3]. In this circuit the anode potential V_a of the EFP60 is set as high as possible without damaging the tube. This accelerates the rise in dynode potential. The dynode potential rise is clamped at +250 volts by the germanium diodes D_1 and D_2, and the E1T is ready for the next step.

The stepping pulse into the stepping triode may be the square wave at the plate of V_2 of Figure 16 (Schmitt trigger circuit). The Schmitt trigger circuit may be redesigned to give a current pulse of greater than 10 ma by using higher current pentodes. A 6CB6, for example, may be biased to pass a plate current of 20 ma without exceeding its rated plate dissipation of two watts, a 6AH6 30 ma without exceeding 3.2 watts, and a 6CL6 60 ma without exceeding 7.5 watts. Employing a large enough plate load resistor to obtain a plate voltage swing of at least 50 volts, and clamping diodes to limit this swing to about 20 volts, a stepping time of less than 0.05 usec might be obtained, especially if a Doba network is

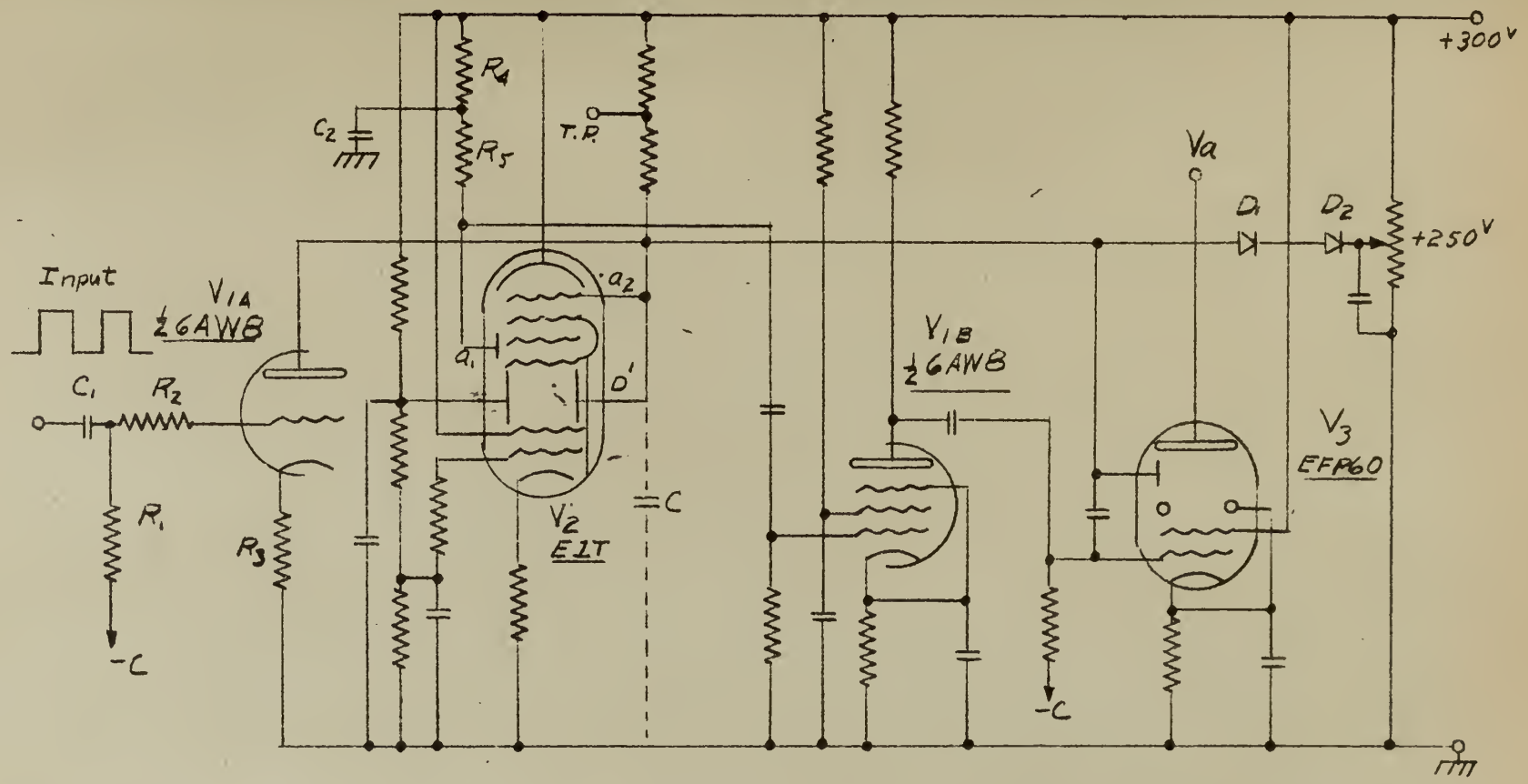

Fig. 32. Modification of Fig. III-5, Employing a Pentode Reset Pulse Amplifier and High-level Clamping of the EFP60 Dynode Potential Rise

used as the plate load impedance. A triode-connected 6AK5 or 6BH6 may be used as a stepping triode, in lieu of the 6AW8 triode section. A grid current limiting resistor R_2 will be required to eliminate the grid-current pulse, as pointed out in Chapter III.

A 6BH6 or 6AK5 pentode could also be used as the reset pulse amplifier, in lieu of the 6AW8 pentode section V_{1B}. Decoupling capacitor C_2 is inserted between R_4 and R_5, the reset anode load resistors, to provide a small enough AC load resistance to insure a fast rise time of the reset pulse, while limiting the DC current drawn by the reset anode to a safe value. As an alternative, a very large AC reset anode resistance might be used, developing a large negative reset pulse. By means of a clamping diode between a_1 and about +290 volts, only a few volts of this large negative excursion would be used to cut off V_{1B}, which may or may not decrease the reset time.

7. Proposed Decade Counter Tube that Eliminates the Reset Operation.

In Figure 33 is shown schematically a proposed decade counter tube, utilizing electrostatic focusing and electromagnetic deflection, yet retaining the cathode ray tube zero-to-nine count readout on the end of the tube. Electron gun g_1, a_1, and a_2 provides a beam of circular cross-section, focused on the luminous screen S. The circular apertures in g_4 and a_3 are located 36° apart around the periphery of the electrodes, with the apertures of g_4 in alignment with those of a_3. Anode #3 is connected to the electromagnets m_1 and m_2 at D', providing some stabilizing feedback to maintain the beam in one position between steps, as in the E1T. Stepping would be accomplished by means of a stepping triode or diode (V_1)

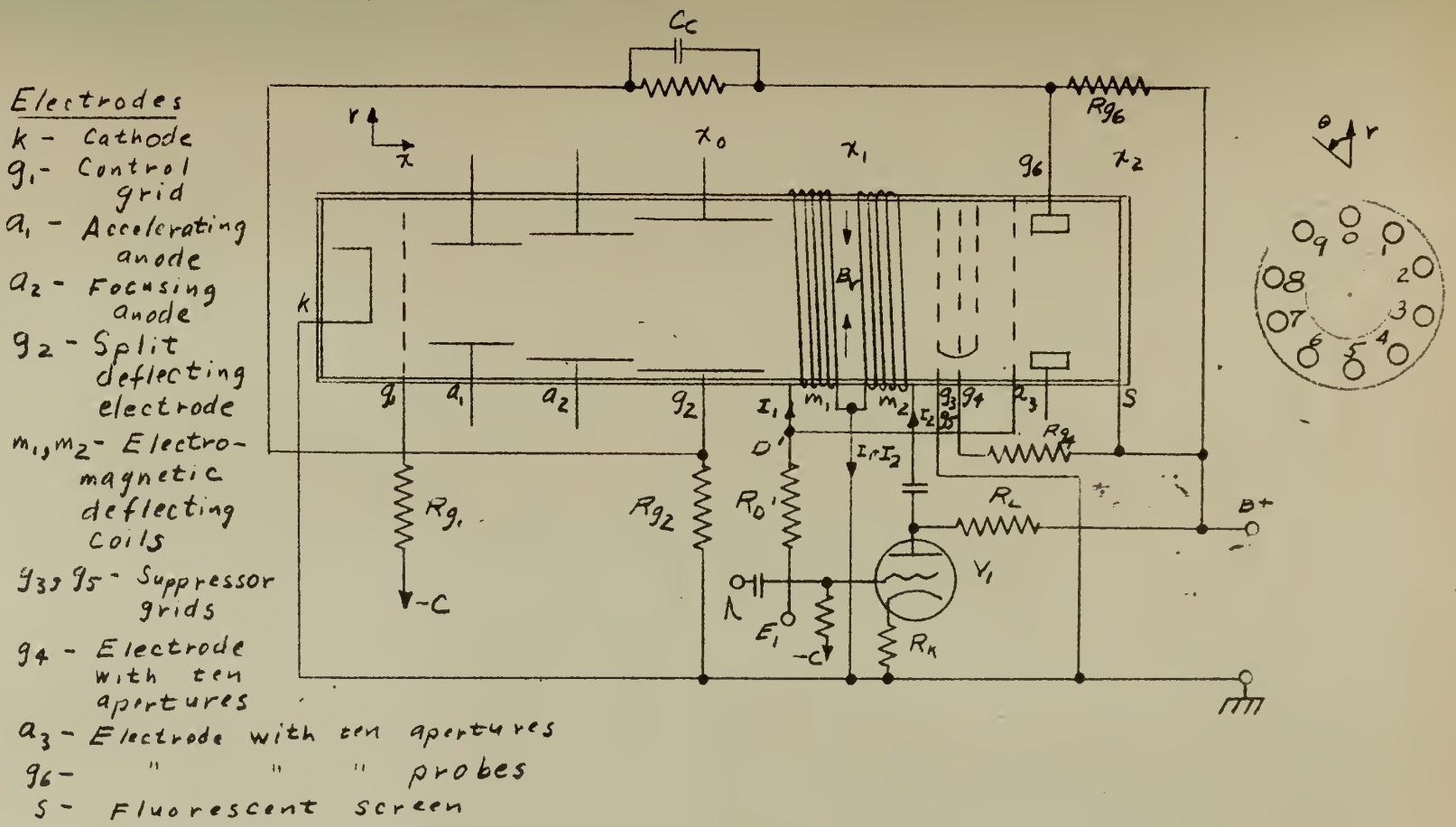

Fig. 33. Schematic of Proposed Decade Counter Tube, using Electrostatic and Electromagnetic Deflection

whose plate is connected to D' and a_3, and is normally biased non-conducting. When a positive stepping pulse is applied to the grid of this stepping triode (or negative pulse to the cathode of a stepping diode), the current normally flowing through the two opposing electromagnets m_1 and m_2 is diverted through the stepping tube. This reduces the radial magnetic field strength in the gap between the two electromagnets, thus reducing the amount of angular deflection experienced by an electron travelling through this magnetic field. By controlling the tube dimensions, electron velocity, and change of magnetic field strength produced by the stepping tube, an electron can be made to shift its angular deflection during stepping by an amount such that it passes through the next set of holes in g_4 and a_3, illuminating the next digit on the luminous screen S.

In order for the electrons in the beam to experience an angular deflection by the radial magnetic field they must be given an initial radial acceleration away from the tube axis. This may be accomplished by means of feedback from ten separate probes, g_6, each in line with an aperture of a_3, to ten separate deflecting electrodes, g_2, located 36° apart around the periphery of the tube between a_2 and m_1. When the electron beam passes through aperture zero of a_3 it strikes probe zero of g_6, reducing the potential of this probe. This decrease of potential is directly coupled to deflecting electrode six of g_2, deflecting the electron stream toward position one. Due to the angular deflection experienced by the electrons when passing through the radial magnetic field B_r between magnets m_1 and m_2, the electrons arrive at the fluorescent screen S at position zero instead of position one.

A carry pulse to the next decade stage may be obtained at probe zero of g_6.

In order to insure that the tube will initially set to zero, a manual and/or automatic mechanical zero set would probably have to be used, which by means of a switch removes B+ voltage from all probes of g_6 except probe zero.

Grids #3, #4, and #5 may not be necessary, since final acceleration of the electrons is provided by connecting the fluorescent screen S to B+. Grids #3 and #5 are suppressors. If grid #4 is eliminated, these suppressors may have to be located on either side of a_3 to suppress secondary emission electrons from s.

The overall length of this tube could be about five inches, requiring electron transit times of the order of 10 musec or less, with accelerating voltages of 300 volts or higher. The stepping time could probably be reduced to 0.05 usec or less, raising the possibility of a decade counter tube with direct readout, having counting speeds considerably in excess of 10 Mc.

For the electrostatic deflection, from Spangenberg [5], Section 6.3,

$$y_s = \frac{\ell b V_d}{2a V_o},$$

where y_s = distance from center line of tube to point where electron beam strikes the fluorescent screen,

ℓ = distance from center of deflection plates to fluorescent screen,

b = length of deflection plates,

a = separation of deflection plates,

V_d = potential between plates,

and V_o = potential corresponding to the electron initial velocity.

The above dimensions are diagrammed in Figure 35 (a). For Y_s = 0.5", b = 1", a = 0.5", ℓ = 3", and V_o = 200 volts,

$$V_d = \frac{2a\ V_o\ y_s}{\ell\ b} \simeq \frac{2\ (1/2)\ 200\ (1/2)}{3\ (1)} = 33.3 \text{ volts},$$

which is the potential decrease necessary at g_6. If Rg_6 = 1M, then 33μa of the beam current must be collected by g_6, to produce this potential drop. From Spangenberg [5], section 15.5, beam currents of at least 50 ma appear to be reasonable with this size tube, rendering V_d = 33 volts quite feasible.

For the electromagnetic deflection, assume a net radial magnetic field, B_r, is concentrated at x_1, midway between the opposing electromagnets m_1 and m_2, as shown in Figure 34. (Actually this will be a distributed field.) An angular deflecting force, $\bar{f} = e\ \bar{B} \times \bar{v}$ will be experienced by an electron passing through this magnetic field with velocity v. For stepping to the next higher digit, $-\Delta I$ through the magnet causes $-\Delta B_r$, which in turn causes $-\Delta f$ and the electrons are deflected less.

$$\bar{f} = e\ \bar{B} \times \bar{v} = \frac{m\ \bar{v}^2}{R}$$

where R is the radius of curvature of the electron path (from Spangenberg [5], section 15.3).

$$R = 3.37\ (10^{-6})\ \frac{V}{B_r},$$

where V is the electron velocity in equivalent volts.

In order to specify a value of R, the dimensions of the tube must be established. In Figure 35, y_s is the radial distance from the tube axis

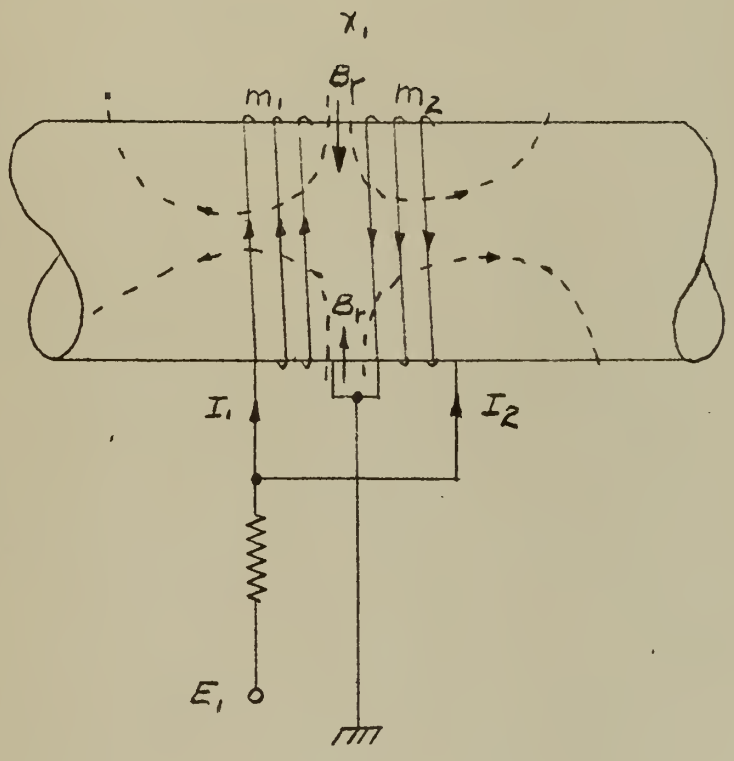

Fig. 34. Radial Magnetic Field Caused by Current in Coils m_1 and m_2

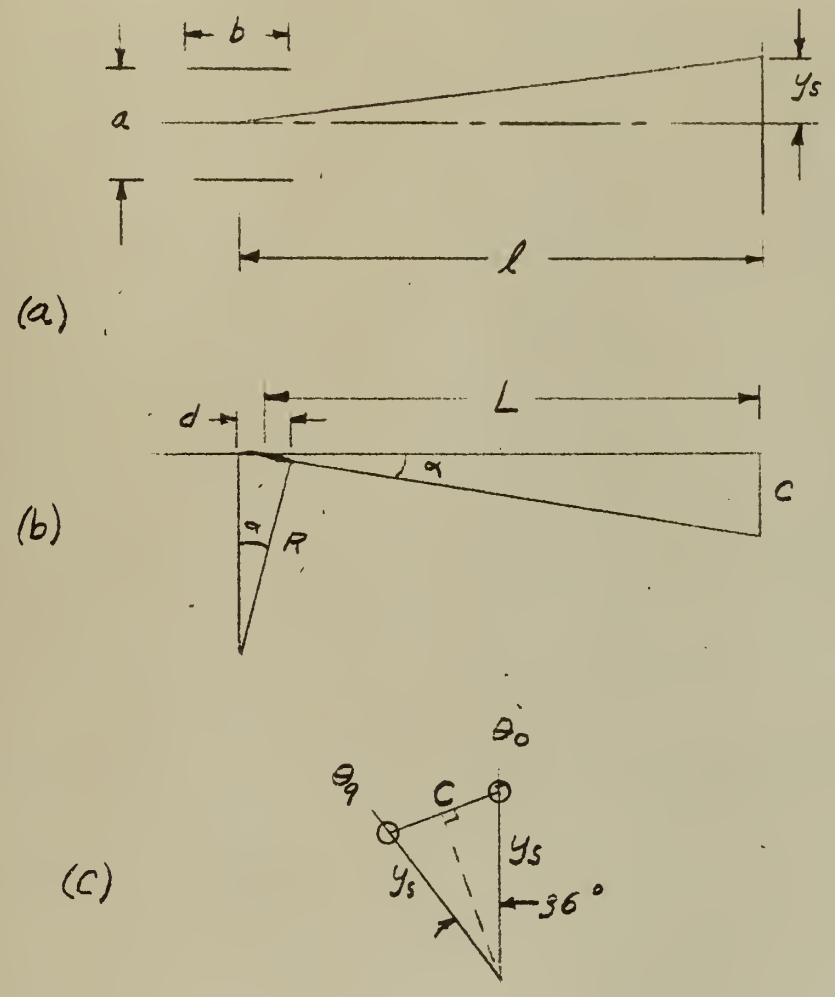

Fig. 35. Diagram for Explaining Electron Deflection in Counter Tube of Fig. 33

to the spot where the electrons strike the fluorescent screen S. Since

$$\theta = 36°,$$

$$c = 2y_s \sin 18°,$$

For $y_s = 0.5"$, $c = 0.31"$. L is the distance from the midpoint between the magnets m_1 and m_2 (x_1) to the fluorescent screen S. Assuming B_r to be constant over a 1/4" gap (d) between m_1 and m_2, then

$$\arctan \frac{c}{L} = \arctan \frac{d}{R}$$

For $c = 0.31"$, $L = 1.5"$, and $d = 0.25"$,

$$R = \frac{dL}{c} = \frac{0.25(1.5)}{0.31} = 1.21" = 0.0308 \text{ meter}$$

For $V = 200$ volts,

$$\Delta B_r = \frac{3.37\ (10^{-6})\sqrt{200}}{3.08\ (10^{-2})} = 15.5\ (10^{-4})\ \frac{\text{Weber}}{\text{Meter}^2}$$

$$B_r = \mu \Delta H_r$$

$$= 4\pi(10^{-7})$$

$$\Delta H_r = \frac{\Delta B_r}{\mu}\ \frac{15.5\ (10^{-4})}{4\pi(10^{-7})} = 1240\ \frac{\text{amp-turns}}{\text{meter}}$$

$\Delta H_z = \frac{N}{\ell} \Delta I$ at the center of the solenoid, where N = number of turns on the solenoid, and l = length of the solenoid. Due to the fields of the two coils m_1 and m_2 opposing each other, H_r in the gap between the two coils will be more intense than H_z in the center of the solenoids. Assume H_r at $x = x_1$, and r = 1/4" is 4 times as great as H_z at the center of the solenoid. Then

$$\Delta H_z = \frac{N}{\ell}\Delta I = \frac{1240}{4} \approx 300\ \frac{\text{amp-turns}}{\text{meter}}$$

$$\frac{N}{\ell} = \frac{\Delta H_z}{\Delta I} = \frac{100}{.01} = 30{,}000\ \frac{\text{turns}}{\text{meter}},$$

assuming $\Delta I = 10$ ma during a step.

$\frac{N}{\ell} = 300$ turns/cm $= 763$ turns/inch

(Three layers of #39 wire.)

From the Federal Handbook [9], p. 73,

$$L = n^2 Fd,$$

where L = coil inductance in μh,

n = number of turns on coil

F = form factor (from [9], p. 75)

d = coil diameter in inches.

Assume $d = 1.25$" and $d/l = 10$, where

l = coil length. Then

$l = 0.125$"

$n = \frac{763}{10} = 76$ turns

$F = 0.051$

$L = (76)^2\ (.051)\ (1.25) = 370\mu$h

$$\Delta E = L\frac{\Delta I}{\Delta t}$$

$$L\Delta I = E\Delta t$$

$$370\ (10^{-6})\ (.01) = 3.7\ (10^{-6}) = \Delta E \Delta t$$

For $\Delta t = 0.05\mu$s,

$\Delta E = 74$ volts $= \Delta e_b$ of V_1 during a step.

$$f_{max} = \frac{1}{\Delta t} = \frac{1}{.05\ (10^{-6})} = 20 \text{ Mc.}$$

During a step pulse, 10 ma must be diverted from each coil through V_1 (Figure 33). Therefore, the DC current through $R_{D'}$ must be $\geq$20 ma and $R_{D'}$ is limited to a fairly small value by the DC power dissipation (2.5K

for one watt). Thus, $E_1 = (I_1 + I_2)R_{D'} = 20(10^{-3})2.5(10^3) = 50$ volts. The plate voltage for V_1 will have to be obtained through a large load resistor R_{L_1}, and the plate of V_1 capacitively coupled to D'. R_K of V_1 will have to be adjusted so that the proper amount of current is drawn from m_1 and m_2 to insure proper stepping of the tube when positive pulses of constant amplitude are applied to the grid of V_1.

By decreasing y_s, the radius to the spot on the tube face, and/or increasing L, the accelerating voltage V may be increased, decreasing the electron transit time and thus increasing the maximum frequency. Increasing L increases the transit time, however, and an optimum L would have to be found. Carrying this idea further, the minimum practicable tube size might be of the order of 0.5" diameter and two inches long. For convenient observation of the tube face a magnifying lens could be used. Increasing the accelerating voltage as high as possible (to perhaps 600 volts) and/or increasing Δ B, a transit time of perhaps two musec might be realized. Arbitrarily establishing the minimum stepping time τ_s at twice the transit time gives a maximum theoretical counting frequency of

$$f_{max} = \frac{1}{\tau_{s\ min}} = \frac{1}{4(10^{-9})} = 250 \text{ Mc.}$$

Larger tubes, being easier and cheaper to manufacture, could be used for lower frequencies.

8. Recommended Redesign of the ElT to Increase its Frequency Response.

Figure 36 shows a front view of a modified ElT-type of tube, whose cross-section is approximately the same as the ElT, but possibly smaller in diameter. The cathode is lengthened considerably, providing a greater

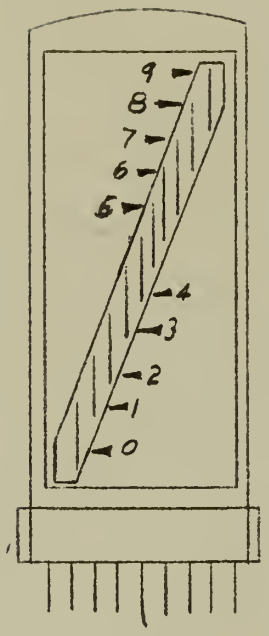

Fig. 36. Front View of Modified E1T-type Decade Counter Tube

beam current in the tube. The slots in g_4 are of approximately the same length as the cathode (three inches or more). The slots in a_2, however, instead of being oriented in two horizontal rows as in the E1T (even digits in the top row and odd digits in the bottom row) are placed on a sloping line, as close together as possible, yet separated sufficiently in azimuth so that the focused electron beam passes through one slot at a time and illuminates the flourescent screen beyond that slot. The beam is focused as sharply as possible on position four or five. The slots are located symmetrically about the center position (between slots four and five), being wider and farther apart as the angular displacement from the center position increases, to compensate for the defocusing caused by the deflection of the beam away from its position of best focus (center). The purpose of this compensation is to insure that the stepping pulses required for each step will all be of the same amplitude, instead of variable as in the E1T. This in turn will simplify the external circuitry required.

With the longer cathode and consequent larger beam current, a smaller change of deflection plate voltage would be required to step the beam to the next higher digit (perhaps five volts for stepping and thus fifty volts for resetting). Using a difference amplifier for push-pull deflection, and high-level clamping during reset, the stepping time could probably be reduced to about 0.02 usec, using a suitably designed trigger circuit, and the reset time to about 0.1 usec, thus increasing the maximum counting frequency to about ten Mc. The reset anode should be made as large as possible to increase the reset anode current, thus decreasing the reset time.

For the slower decades, the reset anode resistance can be made very large, providing a negative reset pulse of amplitude greater than the amount of positive voltage excursion required at the right deflection plate D' to reset the tube to zero. Thus, by capacitively coupling the reset anode to the right deflecting plate, and employing clamping if necessary, the tube can be reset to zero as the reset anode potential returns to B+, with no auxiliary reset tube. A portion of this negative reset pulse can be capacitively coupled to D' of the succeeding decade tube for the carry pulse.

The B+ voltage should be as high as possible without damaging the tube (400 volts or greater, possibly) to decrease the electron transit time and increase the beam current.

This type of counter tube, with a minimum of auxiliary circuitry, should lend itself well to applications requiring miniturization and small power drain.

BIBLIOGRAPHY

1. Kandiah, K. — DECIMAL COUNTING TUBES, Electronic Engineering, p. 56-63, Feb. 1954.

2. Amperex Electronic Corp. — E1T DECADE COUNTER TUBE (Pamphlet 20/0/4602), Amperex Electronic Corp., July 1955.

3. van Barneveld, E. J. — FAST COUNTER CIRCUITS WITH DECADE SCALER TUBES, Philips Technical Review, Vol. 16, No. 12, June 1955.

4. Clark, J. R. — LOW POWER BLOCKING OSCILLATORS, Proceedings, National Electronics Conference, Vol. VIII, 1952.

5. Spangenberg, K. R. — VACUUM TUBES, McGraw-Hill, New York, 1948.

6. Valor Electronic Components Co. — VALOR PULSE TRANSFORMERS, Valor Circuit Notes, No. III, July 1955.

7. Langford-Smith, F. — RADIOTRON DESIGNER'S HANDBOOK, 4th ed., Radio Corp. of America, 1953.

8. Moskowitz, S. and Racker, J. — PULSE TECHNIQUES, Prentice-Hall, New York, 1951.

9. Federal Telephone and Radio Co. — REFERENCE DATA FOR RADIO ENGINEER'S, Federal Telephone and Radio Co., 1949.

10. Kuchinsky, S. — THE MAGNETRON BEAM SWITCHING TUBE - A NEW CONCEPT IN VACUUM DEVICES, Hayden Bros. of New Jersey, 1955.

11. Terman, F. E. — RADIO ENGINEER'S HANDBOOK, McGraw-Hill, New York, 1943.

12. Chance, et al. — WAVEFORMS, Vol. 19, M.I.T. Radiation Laboratory Series, McGraw-Hill, New York, 1947.

13. Seely, S. — ELECTRON TUBE CIRCUITS, McGraw-Hill, New York, 1950.

14. Terman, F. E. — RADIO ENGINEERING, 3rd ed., McGraw-Hill, New York, 1947.

15. Radio Corporation of America — RCA RECEIVING TUBE MANUAL, Radio Corporation of America, 1955.

APPENDIX I

E1T TECHNICAL DATA

Heater Data

Supply		Indirect by A.C. or D.C.; series or parallel supply
Heater voltage	V_f	= 6.3 V ± 10%
Heater current	I_f	= 0.3 A

Operating Characteristics

Supply voltage	V_b	= 300 V*)
Cathode current	I_k	= 0.95 mA
Cathode resistor	R_k	= 15 k ± 1%
Control-grid voltage	V_{g1}	= 11.9 V*) ± 0.15V
Accelerating-electrode voltage	V_{g2}	= 300 V*)
Left deflection electrode voltage	V_D	= 156 V*) ± 1.5 V
Slotted-electrode resistor	R_{g4}	= 47K ± 5%
Conducting-layer voltage	V1	= 300 V*)
Anode resistor	R_{a_2}	= 1M ± 1%
Reset-anode resistor	R_{a_1}	= 39K ± 10%
Accelerating-electrode current	I_{g_2}	= 0.1 mA

Capacitances

Anode capacitance	C_{a_2}	= 10.5 uuF

*) All voltages are quoted with respect to the chassis. Provided the ratios of the supply voltages are strictly maintained by using a suitably designed voltage divider consisting of 1% precision resistors, there is no need to stabilize the supply unit, voltage fluctuations of ± 10% then being permissible. It should be borne in mind, however, the during life a change may occur as a result of lack of stability of the resistors. V_B = 400 volts maximum.

Capacitances, Contd.

Left deflection electrode capacitance . .	C_D	= 3.5 uuF
Right deflection electrode capacitance .	$C_{D'}$	= 3.8 uuF
Reset-anode capacitance	C_{a_1}	= 4.9 uuF
Control-grid capacitance	C_{g_1}	= 6.8 uuF
Slotted-electrode capacitance	C_{g_4}	= 7.7 uuF

Sensitivity to Magnetic Fields.

Care should be taken to prevent magnetic fields from upsetting the operating of the counter tube, the electron beam being sensitive to the influence of external fields. The flux density of these fields should not exceed 2 X 10^{-4} Wb/m^2 (=2 gauss) in any direction.

Ambient Illumination.

In order to obtain a clear reading, the ambient illumination should range from 40 lux to 400 lux, to be measured by means of a luxmeter, set up vertically. At too low a value of the ambient illumination, it may become difficult to read the figures on the masks of the counter tubes, and some inconvenience may occasionally be experienced by the two neighbouring spots showing some fluorescence. When, on the other hand, the ambient illumination exceeds 400 lux, it may become difficult to discern the luminescent spot.

Mounting Position.

Any, except with the tube horizontal and the fluorescent screen downward.

Socket.

Duodecal socket type S-13264.

APPENDIX II

THE COUNTING OF RANDOM PULSES WITH THE ElT

In counting completely random pulses; such as the output of Geiger-Müller or scintillation counters, a fraction of the pulses produced will escape detection, due to the inherent dead time required for the counter (scaler) tube to record one digit. During this dead time the tube is insensitive and any pulse arriving will not be counted. Such losses occur in all electronic scalers and the loss is even more serious in mechanical counters. It is customary to specify this characteristic property of a scaler.

The ElT has two inherent dead times, a stepping time τ_s required to step the beam from one position to the next, and a reset time τ_r required to reset the beam from position nine to position zero. For periodic pulses, the counting rate with zero counting loss is limited by τ_r; that is, if the interval between pulses is less than τ_r, pulses arriving during τ_r will not be counted. This loss obviously increases as the counting rate increases beyond $\frac{1}{\tau_r}$.

Considering random pulses, let n represent the average number of pulses recorded per second. This also represents the number of times per second that the counter is insensitive. In nine out of ten cases, the cause of this insensitivity is a step of duration τ_s, and in one out of ten cases it is a reset of duration τ_r. Therefore, let an average dead time τ_m be defined:

$$\tau_m = 0.9\,\tau_s + 0.1\,\tau_r \qquad (1)$$

On the average, the counter is insensitive for $n\tau_m$ second per second. Thus, the number of pulses actually arriving per second is:

$$N = \frac{1}{1 - n\tau_m} n \tag{2}$$

Solving for n,

$$N - Nn\tau_m = n$$

$$n = \frac{N}{1 + N\tau_m}, \text{ or} \tag{3}$$

$$n = \frac{1}{\tau_m} \cdot \frac{N - n}{N}, \tag{4}$$

where $\frac{N - n}{N}$ may be defined as the relative loss (δ), or accuracy of indicating the actual count N.

Let Δ be the accuracy of measurement of τ_m. If τ_m could be measured with no error, then $n\tau_m \leq$ one second. With Δ% error in the measurement of τ_m, $n\tau_m + \Delta \leq$ one second. Dividing by $n\tau_m + \Delta$,

$$1 \leq \frac{1}{\Delta + n\tau_m}.$$

Multiplying by $n\tau_m$,

$$n\tau_m \leq \frac{n\tau_m}{\Delta + n\tau_m} = \frac{\delta}{\Delta + \delta}, \tag{5}$$

from equation (4).

For example, if the required accuracy of counting N pulses is 1%, and τ_m can be measured within 10%, then:

$$n = \frac{1}{11\tau_m}$$

will be the maximum indicated counting rate that will insure the required counting accuracy.

APPENDIX III

CIRCUIT FOR OPERATING THE E1T DECADE COUNTER TUBE AT FREQUENCIES UP TO 2.2 MEGACYCLES

1. Introduction.

Auxiliary circuits capable of operating the E1T decade counter tube at frequencies up to 2.2 Mc have been described by van Barneveld [3]. The techniques utilized to accomplish this are:

(a) Reducing the stepping time by means of a stepping triode, and

(b) Reducing the reset time by means of a secondary emission tube.

2. Reducing the Stepping Time.

The stepping time τ_s is the time required to discharge the total capacity C existing at electrodes D' and a_2 of the E1T by an amount of charge sufficient to decrease its potential (ΔV) to that corresponding to the next stable position of the E1T. From the relation

$$\tau_s = \frac{C \Delta V}{\bar{I}},$$

where $\bar{I}$ is the average current flowing during the stepping time τ_s, it is apparent that to decrease τ_s, $\bar{I}$ must be increased. Assuming typical values of C (23 uuf) and Δ V (14 volts), for τ_s = 0.1 usec, $\bar{I}$ must be = $\frac{23\ (10^{-12})\ 14}{(0.1)\ 10^{-6}}$ = 3.22 ma. This amount of current cannot be supplied by the E1T itself, since its normal total tube current is about one ma. However, the additional current can readily be supplied by

connecting the plate of a triode to D' and a_2 as shown in Figure III-1, and biasing the triode non-conducting between stepping pulses. During a stepping pulse the current flowing through V_1 is drawn from the capacity C existing at D' and a_2, lowering the potential of D' and a_2 sufficiently to step the ElT to its next stable position.

The amplitude of the change of voltage necessary to step the ElT from one stable position to the next decreases as the beam is shifted further to the left, being about 17.5 volts for the step from position zero to position one, and about 12.8 volts for the step from position nine to the reset anode. The ratio of the maximum step amplitude to the minimum step amplitude is thus about 4:3. In order to provide stepping currents of the proper amplitude for each step, advantage is taken of the transfer characteristics of a triode, shown in Figure III-2. As the plate voltage of V_1 (in this case V_{D',a_2}) decreases, the I_b vs. E_c curve moves to the right on the transfer characteristic plot. For an unbypassed cathode resistance R_K in Figure III-1, $e_c = R_K i_b$, $R_K = \frac{-e_c}{i_b}$, or $R_K = \cot \alpha$. Locating the points A and B on the transfer characteristic curves for $V_{D',a_2} = 250$ volts and 100 volts, such that $I_A = 4/3\ I_B$, determines a cathode resistor load line. The slope of this load line determines the value of R_K required to insure the correct amplitude of each step (2.5K for the parameters given in Figure III-2). The amplitude of the positive pulse required at the grid of V_1 must be equal to the negative grid cutoff bias plus the amount that the grid must swing positive in order for the cathode resistor load line to intersect the $E_b = 250$ volts curve at point A (16 volts for the triode characteristics shown in Figure III-2).

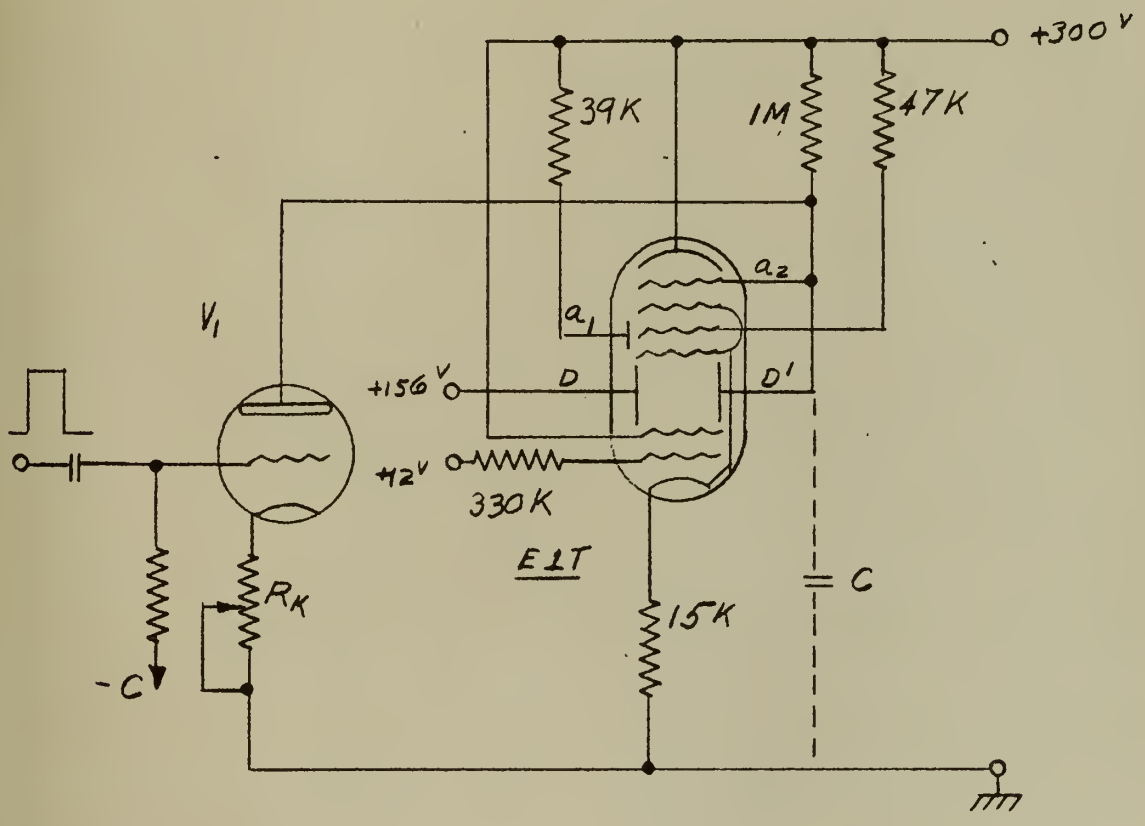

Fig. III-1. Circuit to Reduce the Stepping Time Using an Auxiliary Triode

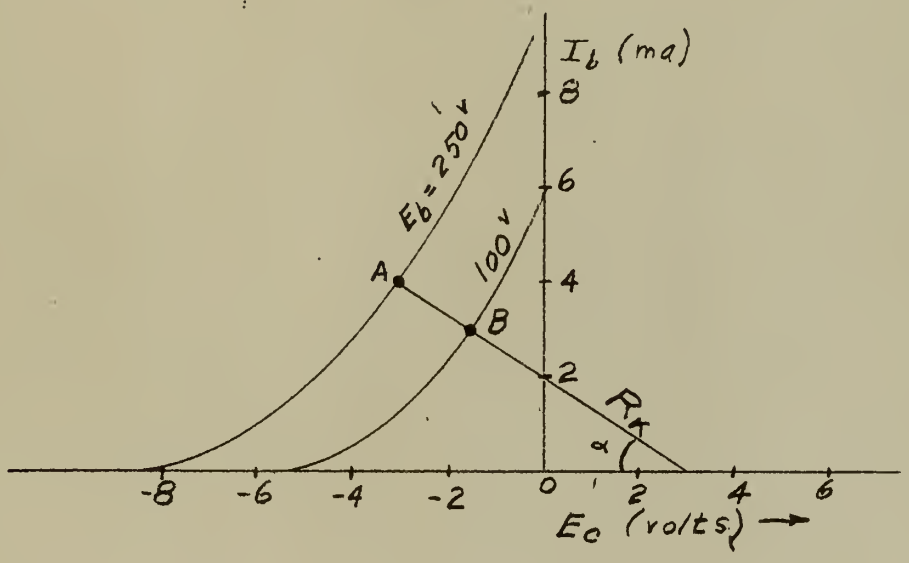

Fig. III-2. Triode Transfer Characteristic

3. Reducing the Reset Time.

The reset time of the ElT may be reduced to about four usec by means of the monostable multivibrator circuit shown in Figure III-3, which is a modification of the circuit of Figure 11, and operates in essentially the same manner. The disadvantages of this circuit are the same as for that of Figure 11, high heater-to-cathode and cathode-to-grid voltages, and the possibility of a small cathode-to-heater leakage current effectively shunting R_{a_2}. The heater-to-cathode voltage may be reduced to about 80 volts maximum by installing a heater isolation transformer for V_2, with its secondary center tap connected to about +170 volts (midway between the extreme values of V_{D',a_2} of 90 and 250 volts). The above disadvantages may be eliminated by using a secondary emission tube, whose auxiliary cathode (dynode) employs secondary instead of thermionic emission. Figure III-4 shows a reset circuit employing such a tube (EFP60). In this tube, primary electrons are produced by a thermionic cathode k_1, pass three grids (g_1 and g_2, and g_3), and then strike the dynode k_2. The dynode is coated with a substance with a high secondary emission factor, that is, each incident primary electron releases several secondary electrons. The anode a is positive with respect to the dynode, thus drawing the secondary electrons released to the anode. By means of this secondary emission, the anode current of the tube exceeds its cathode current, the difference being supplied by the dynode. When the dynode is connected to D' and a_2 of the ElT as shown in Figure III-4, and the EFP60 is rendered conducting by means of a positive pulse applied to its control grid, the secondary emission electrons from the dynode are drawn from the total capacity C at D' and a_2. This action raises the potential of D' and a_2 at a rate

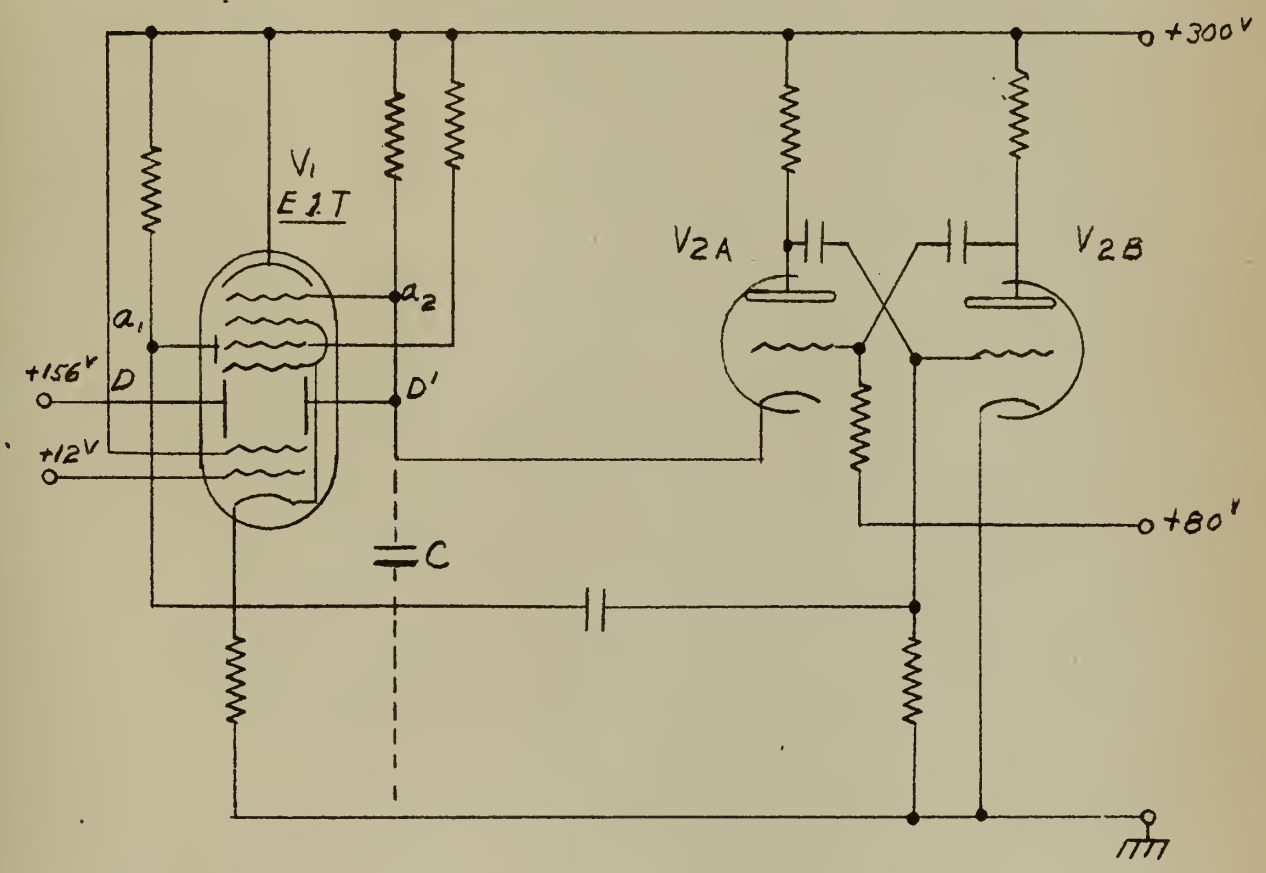

Fig. III-3. Monostable Multivibrator Reset Circuit

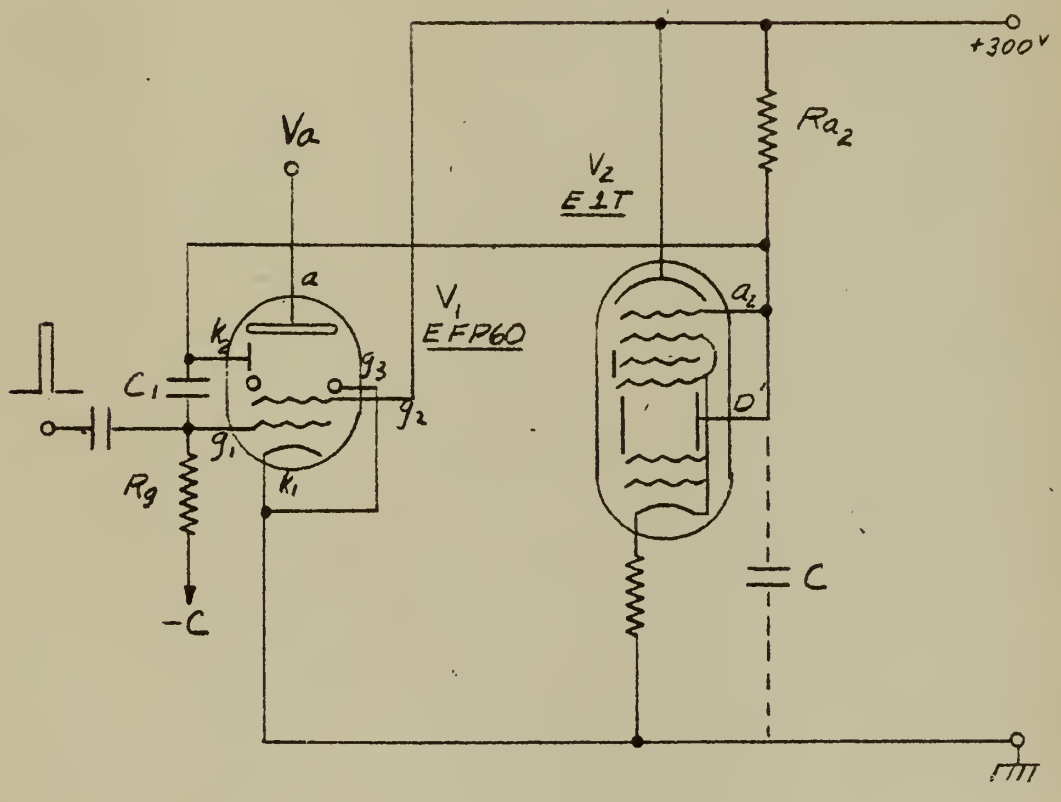

Fig. III-4. E1T Reset Circuit using an EFP60 Secondary Emission Tube

determined by the rise time of the pulse applied to the grid of the EFP60. In order to terminate this action as soon as possible after the potential of D' and a_2 has been raised by about 160 volts (i.e., reset to zero), the control grid g_1 is coupled to the dynode through capacitor C_1. The dynode potential rises until nearly equal to the anode potential. Secondary electrons then return to the dynode. A portion of the increase in dynode potential has been transmitted to g_1 through C_1, thus maintaining the tube conducting. When the dynode potential rise ceases, the potential of g_1 relaxes toward the negative cutoff bias potential at a rate determined by the R-C time constant R_gC_1, but accelerated by the drop of the dynode potential caused by the return of secondary emission electrons to the dynode. This accelerated drop of control grid potential causes the EFP60 to cut off rapidly, similar to a blocking oscillator. The potential of D' and a_2 of the ElT remains at its stable zero position until the next stepping pulse arrives at the grid of the stepping triode.

Since a positive pulse is required at the grid of the EFP60 to accomplish this reset operation, and a negative pulse is available at the reset anode when it is struck by the electron beam, a triode amplifier may be used to amplify and invert the reset anode pulse to drive the EFP60, as shown in Figure III-5. Potentiometer P provides for individual adjustment of the amplitude of the dynode voltage rise necessary to reset the ElT to zero. This circuit enables the reset operation to be accomplished in 0.45 usec, permitting a maximum counting rate of 2.2 Mc for regularly recurring pulses.

For counting random pulses, using the terminology of Appendix II,

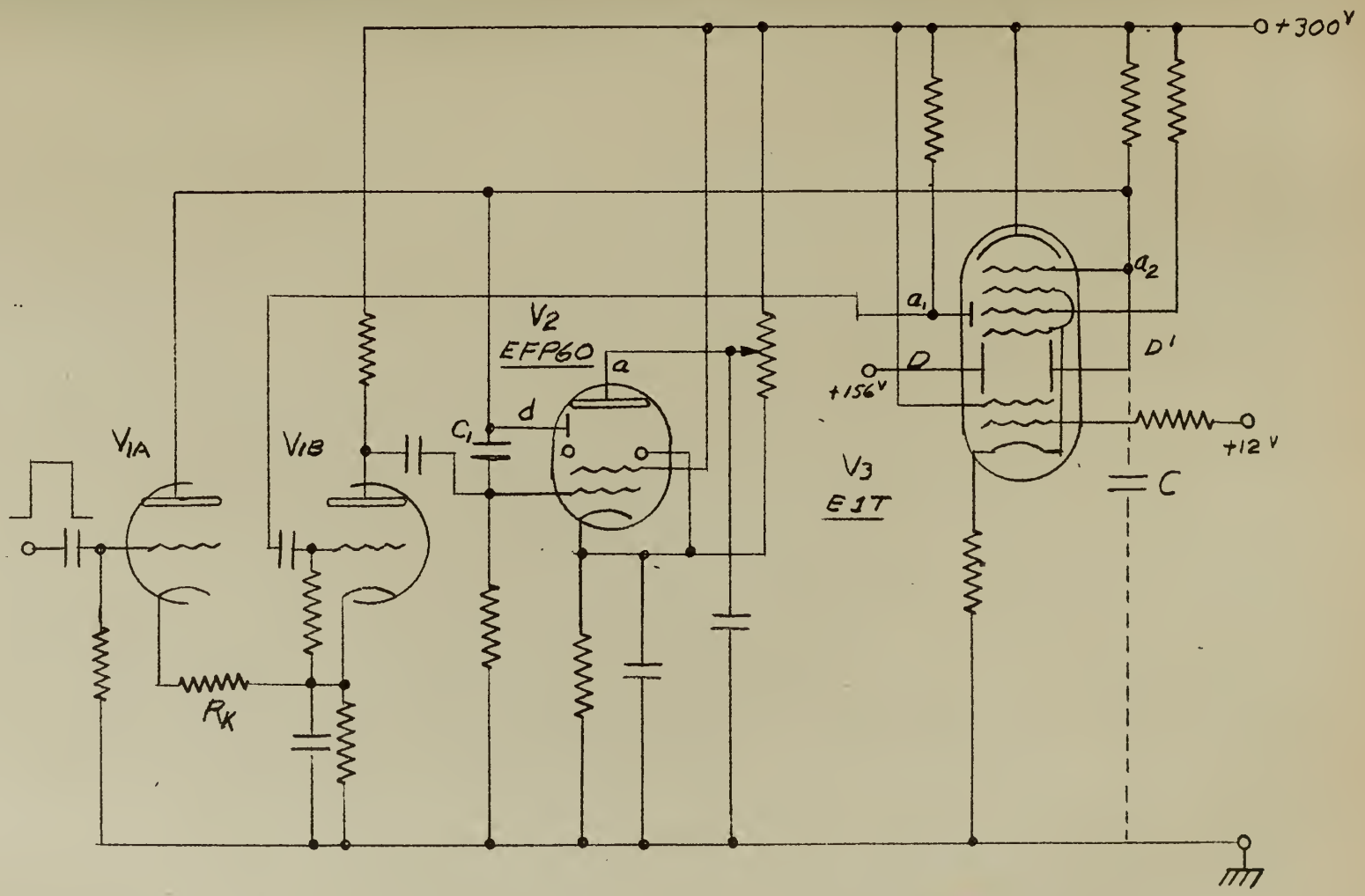

Fig. III-5. E1T Circuit Using a Triode Stepping Tube and a Secondary Emission Reset Tube.

for τ_s = 0.2 usec, and τ_r = 0.45 usec,

$$\tau_m = 0.9 \text{ X } 0.2 + 0.1 \text{ X } 0.45 = 0.225 \text{ usec.}$$

Accepting a 1% counting loss, δ = 1% and let Δ = 10%. Then

$$n = \frac{1}{11\tau_m} = \frac{1}{11\ (0.225)\ 10^{-6}} = 40.5 \text{ kc.}$$

This maximum counting rate increases in proportion to the percent counting loss acceptable.

APPENDIX IV

PARALLEL - TRIGGERED BLOCKING OSCILLATOR

1. Trigger - ability of parallel - triggered blocking oscillator circuits.

Referring to Fig. IV-1, blocking oscillator action is initiated when the triggering voltage e_2, developed across the secondary of the pulse transformer causes the grid of the blocking oscillator tube to rise to its cutoff level, or when

$$e_2 = E_{cc} - E_{co},$$

where E_{cc} is the grid bias voltage and E_{co} is the cutoff voltage of the tube. The actual voltage which is developed across the pulse transformer by the triggering tube is dependent on the rise time of its triggering voltage, the tube transconductance, and the inductance of the pulse transformer. This is given by the relationship:

$$e_2 = L_p G_m \frac{de_s}{dt},$$

where L_p is the primary inductance of the pulse transformer, G_m the transconductance of the trigger tube, and $\frac{de_s}{dt}$ is the rate of rise of the trigger voltage. The trigger-ability is also affected by the sharpness of the cutoff characteristic of the trigger tube and the ratio between the initial and the average inductance of the pulse transformer.

It is to be emphasized that regardless of how large

the amplitude of the triggering signal applied to the grid of the trigger tube, the blocking oscillator will not be triggered unless this signal has sufficient rise time for the combination of trigger tube and pulse transformer in use.

This triggering method is one of the most reliable and easily implemented triggering circuits. The advantages of parallel triggering are the additional amplification of the triggering signal, and the relative freedom from retriggering of the triggering signal persists after the blocking oscillator has passed through its cycle of operation.

2. Pulse duration.

Clark [4] refers to experimental tests made with a wide variety of tube, transformer and coupling capacitor combinations using the circuit shown in Fig. IV-2. These tests showed a marked porportionality of pulse width to coupling capacitor size and an even more remarkable independence of pulse width from transformer inductance in the range of smaller coupling capacitors and hence narrower pulses.

In pursuit of an explicit solution for pulse duration, Clark points out that the pulse termination coincides with the return of the grid current to zero. To use this idea, we first set up a simplified equivalent circuit for the blocking oscillator as shown in Fig. IV-3. We then write the mesh equations and, using the method of Laplace Trans-

forms, solve for the transformed grid current. This yields an expression of the form:

$$Ig(s) = \frac{e}{Rg} \cdot \frac{s^3 + As^2 + Bs + C}{s^4 + Ps^3 + Qs^2 + Rs + U}, \qquad (1)$$

in which the coefficients of the denominator do not lend themselves to an explicit solution in literal form. However, by dividing the polynomials in s, we get the series:

$$Ig(s) = \frac{e}{Rg}\left\{\frac{1}{s} + (A-P)\frac{1}{s^2} + (B+P^2-Q-AP)\frac{1}{s^3} + \ldots\right\}, \qquad (2)$$

whose term by term inverse transform is:

$$ig(t) = \frac{e}{Rg}\left\{1 - \frac{1}{T}t - \frac{1}{2}\frac{E/e}{L_L C_d} - \frac{1}{T^2} + \ldots\right\}, \qquad (3)$$

where $T = Rg\left(\frac{Cg\ Cd}{Cg + Cd}\right)$. (4)

This process is valid providing the convergence of the series can be established. From observation of the grid current waveform of a blocking oscillator, it is apparent that a power series representation of the grid current not only converges, but should require nothing higher than a term in t^2 for a good approximation. In fact, when the coupling capacitance is small, the grid current waveform is so nearly triangular that even a term in t^2 would not appear to be necessary.

To proceed, we then solve the first three terms of the above series for the time at which the grid current reaches zero. This yields the expression for pulse duration:

$$\tau = T \quad \frac{1 - \sqrt{2KT^2 - 1}}{1 - KT^2} \quad , \qquad (5)$$

where

$$K = \frac{E}{eL_L C_d} \quad . \qquad (6)$$

Had we used only two terms of the series we would have simply $\tau = T$, which in itself does agree in general shape with experiment, particularly at low values of τ. The complete expression, on the other hand, shows a smaller variation of τ with T than that obtained by experiment. It should be emphasized that these expressions predict only the relative changes of τ with variation of the parameters.

Let us consider the simpler expression:

$$\tau \approx T = Rg \left(\frac{Cg\ Cd}{Cg + Cd}\right) = RgCd \left(\frac{1}{1 + \frac{Cd}{Cg}}\right) \quad . \qquad (7)$$

This predicts a maximum value of $\tau = Rg\ Cd$ and shows that Cg must be comparable to Cd, the total effective shunt capacitance, before the pulse width is materially affected. It also points out that the grid circuit resistance, Rg, will affect the pulse width.

The trailing edge of the blocking oscillator pulse can probably be most readily described as the damped oscillation of the transformer magnetizing inductance and the total effective shunt capacity. The damping is provided by core losses in the transformer as well as any resistive load which might be connected to one of the transformer windings.

For maximum amplitude of the plate voltage pulse, the transformer turns ratio should be "step down" from plate to grid. The reverse ratio will give increased tube currents. As the plate to grid ratio is increased, the pulse duration is decreased, providing that the inductance of the plate winding is held constant.

3. Pulse transformer shunt capacitance.

In the construction of pulse transformers there are ordinarily several sources of shunt capacitance which will act to reduce the high frequency response of the unit. Among these are:

a. Winding-to-core capacitance,

b. Inter-layer winding capacitance,

c. Coupling capacitance between primary and secondary windings, and

d. Capacitance between adjacent turns.

In the use of a bifilar wound, ferrite core transformer, however, the more significant of these capacitances can be reduced to negligible values. First, due to the high resistance of the core material, the winding to core capacitance is effectively eliminated. Second, the bifilar winding can be of a progressive type so that no inter-layer capacitance is present. This leaves only the capacitance between adjacent turns of each winding and the turn-to-turn coupling capacitance between primary and secondary. (See Fig. IV-4). Since the fraction of the applied signal vol-

tage which appears across the capacitance of each of the adjacent turns capacitances is divided by the total number of turns in the winding, the effective capacitance from this source is correspondingly reduced. Also, if the transformer is not used to invert signal polarity (See Fig. IV-5A), no voltage will appear across the turn-to-turn coupling capacitance from primary to secondary. This means that the total effective shunt capacitance of the bifilar wound ferrite core pulse transformer can be as low as one $\mu\mu$f.

On the other hand, if the transformer is used to invert signal polarity (See Fig. IV-5B), the entire signal voltage will appear across each of the turn-to-turn coupling capacitances between primary and secondary. For this connection, the effective shunt capacitance will be the total coupling capacitance between primary and secondary. This can be as high as 10 $\mu\mu$f or more for typical commercial pulse transformers.

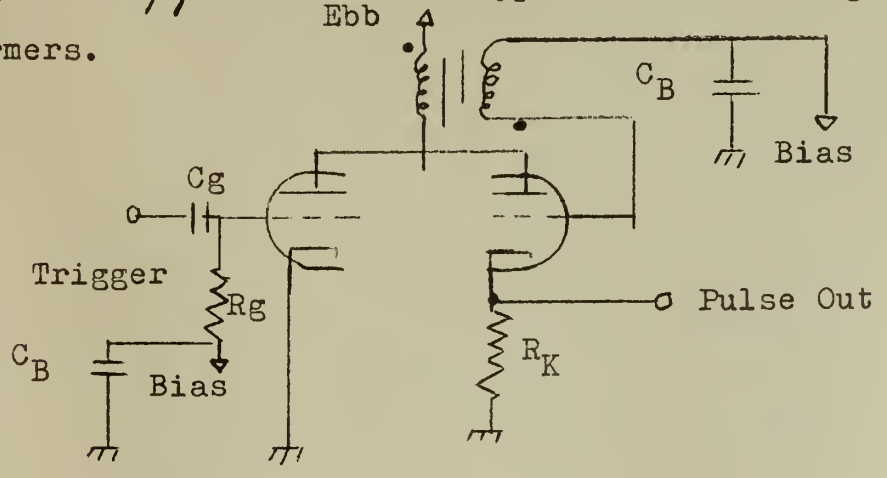

Fig. IV-1. Parallel-triggered blocking oscillator circuit.

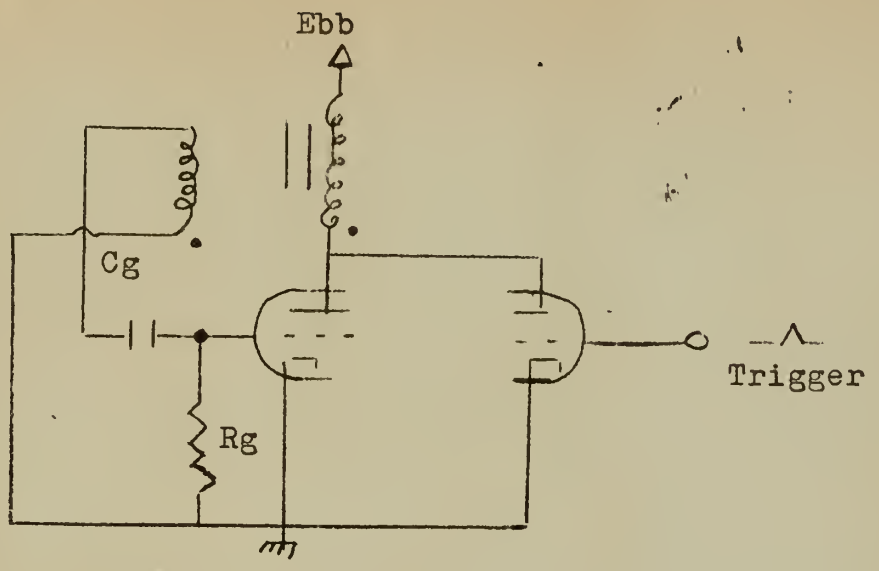

Fig. IV-2 Parallel-triggered blocking oscillator circuit.

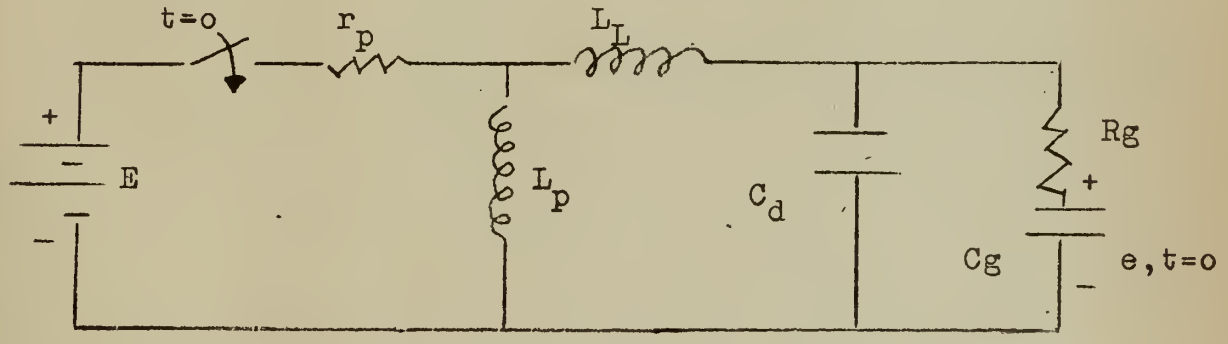

Fig. IV-3. Equivalent circuit of Fig. IV-2 for determining pulse duration. Cd is the total effective shunt capacity across the pulse transformer secondary, L_p the primary inductance, L_L the leakage inductance, and r_p the tube plate resistance. R_g and C_g are the grid resistance and capacity, as in Fig. IV-2.

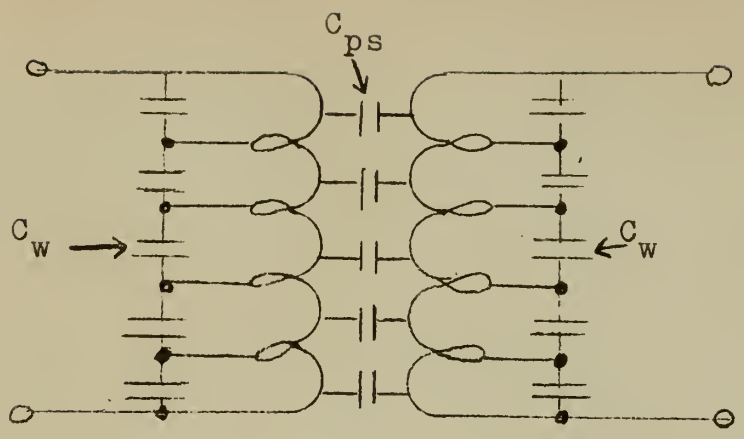

Fig. IV-4. Pulse transformer schematic showing the various inherent capacitances.

C_w - Capacitance between adjacent turns of each winding.

C_{ps} - Coupling capacitance between adjacent turns of primary and secondary.

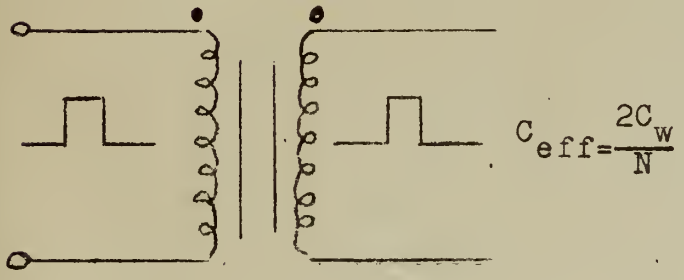

Fig. IV-5A Pulse Coupling

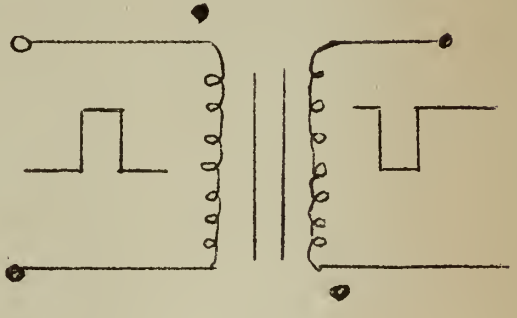

Fig. IV-5B Pulse coupling, Reversed polarity.

APPENDIX V

CALCULATION OF THE MAXIMUM ELECTRON TRANSIT TIME IN THE ElT

From Spangenberg [5], Section 6.1, the equation of motion of an electron in a uniform electric field is:

$$m \frac{d^2x}{dt^2} = -Ee, \tag{1}$$

$$\frac{dx}{dt} = - \frac{Ee}{m} t + v_o, \tag{2}$$

$$x = - \frac{Ee}{2m} t^2 + v_o t + x_o \tag{3}$$

where m is the mass of an electron in kilograms,

e is the negative charge on an electron in coulombs,

x is the distance traveled by the electron in the uniform electric field, and

E is the magnitude of the electric field in the positive x direction. Let $x_o = o$ for all $x_1 \ldots\ldots x_6$, and assume that the electric field is uniform in each of the six zones of electron travel in the ElT shown in Figure V-1. Then,

$$- \frac{Ee}{2m} t^2 + v_o t - x = o,$$

$$t_n = \frac{-v_{on} \pm \sqrt{v_{on}^2 - \frac{2E_n e}{m} x_n}}{- \frac{E_n e}{m}}, \qquad (n = 1....6) \tag{4}$$

and

$$v_{on} = v_{on-1} - \frac{E_{n-1} e}{m} t_{n-1}. \qquad (n = 1....6) \tag{5}$$

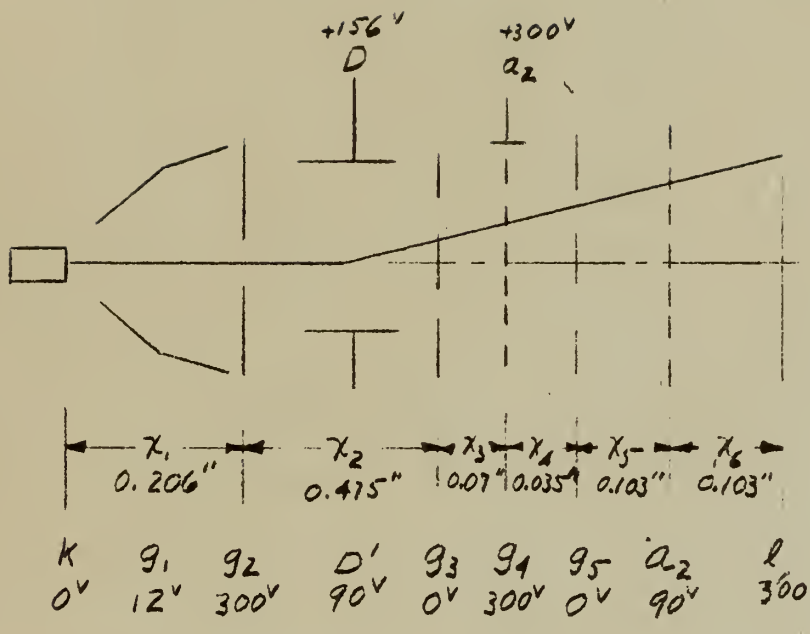

Fig. V-1. Schematic of Interior Construction and Dimensions of E1T

Maximum electron transit time occurs in the ElT when the beam is at or near the reset anode, and $V_{D',a_2} = 90$ volts, as indicated in Figure V-1.

The lengths of the six zones of electron travel are:

$$x_1 = 0.206" = 5.24\ (10^{-3})\ \text{meter}$$

$$x_2 = 0.475" = 12.1\ (10^{-3})\ \text{meter}$$

$$x_3 = 0.07" = 1.78\ (10^{-3})\ \text{meter}$$

$$x_4 = 0.035" = 0.89\ (10^{-3})\ \text{meter}$$

$$x_5 = x_6 = 0.103" = 2.62\ (10^{-3})\ \text{meter}$$

The electric fields in each of these zones are:

$$\bar{E}_1 = \frac{V_{g_2} - V_K}{x_1}(-\bar{a}_x) = \frac{(300-0)(-\bar{a}_x)}{5.4\ (10^{-3})} = -5.56(10^4)\bar{a}_x \quad \frac{\text{Volts}}{\text{meter}}$$

$$\bar{E}_2 = \frac{V_{g_3} - V_{g_2}}{x_2}(-\bar{a}_x) = \frac{(0-300)(-\bar{a}_x)}{12.1\ (10^{-3})} = 2.48\ (10^4)\,\bar{a}_x \quad \frac{\text{Volts}}{\text{meter}}$$

$$\bar{E}_3 = \frac{V_{g_4} - V_{g_3}}{x_3}(-\bar{a}_x) = \frac{(300-0)(-\bar{a}_x)}{1.78\ (10^{-3})} = -16.9\ (10^4)\,\bar{a}_x \quad \frac{\text{Volts}}{\text{meter}}$$

$$\bar{E}_4 = \frac{V_{g_5} - V_{g_4}}{x_4}(-\bar{a}_x) = \frac{(0-300)(-\bar{a}_x)}{0.89\ (10^{-3})} = 33.7\ (10^4)\,\bar{a}_x \quad \frac{\text{Volts}}{\text{meter}}$$

$$\bar{E}_5 = \frac{V_{a_2} - V_{g_5}}{x_5}(-\bar{a}_x) = \frac{(90-0)(-\bar{a}_x)}{2.62\ (10^{-3})} = -3.44\ (10^4)\,\bar{a}_x \quad \frac{\text{Volts}}{\text{meter}}$$

$$\bar{E}_6 = \frac{V_g - V_{a_2}}{x_6}(-\bar{a}_x) = \frac{(300-90)(-\bar{a}_x)}{2.62\ (10^{-3})} = -8.0\ (10^4)\,\bar{a}_x \quad \frac{\text{Volts}}{\text{meter}}$$

$$\frac{2m}{e} = \frac{2\ (9.1)\ 10^{-31}}{1.6\ (10^{-19})} = 1.14\ (10^{-11}) \quad \frac{\text{kilogram}}{\text{coulomb}}$$

$$\frac{e}{m} = \frac{1.6\ (10^{-19})}{9.1\ (10^{-31})} = 1.76\ (10^{11}) \quad \frac{\text{coulombs}}{\text{kilogram}}$$

Substituting in equations (4) and (5),

$$v_{o_1} = 0$$

$$t_1 = 1.035 \text{ musec}$$

$$v_{o_1} = 1.01\ (10^7) \text{ meters/sec}$$

$$t_2 = 2.31 \text{ musec}$$

$$v_{o_3} = 0$$

$$t_3 = 0.35 \text{ musec}$$

$$v_{o_4} = 1.04\ (10^7) \text{ meters/sec}$$

$$t_4 = 0.147 \text{ musec}$$

$$v_{o_5} = 2.0\ (10^6) \text{ meters/sec}$$

$$t_5 = 0.658 \text{ musec}$$

$$v_{o_6} = 11.28\ (10^6) \text{ meters/sec}$$

$$t_6 = 0.213 \text{ musec}$$

$$\text{Transit time} = \sum_{n=1}^{6} t_n = 1.04 + 2.31 + 0.35 + 0.15 + 0.66 + 0.21$$

$$= 4.72 \text{ musec}$$